THE LUMINESCENCE OF PERHYDRO, DEUTERO AND HALO-PHENYLACETYLENES IN RIGID SOLUTIONS AT 77°K

by

HALVIDAR SINGH

A Thesis

Submitted to the School of Graduate Studies

in Partial Fulfilment of the Requirements

for the degree

Doctor of Philosophy

McMaster University

May, 1976

LUMINESCENCE OF PHENYLACETYLENES

In Memory of My Parents

Shivprasad and Rajdaya

DOCTOR OF PHILOSOPHY — MCMASTER UNIVERSITY

(Chemistry) — Hamilton, Ontario

TITLE: The Luminescence of Perhydro, Deutero, and Halo-Phenylacetylenes in Rigid Solutions at 77°K

AUTHOR: Halvidar Singh, B.Sc. (University of Guyana)

SUPERVISOR: Dr. J. D. Laposa

NUMBER OF PAGES: xi; 181.

ABSTRACT

The fluorescence and phosphorescence spectra of phenylacetylene-H_6, -D_1, -D_5 and -D_6 as dilute (10^{-3}M or less) solutions at 77°K are reported.

Vibrational analyses of the fluorescence and phosphorescence spectra of these compounds in polycrystalline methylcyclohexane indicate that the geometries of the emitting singlet (S_1) and triplet (T_1) states are different. The fluorescence spectra are interpreted in terms of a weak allowed component and a strong forbidden one, the latter based on one quantum of non-totally symmetric b_2 vibrations. The main progression in up to five quanta of the ring breathing fundamental is explained to signify a planar, slightly expanded regular ring geometry of S_1. The phosphorescence spectra show a relatively long progression in the totally symmetric C-C ring stretching mode indicating a planar, non-regular-hexagonal ring in the T_1 state.

Polarization of the fluorescence and phosphorescence spectra of phenylacetylene-H_6 in a rigid glass at 77°K are used to assign the orbital symmetries of the T_1 state as well as the symmetries of the major bands of these spectra.

The phosphorescence lifetimes of -H_6, -D_1, -D_5 and -D_6 in rigid glasses at 77°K show that deuterium substitution for the single acetylenic hydrogen has almost the same effect as deuterium substitution for all five ring hydrogens in altering

the radiationless deactivation of T_1. These results are interpreted on the basis of a current theory of radiationless transitions.

The effect of halo-substitution in the ring on radiative and non-radiative rates is investigated for seven monohalophenylacetylenes. The phosphorescence lifetimes (in 10^{-3} M glassy solutions) decrease markedly with increasing mass of the halogen, and the effect is greatest for the <u>para</u> position. Heavy atom perturbation affects the $\int \epsilon d\bar{\nu}$ values of the $S_1 \leftarrow S_0$ and $S_1 \leftarrow S_0$ absorptions only slightly. Intersystem crossing yields are also found to increase with halogen mass. The vibrational analyses of the phosphorescence spectra of the halophenylacetylenes (in rigid solutions at 77°K) indicate the presence of two subspectra. Subspectrum I consists of the 0,0 band and bands due to in-plane modes (mainly totally-symmetric) while Subspectrum II arises from out-of-plane modes. Subspectrum II is found to increase relative to Subspectrum I with halogen substitution. Polarization measurements of the main bands of the phosphorescence spectra are interpreted in terms of contributions from several spin-orbit mechanisms.

ACKNOWLEDGEMENTS

Firstly, I would like to thank my Research director Dr. J. D. Laposa for helpful suggestions, comments, unfailing encouragement and guidance.

I am grateful to the Chemistry Department of McMaster University for financial support and to my supervisory committee for useful advice.

I appreciate the constructive discussions with my fellow graduate students [illegible], [illegible], [illegible], and Dave Condirston. Also my thanks to Mrs. [illegible], for running the Raman Spectra, Mr. William Sayer for running the ^{13}C Spectra, and Mrs. Jacqueline [illegible], for typing the final draft of this thesis.

Sincere thanks goes to my friends and relatives who contributed in some way.

Finally, but most important, I cherish the [illegible] and companionship of [illegible] who gave [illegible] to [illegible].

TABLE OF CONTENTS

LIST OF DIAGRAMS

LIST OF TABLES

CHAPTER 1

INTRODUCTION

Molecular spectroscopy deals with the interaction of electromagnetic radiation with molecules. Both absorption and emission spectroscopy give insights into the geometry and nature of the ground and excited states of molecules. Luminescence is light emission by molecules after being supplied with some form of energy from some source. In photoluminescence this energy is provided by the absorption of infrared, visible or ultraviolet light. Photoluminescence gives information on the chemical composition of the emitting system and of the processes which takes place after the absorption of the excitation energy. These processes are closely associated with those that result in photochemical reactions.

Benzene and substituted benzenes have been subjected to intensive spectroscopic research within recent years. The absorption spectra of phenylacetylene-H_6(C_6H_5CCH) has been studied in the near[1-3] and far[4] ultraviolet, infrared[5] and microwave[6] regions. Raman scattering[7, 8] has been done. Emission in rigid solutions was investigated by Khuravleva[3]. The deuterium substituted acetylenic hydrogen derivative phenylacetylene-D_1(C_6H_5CCD) was studied by infrared and Raman techniques[9]. King and So[10-12] recently extended some of these studies to include the ring deuterated phenylacetylene-D_5(C_6D_5CCH) the completely deuterated phenylacetylene-D_6(C_6D_5CCD). These

studies completely assigned the frequencies of all 36 ground state fundamental vibrational modes of phenylacetylene. They also established that the $S_0(A_1)$ - $S_1(B_2)$ electronic transition is a π π^* transition consisting of an allowed component and a much more intense forbidden component based on one quantum of a b_2 mode. Evans[13] reported the spin forbidden singlet-triplet absorption spectrum using oxygen as a perturber. The electron spin resonance (ESR) spectrum of phenylacetylene was reported for the single crystal[14] and in glassy hosts[15] at 77°K.

In this study, the vibrational analyses of the luminescence spectra of phenylacetylene-H_8, $-D_1$, $-D_5$ and $-D_6$ in rigid solutions (both glassy and polycrystalline) at 77°K are presented. Zhuravleva originally studied the electronic spectra of phenylacetylene-H_8 to help in the understanding of some photochemical activities of this and related molecules. Phenylacetylene forms radicals in alcoholic matrices[16]. From the work of King and So, a complete vibrational analysis of the emission spectra is possible, leading to a description of the geometry and symmetry of the S_1 and T_1 states. Whereas the S_1 state is accessible by both absorption and emission measurements, the T_1 state is not easily accessible by direct absorption measurement since the T_1 - S_0 electronic transition is spin forbidden. Emission studies give a direct handle on the nature of the T_1 state.

The results are interpreted qualitatively in terms of the Franck-Condon principle. The appearance of a prominent

progression in a particular normal mode of vibration is indicative of a molecular distortion along that normal coordinate. Qualitatively, the method developed by Nieman[17] for the calculation of geometry changes by relative intensity measurements on the members of the progression for emission data was applied to the phosphorescence spectrum of phenylacetylene-H_6.

Polarization studies (by the method of photoselection) are used to assign the orbital symmetry of the lowest triplet state of phenylacetylene.

The internal heavy-atom effect on the phosphorescence of $\pi\,\pi^*$ transitions has been studied in detail for naphthalene[18-20] and a few other aromatics[19]. In this study the phosphorescence spectra of seven halo-substituted phenylacetylenes are recorded in polycrystalline matrices, for which vibrational analyses are attempted, and in rigid glasses, for which polarization data are presented. An attempt is made to correlate the intensities and polarizations of two subspectra with the nature of the heavy-atom. The phosphorescence spectrum of phenylacetylene consists mainly of Subspectrum I, while those of its halo-derivatives contain a large amount of Subspectrum II, which is of vibronic origin.

The lifetimes of the triplet emission are presented to demonstrate the effect of complete and partial deuteration and the effect of the internal heavy atoms on these lifetimes in rigid solutions at 77°K. Changes in lifetimes are related to changes in the rate of the non-radiative processes,[21, 22, 36] plus, for the heavy atom derivatives, alterations in the radiative rates.[22, 69]

Furthermore, the luminescence spectra of phenylacetylene is compared with those of benzene and other substituted benzenes, including the isoelectronic molecules, phenylisocyanide and benzonitrile.

CHAPTER 2

THEORETICAL *

2.1 Symmetry Classification of the Phenylacetylenes (Ethynylbenzenes)

Although the ground state geometry of phenylacetylene - H_6 is not known experimentally, the isolated molecule can be classified as belonging to the C_{2v} symmetry point group by assuming that the molecule is planar, with the - C ≡ C - H substituent group lying on a straight line bisecting the ring. Each isotopic species (C_6H_5CCH, C_6H_5CCD, C_6D_5CCH and C_6D_5CCD) has the same symmetry elements.

A halogen substituent in the para-position does not change the symmetry. However, an ortho- or meta-halogen changes the symmetry to C_s (or C_{1h}). Mulliken's convention[27] is used in assigning the principal axes. (See Figure 2.1)

Microwave measurements on phenylacetylene - H_6 and benzonitrile[6,28] suggest both molecules are similar in geometry. Benzonitrile was found experimentally to be of C_{2v} symmetry in the ground state equilibrium configuration, with a slightly non-regular hexagonal ring[28, 29]. This is the only mono-substituted benzene with a completely determined ground state structure. King and So[10, 11] estimated the ex-

---

*Throughout this thesis it is assumed that the reader has an elementary knowledge of quantum mechanics[22], group theory[23], and spectroscopy[24, 25].

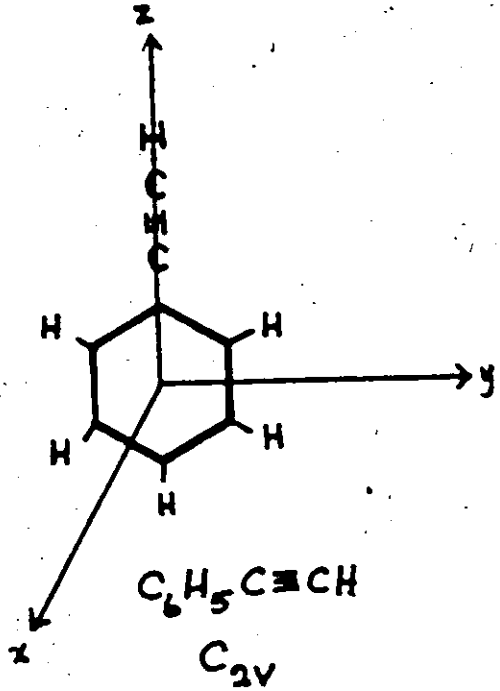

$C_6H_5C\equiv CH$

C_{2v}

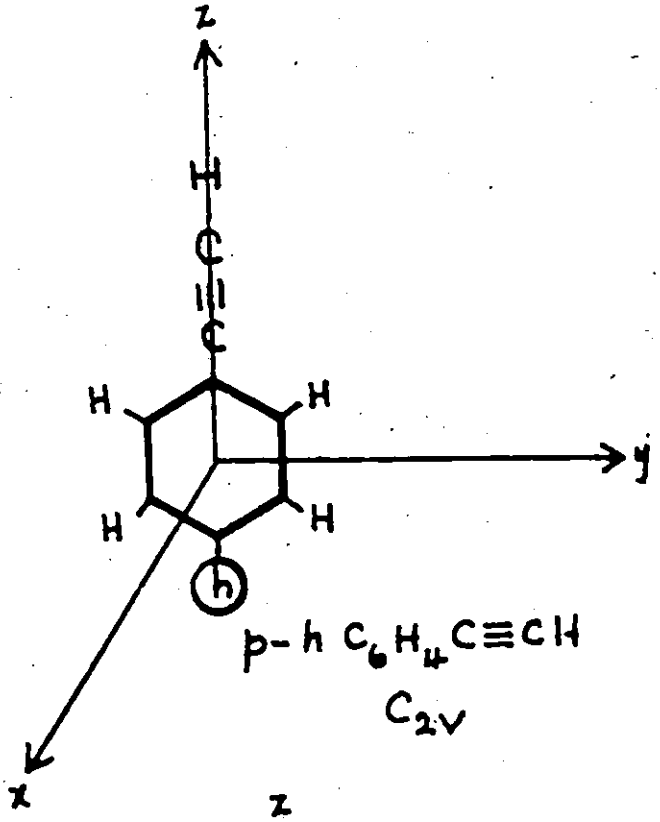

p-h $C_6H_4C\equiv CH$

C_{2v}

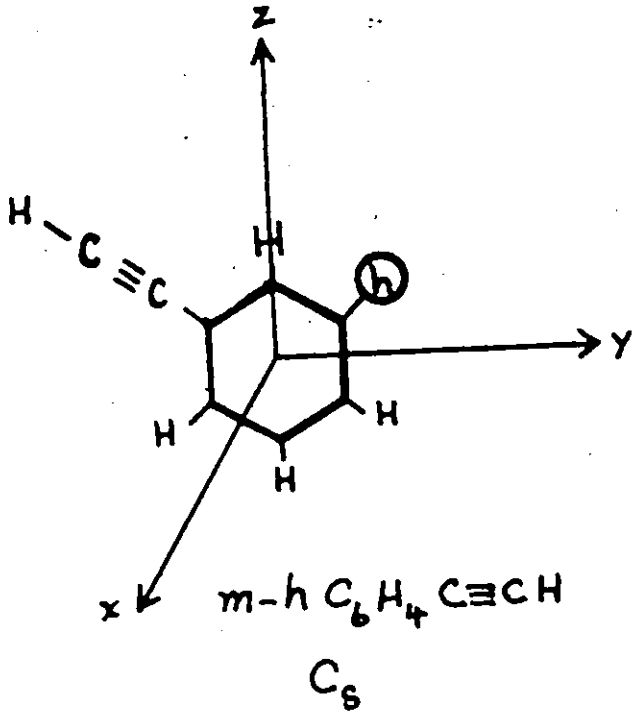

m-h $C_6H_4C\equiv CH$

C_s

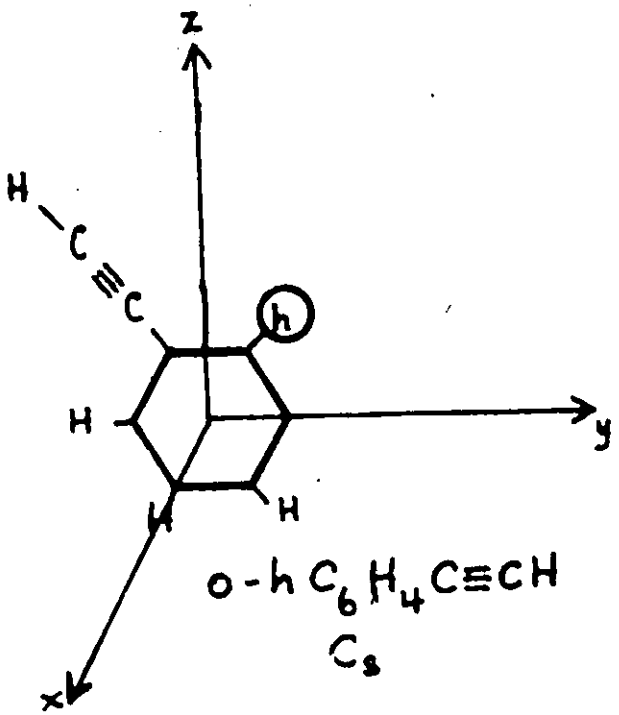

o-h $C_6H_4C\equiv CH$

C_s

FIG. 2.1 DEFINITION OF THE COORDINATE (x, y, z) AXES FOR $C_6H_5C\equiv CH$ AND h-$C_6H_4C\equiv CH$

cited state parameters of phenylacetylene. From the rotational structure obtained from the electronic absorption spectra analysed by King and So and from the infrared and Raman work of these authors and of Evans and Nyquist[9] phenylacetylene can be treated as having a planar C_{2v} geometry in the excited state.

2.2 Classification of Electronic States

Detailed discussions on the classification of the electronic states of polyatomics were done by King[26], Herzberg[25], and Sponer and Teller[31]. For a molecule belonging to the C_{2v} or C_s point group there are no degenerate representations. All the possible electronic states for phenylacetylenes are $^{1,3}A_1$, $^{1,3}A_2$, $^{1,3}B_1$ and $^{1,3}B_2$ for C_{2v} and $^{1,3}A'$ and $^{1,3}A''$ for C_s.

2.3 Electronic Absorption and Emission

During electronic absorption electromagnetic radiation excites a molecule by promoting one (or more) electrons from an occupied molecular orbital (MO) to an unoccupied MO at higher energy. Some of the intramolecular photophysical processes[19, 33] leading to the depopulation of electronically and vibrationally excited molecules are shown in Figure 2.2.

The radiative processes usually consist of two emissions named fluorescence and phosphorescence. Fluorescence is a transition between states of the same multiplicity while phosphorescence (a spin-forbidden transition) occurs between states of different multiplicities.

Radiationless transitions occur between vibronic states of the same kinetic energy. Isoenergetic transitions are called Internal Conversion (IC) between states of equal spin and Inter-System Crossing (ISC) between states of different spins.

Any vibrationally excited electronic state can reach its vibrationless state via vibronic relaxation by dissipating heat energy to the environment.

Besides these processes, the excited molecules may react, dissociate or transfer their energy to other molecules.

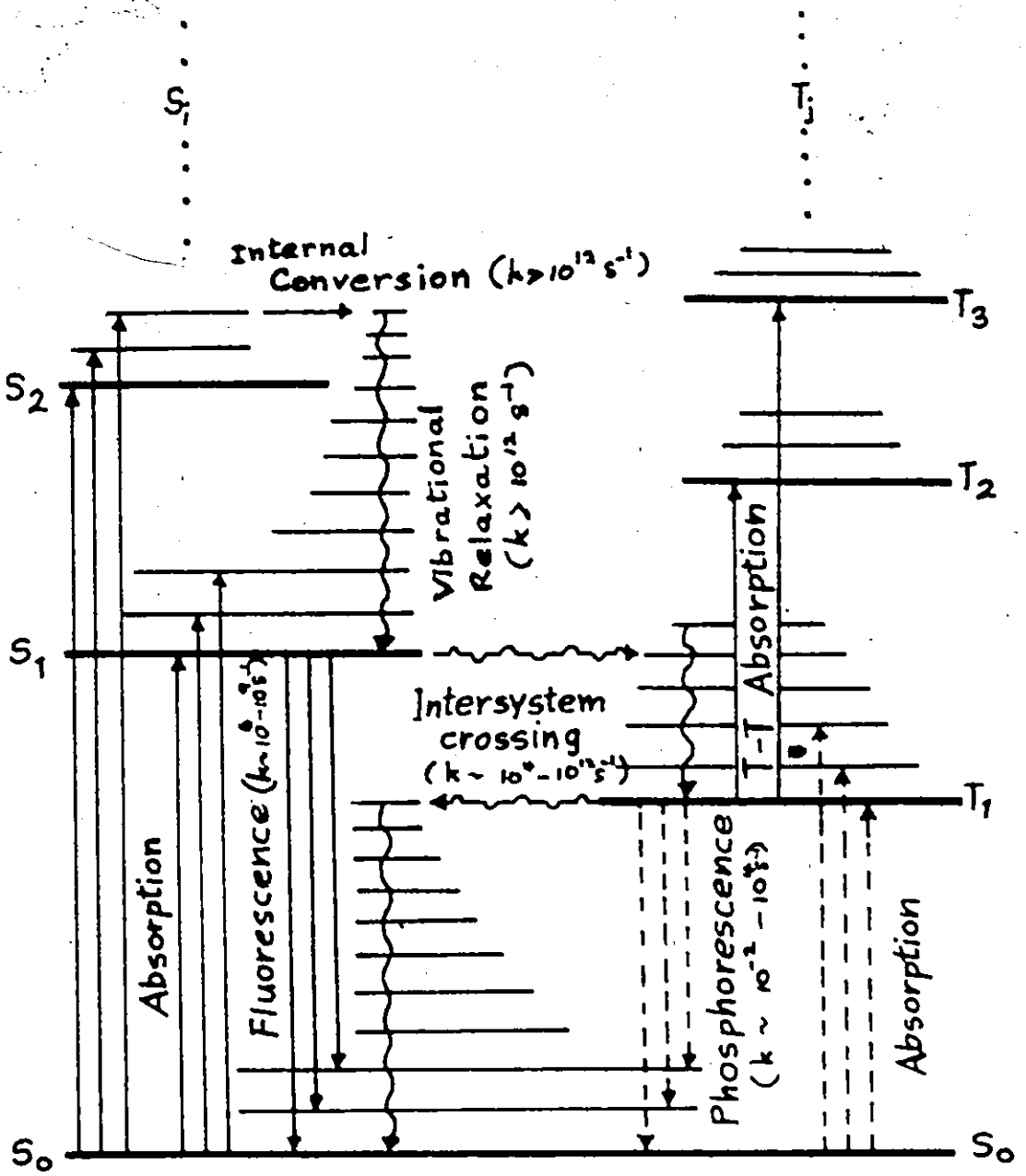

FIG. 2.2 SCHEMATIC ENERGY LEVELS WITH RADIATIVE AND NON-RADIATIVE INTRAMOLECULAR ENERGY LOSS.

2.4 The Theory of Electronic Spectra

(a) Allowed Transitions

The selection rules for electric dipole transitions [illegible] in polyatomics are more easily treated by the use of group theory. The transition moment for the vibronic non-[illegible] levels Ψ_{ev} and $\Psi_{e'v'}$ is given by the integral

$$R_{e'v'ev} = \langle \Psi_{e'v'} | \mu | \Psi_{ev} \rangle$$

The electric dipole vector [illegible] can be resolved into electronic and a nuclear part:

$$\mu = \mu_e + \mu_n$$

With the Born-Oppenheimer (BO) approximation the interactions between the electronic and nuclear motions are neglected by writing the vibronic eigenfunction Ψ_{ev} as the product $\Psi_e \Phi_v$. Hence equation 2.1 can be written as

$$R_{e'v'ev} = \langle \phi_{v'} | R_{e'e} | \phi_v \rangle + \langle \Psi_{e'} | \Psi_e \rangle \langle \phi_{v'} | \mu_n | \phi_v \rangle$$

The second term on the right is zero because of the orthogonality of electronic states. The electronic transition moment in equation 2.3

$$R_{e'e} = \langle \Psi_{e'} | \mu_e | \Psi_e \rangle$$

is a function of nuclear coordinates because the electronic wavefunctions contain these coordinates explicitly. The final value of R,

$$R^0_{e'e} = \langle \Psi^0_{e'}(r, \ldots, r_n) | \mu_e | \Psi^0_e(r, \ldots, r_n) \rangle$$

where r_0 is the equilibrium [illegible] positions in the initial

state and q is the electronic coordinates. Therefore equation 2.2 can be written as

$$R_{e'v'e''v''} = R^{o}_{e'e''} \langle \phi_{v'} | \phi_{v''} \rangle$$

In this approximation an electronic transition between the electronic states $\Psi_{e'}$ and $\Psi_{e''}$ is allowed if $R^{o}_{e'e''}$ is non-zero. In group theoretical language, for this integral to be non-zero, then

$$\Gamma\Psi_{e'} \times \Gamma\Psi_{e''} = \Gamma_{\ldots}, \ldots \text{or} \ldots$$

The overlap integral $\langle \phi_{v'} | \phi_{v''} \rangle$ determines the vibronic intensity distribution. This integral is non-zero if $\Gamma\phi_{v'} \times \Gamma\phi_{v''}$ is totally symmetric. For a transition from the zero-point vibrational level of the initial electronic state to the various vibrational levels of the final state the overlap integral is non-zero for zero and any number of quanta of a totally symmetric vibration and for zero or even quanta of a non-totally symmetric vibration.

(b) Vibronic Transition

When $R^{o}_{e'e''}$ is zero, the transition is said to be electronically forbidden. However vibronic interactions via the Jahn-Teller effect[31] can remove this forbiddenness. The total Hamiltonian can be written as

$$H = H_{e} + H_{n} + \ldots$$

Here the operator H_{e} is the sum of the kinetic energy operators of all the electrons, the operator for the electrostatic interactions of all the nuclei for the electrons, and the operator

the repulsions between pairs of electrons. [illegible] is the sum of the kinetic energy operator of all the nuclei [illegible] operator for the electrostatic attraction of all the nuclei for the electrons, and the operator for the repulsions [illegible] nuclei. The operator [illegible] = [illegible] (,), [illegible] function of both electronic and nuclear coordinates. This [illegible] is responsible for vibronic interaction. [illegible] Taylor [illegible] about the equilibrium nuclear configuration [illegible]

$$H(\; , \; _o) = \; (\; , \; _o) + \sum_i \left[\frac{\partial \; (\; , \;)}{\partial \; _i} \right]_o \; \cdots \; + \; \sum \left[\frac{\partial \; \cdots}{\partial \; \; \partial \; } \right] \; \cdots$$

$$+ \; \cdots$$

The third term on the [illegible] is [illegible]. In the usual treatment, it is assumed that only the [illegible] Ψ_e, is affected by the perturbation [illegible] term in the [illegible]. A set of zero-order [illegible] be written:

$$\Psi_e{}' = \Psi_m^o + \sum_k \; C_{mk} \; \Psi_k^o$$

where the [illegible] coefficients [illegible]

$$C_{mk} = \frac{\langle \Psi_m(\; , \; _o) \,|\, \sum_i \left[\frac{\partial \; (\; , \;)}{\partial \; _i} \right]_o \,|\, \Psi_k(\; , \; _o) \rangle}{E_m(\; _o) - E_k(\; _o)}$$

The integral in the numerator is non-zero if the [illegible] of the nuclear displacement belongs to some appropriate [illegible] causing the mixing of adiabatic [illegible] function [illegible]. This is the case when the [illegible] state in [illegible] allowed [illegible]

, transition from [illegible] to the ground state is said to be "stolen" from this allowed transition. [illegible] or non-totally symmetric [illegible] theoretical language [illegible] space as Q_i transforms in vibrational space. [illegible] in equation 2.7 is non-zero for

$$\Gamma\psi^{o}_{[illegible]} \times \Gamma\psi^{o}_{m} = \Gamma_{[illegible]}$$

2.5 The Franck-Condon Principle

Since the time required for an electronic transition is negligible compared with that of the nuclear motion, the most probable vibrational transition is the one which involves no change in the nuclear coordinates i.e. a vertical transition. This is known as the Franck-Condon Principle. Quantum mechanically, this maximum corresponds to maximum overlap between the ground state vibrational wavefunction and the excited state vibrational wavefunction.

The envelope of vibronic bands of the absorption band system is called the Franck-Condon envelope and the maximum approximates to the most intense vibronic band. If the maximum is the 0, 0 then the mean nuclear configuration of the excited state is similar to that of the ground state. When

the 0, 0 is absent or weak the transition is symmetry forbidden. An analysis of the vibronic structure and Franck-Condon envelope yields information of the nuclear configuration of an electronic excited state and its vibrational modes.

In general the positions of the electronic levels depend on the excitation state of the molecule. Figure 2.3 shows the electronic levels for a molecule in the ground electronic state (a) and for the molecule in the first excited state (b). For luminescence only these states need be considered since the highly excited states E_2, E_3 . . . are transformed by the conversion of electronic energy into vibrational energy into the first excited states of a given multiplicity.

Absorption of a quantum, $G \rightarrow E_1$ (FC), transforms the molecule from the stationary ground state G into the instantaneous Franck-Condon excited state E_1(FC). The molecule relaxes, by rearranging its electron shell and nuclear structure, $E_1(FC) \rightsquigarrow E_1(S)$, to a stationary excited state $E_1(S)$ which is self-consistent with respect to the nuclear configuration and the electronic structure. With emission of a quantum, $E_1(S) \rightarrow G(FC)$, the molecule goes to the non-stationary FC ground electronic level, G(FC), which relaxes to G. Since the total probabilities of the vibronic transitions $B_G \rightarrow E_1(FC)$ and $B_{E_1(S)} \rightarrow G(FC)$ may differ, so do the intensities of the bands in the systems (a) and (b).

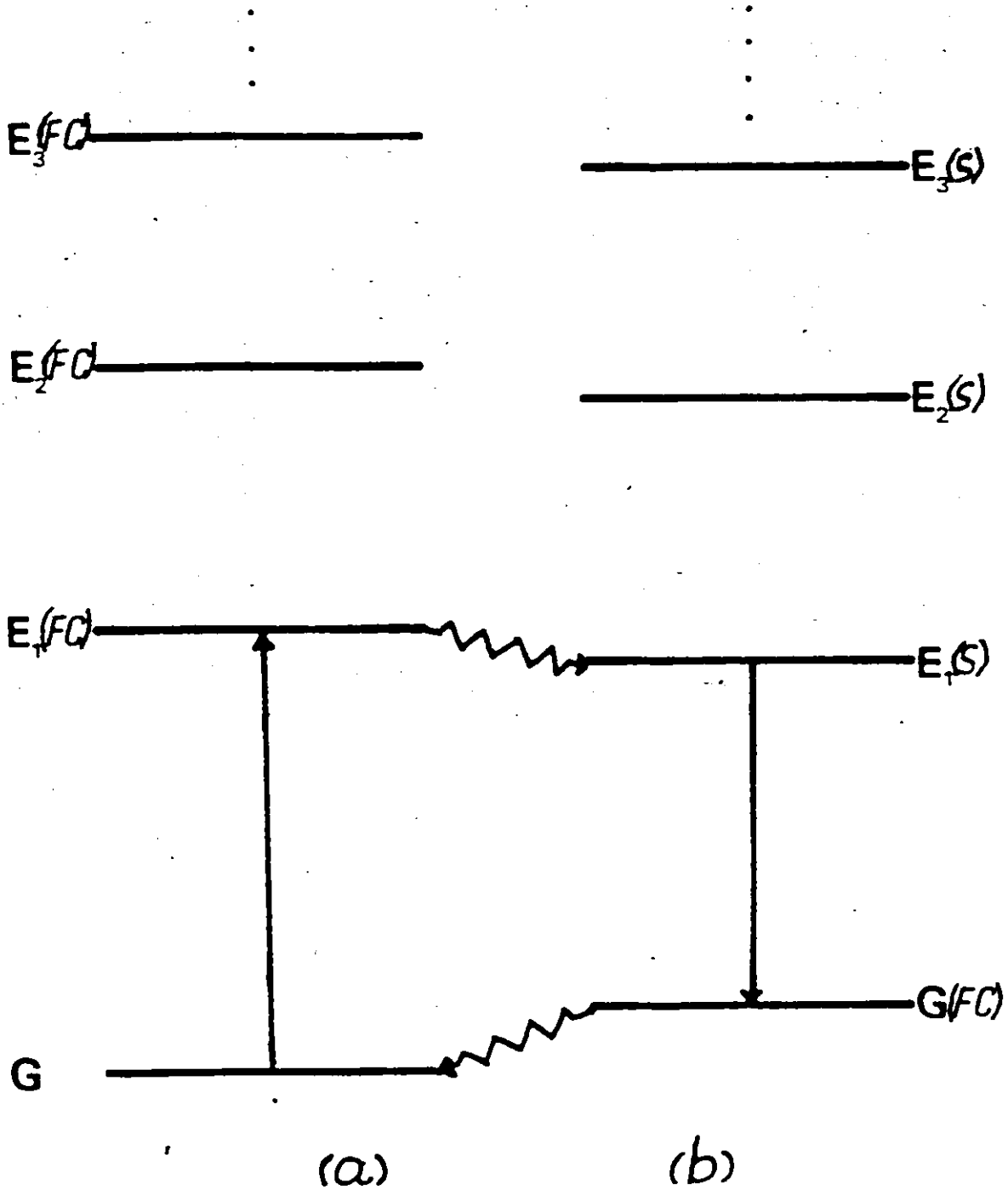

FIG. 2.3 FRANCK-CONDON AND STATIONARY ELECTRONIC STATES

2.6 Radiationless Transitions in Condensed Media

As yet no comprehensive theory on radiationless transitions has evolved. The main reason for this is the lack of experimental data. Arbitrary choices of variables are made in calculations because the observed factors are not due to one isolated effect. Several reviews [19, 33, 44] have discussed the advances made both experimentally and theoretically.

After excitation into the various vibronic levels of S_1, the 'hot' molecule in a condensed phase dissipates its excess vibrational energy to the medium to reach thermal equilibrium. Since this dissipation is fast (10^{-11}s.) compared with normal fluorescence, the flourescent properties of a molecule in dilute solutions are independent of the initial vibronic state in the $S_0 \rightarrow S_1$ absorption band system to which the molecule is excited initially. When excited into S_2 the molecule dissipates energy rapidly by crossing into an isoenergetic state of S_1 which, in turn, dissipates rapidly to the zeorth vibrational level of S_1. Most molecules fluoresce from S_1. The $S_2 \rightsquigarrow S_1$ IC rate is about $10^{12}s^{-1}$ for most aromatics.

Singlet-triplet ISC occur either from the zeroth or thermally populated vibrational levels of S_1 either to the excited vibrational levels of T_1 or to the higher excited triplet states T_q which lie nearer S_1. T_q then dissipates to T_1 by triplet-triplet IC in $\sim 10^{-11}$s.

In the highly excited vibrational levels the level density is large because there are many combinations of vibrational energy that give a total energy. For a large molecule the vibrational level density of a highly excited vibrational state may be quite large and is almost continuous. At high pressures in the gaseous state and in solutions the molecular interactions further increase the level density.

The observed decay of an excited state has a lifetime τ_{obs} given by the equation:

$$\tau_{obs}^{-1} = k_e + k_i$$

Here k_e is the radiative transition probability and k_i is the sum of the various radiationless probabilities; k_i varies largely depending on the environment of the excited state. The reason for the large variations of k_i of the phosphorescent state is not very clear at present. It may be due to the general relaxation processes caused by the interactions with the surrounding solvent molecules; and to the effects of some impurities which can deactivate the excited molecule by causing collisional interaction.

Since vibrational relaxation time in condensed phases is fast (about 10^{-12}s) the observed radiationless transition probability will be determined approximately by the transition probability of the IC and ISC processes. In more highly excited states it is not certain which of IC and ISC or vibrational relaxation is rate determining.

2.7 Spin-Orbit Coupling

Extensive reviews on spin-orbit coupling in molecules are given by various authors[19, 37, 38, 39].

Spin-orbit coupling perturbs "pure" spin states and allows transitions between states of different spin multiplicities. In the case of singlet-triplet transitions, the nominal triplet state has a little singlet character mixed into it and vice versa. The wave-function of the lowest triplet state, T_1, is written as:

$$T_1 = t_1 + \sum_K \frac{\langle t_1 | H_{so} | s_K \rangle}{E(t_1) - E(s_K)} \; s_K \qquad (...1)$$

and that of the lowest singlet state, S_0, as:

$$S_0 = s_0 + \sum_m \frac{\langle s_0 | H_{so} | t_m \rangle}{E(s_0) - E(t_m)} \; t_m \qquad (...1)$$

where t_1 and s_0 are the unperturbed triplet and singlet states, H_{so} is the Hamiltonian operator for the spin-orbit interaction, and s_K and t_m are the perturbing singlet and triplet states.

The transition moment of the singlet-triplet transition is:

$$R = \langle S_0 | er | T_1 \rangle$$
$$= \sum_K \langle S_0 | er | \frac{\langle t_1 | H_{so} | s_K \rangle}{E(t_1) - E(s_K)} \; s_K \rangle + \sum_m \langle t_1 | er | \frac{\langle s_0 | H_{so} | t_m \rangle}{E(s_0) - E(t_m)} \; t_m \rangle \qquad (...1)$$

Hence an S-T transition is due to the spin allowedness of transitions between different pairs of singlet states and between different pairs of triplet states. Since the allowedness is "stolen" from some $s_0 \leftrightarrow s_K$ and $t_1 \leftrightarrow t_m$ transitions, the polarization of a singlet-triplet transition is governed by the polarization of the $s_0 \leftrightarrow s_K$ and $t_1 \leftrightarrow t_m$ transitions.

2.8 Polarization of Luminescence

For C_{2v} the transition moment has components in the x, y and z directions. For an oriented molecule, excited by polarized light, the maximum probability of transition occurs when the electric vector is parallel to the transition axis. This probability is zero when the electric vector is at right angles to the transition axis. The effective amplitude in any directional angle θ is proportional to COS θ. Hence the probability is proportional to $COS^2\theta$.

The method of photoselection[40] is used for randomly oriented molecules e.g. in a frozen glass. The molecules are selectively excited by light of a certain oriented electric vector. Therefore, molecules with transition axes parallel to the exciting electric vector are excited preferentially, while molecules in other orientations have a smaller probability of being excited and hence contribute less to the total transition intensity.

The degree of polarization is defined as:

$$P = \frac{I_{\parallel} - I_{\perp}}{I_{\parallel} + I_{\perp}} = \frac{3\ COS^2\ x - 1}{COS^2\ x + 3}$$

where x is the angle between the absorption and emission vectors. P ranges from $+\frac{1}{2}$ to $-\frac{1}{3}$; the upper limit corresponds to $x = 0^o$ and the lower to $x = 90^o$. In practice these limits are hardly observed because of depolarization due to optical inhomogeneities in the rigid glass or its container, deviations from random molecular orientation, and molecular motions. One way of correcting for this is the method of Azumi and McGlynn[41].

2.9 Assignment of Orbital Symmetry

With a vibrational analysis and polarization measurement of the fluorescence and phosphorescence spectra the orbital symmetry of the lowest excited singlet and the lowest triplet states, respectively, can be assigned. For the planar aromatic hydrocarbons, the π-MO's are antisymmetric with respect to reflection in the molecular plane. Therefore in the C_{2v} symmetry the π-MO's transform as a_2 and b_1. The representations of the $\pi\ \pi^*$ orbital configurations are given by the direct product of these two representations and are A_1 and B_2.

The allowed $\pi\ \pi^*$ transitions in planar aromatic hydrocarbons are in-plane polarized. In the C_{2v} point group, these transitions are $A_1 \rightarrow A_1$ (z - polarized) and $A_1 \rightarrow B_2$ (y - polarized). Thus, a $^1A_1 \rightarrow {}^1B_2$ absorption followed by a $^1B_2 \rightarrow {}^1A_2$ fluorescence yields a positive degree of polarization since the absorbing and emitting states have parallel transition moments (y). However, a $^1A_1 \rightarrow {}^1A_1$ absorption followed by a fluorescence from the $^1B_2$ state results in a negative polarization.

McClure[42] has shown the orbital part of H_{so} transforms as the axial rotation operators R_x, R_y, and R_z. If the lowest triplet state is of $^3A_1$ orbital symmetry, the perturbing singlets to t_1 can be $^1A_2$, $^1B_1$, and $^1B_2$, and the perturbing triplets to

S_o can be $^3A_2$, $^3B_1$ and $^3B_2$. Since the transition moment also has the terms $\langle s_o|er|s_k\rangle$ and $\langle t_1|er|t_m\rangle$, the perturbing states are reduced to $^1B_1$, $^1B_2$, $^3B_1$ and $^3B_2$. The $A_1 \rightarrow B_1$ and $A_1 \rightarrow B_2$ transitions are out-of-plane (x) and short axis in-plane (y) polarized respectively. (See Table 2.1). Also shown in the table are the different perturbing states and expected polarization for a $^3B_2$ triplet state. For both $^3A_1$ and $^3B_2$ emitting states there is an out-of-plane (x) contribution to the 0, 0 of the phosphorescence band. However, for $^3A_1$ there is a short axis in-plane (y) contribution, and for $^3B_2$, there is a long axis in-plane (z) contribution. By exciting in the 0, 0 of the absorption bands, $^1A_1 \rightarrow {}^1B_2(y)$ and $^1A_1 \rightarrow {}^1A_1(z)$ and measuring the relative polarization of the 0, 0 of the phosphorescence band the orbital symmetry of the lowest triplet state can be assigned. For $^3A_1$, the polarization is more positive for a (y) excitation, while for a $^3B_2$, it is more positive for a (z) excitation.

TABLE 2.1

SPIN-ORBITAL MIXING OF SINGLET AND TRIPLET STATES

Lowest triplet State t_m (Orbital symmetry)	H_{so} (transform as R's)	Possible perturbing singlet states s_k to the lowest triplet state and polarization of $s_k - s_o$	Possible perturbing triplet states t_m to the ground state and polarization of $t_m - t_1$
$^3B_2$	A_2	$^1B_1$ (x)	$^3A_2$ (x)
	B_1	$^1A_2$ (forbidden)	$^3B_1$ (forbidden)
	B_2	$^1A_1$ (z)	$^3B_2$ (z)
$^3A_1$	A_2	$^1A_2$ (forbidden)	$^3A_2$ (forbidden)
	B_1	$^1B_1$ (z)	$^3B_1$ (x)
	B_2	$^1B_2$ (y)	$^3B_2$ (y)

2.10 Internal Heavy-atom Effect

A heavy-atom substituent enhances spin-orbit coupling. Good reviews of this effect are given by Lower and El-Sayed[37] and by McGlynn, Azumi and Kinoshita[19]. It seems that both the radiative and the radiationless rates increase. This leads to an observed decrease in the phosphorescence lifetime and an increase in the ratio of the quantum yield of phosphorescence relative to that of the fluorescence.

In the halonaphthalenes[18] the phosphorescence was resolved into two subspectra. Subspectrum I originates from the 0, 0 emission band and is polarized perpendicular to the molecular plane. This arises from a first-order perturbation involving out-of-plane or $\sigma\pi^*$ or Rydberg intermediate states. Of vibronic origin is Subspectrum II which is polarized in the molecular plane, and involves $\sigma\sigma^*$ or $\pi\pi^*$ intermediate states.

Friedrich et al[69] extended El-Sayed's work to explain the increasing in-plane polarization of the 0, 0 band of the phosphorescence spectra of the halonaphthalenes. These authors considered second order Herzberg-Teller terms involving out-of-plane promoting modes. The increasing enhancement of the in-plane polarization of the 0, 0 is explained in terms of one center spin-orbit integrals.

The electronic transition matrix element for radiation from the triplet sublevel T_1^r to S_0 is R^r (from equation 2.12). A Taylor expansion to second order gives

$$R^r(Q) = R^r(0) + \sum_p \left[\frac{\partial}{\partial Q_p} R^r\right]_0 Q_p + \frac{1}{2}\sum_{pp'} \left[\frac{\partial}{\partial Q_p}\ \frac{\partial}{\partial Q_{p'}}\ R^r\right]_0 Q_p Q_{p'} \qquad (2.13)$$

In equation 2.13 the first term on the r.h.s represents the transition matrix element at the nuclear equilibrium position while the second and third terms (first and second order Herzberg-Teller (H-T) coupling) represent contributions due to deviations from the equilibrium position.

In "pure" aromatic hydrocarbons the first in equation 2.13 is determined mainly by terms like

$$\langle S_0 | er_x | S_k \rangle \langle S_k | H_{so} | T_1^{i_p} \rangle$$

where x is the oop (out-of-plane) axis and T^{i_p} are the in-plane spin sublevels of T_1. Thus the intermediate states S_k are of $\sigma\pi$-type. The emitted light in the 0,0 band is oop polarized to a high degree. A totally symmetric mode gains its intensity from the same matrix element as the 0,0. For transitions to vibronic states with one quantum of an oop mode, the matrix element $\frac{\partial}{\partial Q_p} R^r(Q)$, the second term in equation 2.13, is of the type

$$\langle S_0 | er_{y,z} | S_k \rangle \left[\frac{\partial}{\partial Q_p} \langle S_k | H_{so} | T^r \rangle\right]$$

where S_k is a $\pi\pi$-type state. The rate constant of a transition involving an oop mode is about 10 times lower than that of the 0,0.

In heavy-atom substituted aromatics the rate constant of the oop radiation originates from similar matrix elements as in the parent, assuming that the triplet character does not change very much on heavy-atom substitution. Intermediate $\sigma\pi^*$-states, where the σ-MO has a large contribution from the σ-, localised at the heavy-atom, can also play a role as the atomic number of the halogen is increased. For the in-plane component of the 0,0, which was of utmost importance in the halonaphthalenes, Friedrich et al.[39] considered only those contributions which exhibit one-center SO integrals in the third term of equation 2.13. They showed that the second order Herzberg-Teller terms exhibit a strong rate enhancement with heavy-atom substitution and that the in-plane rate is governed by coupling of the type

$$\left\langle \frac{\partial}{\partial Q_p} T_1 \left| H_{so} \right| \frac{\partial}{\partial Q_p} S_1 \right\rangle$$

where the most efficient intermediate states originate from aromatic $\pi\pi$-configurations. To explain the additional transitions (and the increasing in-plane polarization) in the halonaphthalenes it was shown that the first derivative of the transition matrix element with respect to an out-of-plane mode became more important than the zero-order term as the nuclear charge of the heavy-atom increased. The leading contributions are charge-transfer $\pi\pi$-configurations, where the electron is transferred from a non-bonding n^*-orbital of the heavy-atom to the π-orbitals of the aromatic ring.

2.11 Deuterium Isotope Effects

There are 36 normal vibrational modes[25, 26, 45] for all the phenylacetylenes in this study. Replacing hydrogen atoms with deuterium negligibly changes the potential energy function. However, the large increase in mass causes large decreases in the frequency of those vibrational mode in which the specific hydrogen atom is oscillating with a large amplitude. A knowledge of the modes affected aids in the vibrational analysis of the electronic spectrum of the parent and deuterated molecules.

Siebrand[21, 22] has shown that for large energy gaps the CH stretching vibrational modes dominate the Franck-Condon factors for radiationless transitions. Deuterium substitution decreases the rate and this leads to a considerable increase in the observed phosphorescence lifetime. Work in E P A at 77°K[46] show essentially no change in the observed fluorescence lifetime on deuterium substitution. This indicates little or no internal conversion from S_1 to S_o.

A radiative deuterium effect[78] was reported for C_6H_6 and C_6D_6 in an argon matrix. The deuterated molecule lost intensity. This radiative effect becomes significant when the electronic transition is made primarily through vibronic interations through CD stretches.

2.12 Environmental Effects

An extensive discussion on the environmental effects on the spectra of molecules is given by Meyer[34]. At low temperatures organic glasses and polycrystalline matrices provide rigid hosts which interact weakly with the guest molecules. Therefore there is little distortion of the electronic configuration of the guest molecules; hence the optical properties observed are those of the guest.

These solvents have a useful spectral range from the uv to the visible spectrum. The solutions, usually stable at room temperature, were 10^{-3}M or less. The samples, prepared by freezing, have a random orientation of the guest molecules.

One drawback in the use of glasses and polycrystalline matrices as hosts is the broadening of the spectral bands because of thermal motion and environmental fields. Very sharp spectra are obtained when the solvent and solute are matched. This effect was first studied by Shpol'skii who used aromatic guests in linear hydrocarbon glasses. For benzene and substituted benzenes, cyclohexane and methyl-substituted cyclohexanes are suitable. For phenylacetylene, meta- and ortho-halophenylacetylenes, methylcyclohexane is the most suitable solvent. For the para-halophenylacetylenes, trans-1, 4-dimethylcyclohexane gives the sharpest spectra. For the xylenes Kalantar[43] used the dimethylcyclohexanes. The solute molecules occupy substitutional sites in the solvent.

At low temperature random motion is restricted. The motion and the excitation of the molecules become coupled. Lattice coupling may also occur. (Lattice vibrations are typically in the range below 150 cm^{-1}). Guest-guest interactions may occur even at 10^{-4} M in emission, leading to senzitized fluorescence, depolarization, changes in decay times, and eximer and polymer emissions.

CHAPTER 3

EXPERIMENTAL

3.1 Chemicals

Samples of phenylacetylene and deuterated phenylacetylene were donated by Dr. G. W. King, McMaster University. The original sources were: phenylacetylene-H_6 (C_6H_5-CCH), reagent grade, from Matheson, Coleman and Bell; phenylacetylene-D_1 (C_6H_5CCD) and -D_5 (C_6D_5CCH) from Merck, Sharp and Dohme Co., Montreal and were over 99% and 98% D atom respectively; phenylacetylene-D_6 (C_6D_5CCD), prepared from C_6D_5CCH by King and So[10] using deuterium exchange, had about 1% C_6D_5CCH as a residual impurity.

Because of polymerization[50] these chemicals were purified by vacuum distillation just before they were dissolved in the solvents.

The following halogen substituted phenylacetylenes were prepared from the corresponding acetophenones:-

para-fluoro-, -chloro, -bromo-, and -iodophenylacetylene;

meta-chloro- and -bromophenylacetylene;

ortho-chlorophenylacetylene.

Para-iodoacetophenone was obtained from K & K Laboratories, Inc., (New York); meta-bromo-, para-bromo, ortho-chloro-, meta-chloro-, para-chloro, and para-fluoroacetophenone were obtained from Eastman Organic Chemicals, (New York). The solid acetophenones (para-iodo- and para-bromo-) were recrystallised from ethanol before use, while the liquids were purified by dis-

tillation under reduced pressure. The method of preparation is discussed in detail by Jacobs[51] and by Allen and Cook[52]. The acetophenone (0.05 mole) was mixed with 0.05 mole Analar phosphorous pentachloride (BDH Chemicals Ltd., England) in a 50 ml round bottom flask fitted with a reflux condenser. After warming to 70 - 75°C (water-bath) the mixture reacted. The reaction, accompanied by a vigorous evolution of hydrogen chloride, was over in 15 minutes and produced an orange-brown clear liquid. Phosphorous oxychloride was removed from the products under reduced pressure at room temperature. The residual liquid, a mixture of the monochloroethylene and the dichloroethane derivatives, was refluxed for 3 - 12 hours with 40 ml of 25% ethanolic potassium hydroxide solution (0.18 mole KOH), and added to 100 ml. ice water. A dark oil separated. The rest of the product was extracted from the water by ether. The oil and ethereal solution were mixed and dried for about 15 min. with anhydrous sodium sulphate[53] (J. T. Baker Chemical Co., N.J.) (Note: Drying overnight with potassium hydroxide pellets[51, 52] caused the ethereal mixture to darken considerably and caused a lower yield)

$$X\text{-}C_6H_4 - \overset{O}{\overset{\|}{C}} - CH_3 \xrightarrow[75^\circ C]{PCl_5} \begin{matrix} X\text{-}C_6H_4 - C\,Cl_2 - CH_3 \\ \text{and} \\ X\text{-}C_6H_4 - C\,Cl_2 = CH_2 \end{matrix} \xrightarrow[\text{Reflux}]{KOH} X\text{-}C_6H_5\,C \equiv CH$$

After the ether was distilled off, the crude product was purified by distillation under reduced pressure over potassium hydroxide pellets.

The products were analysed by ^1H and ^{13}C magnetic resonance

technique (except for para-iodophenylacetylene for which only [illegible] technique was used). All were over 99% pure. All the para-derivatives were white solids while the ortho- and meta- compounds were liquids.

3.2 Solvents

Methylcyclohexane (MC) and EPA (a 5:5:2 mixture of ethyl ether, isopentane and ethanol), spectro-quality, obtained from Matheson, Coleman and Bell were used without further purification. Isopentane (IP) and 3-methylpentane (3MP), pure grade products of Phillips Petroleum Co., were further purified by shaking in Linde 10X molecular sieve. Trans-1,4-dimethylcyclohexane (DMC), 99%, obtained from Aldrich Chemical Co. Inc., were used without further purification. No detectible luminescences of the neat solvents was observed under the experimental conditions used.

Many other solvents were used but these did not improve the sharpness of the spectra. The linear hydrocarbon n-pentane, n-hexane, n-heptane, n-octane, n-nonane (Matheson, Coleman & Bell) were used for all the molecules except the deuterated phenylacetylenes.

A mixture of 98% cis and trans-1,4-dimethylcyclohexane (Aldrich Chemical Company, Inc.) contained a trace of impurity which could not be separated. This impurity yielded a very

sharp luminescence spectrum, which resembled that of paraxylene. The spectra for the ortho- and meta- substituted phenylacetylenes in the solvents 1,2-dimethylcyclohexane and 1,3-dimethylcyclohexane, respectively, were broad.

3.3 Sample Preparation

Rigid glasses were prepared by immersing the sample, contained in a quartz tube (i.d. 8mm), directly into liquid nitrogen in the Dewar. Polycrystalline solutions were cooled by placing the end of the sample tube about 1 cm above the level of the liquid nitrogen. When the sample became a polycrystalline mass the tube was quickly plunged into the liquid nitrogen.

3.4 Apparatus

Figure 3.1 shows the basic apparatus used to obtain the luminescence spectra. The light sources were: a Hanovia 150 W Watt Xenon Lamp or an Osram 150 Watt Xenon Lamp, powered by a Bauch and Lomb power supply; and a 1000 Watt Hanovia Mercury-Xenon Lamp or an Osram 450 Watt Xenon Lamp powered by a DC regulated universal lamp power supply (Model # C-72-50, Oriel Optics Corporation). The light was passed through a mono-

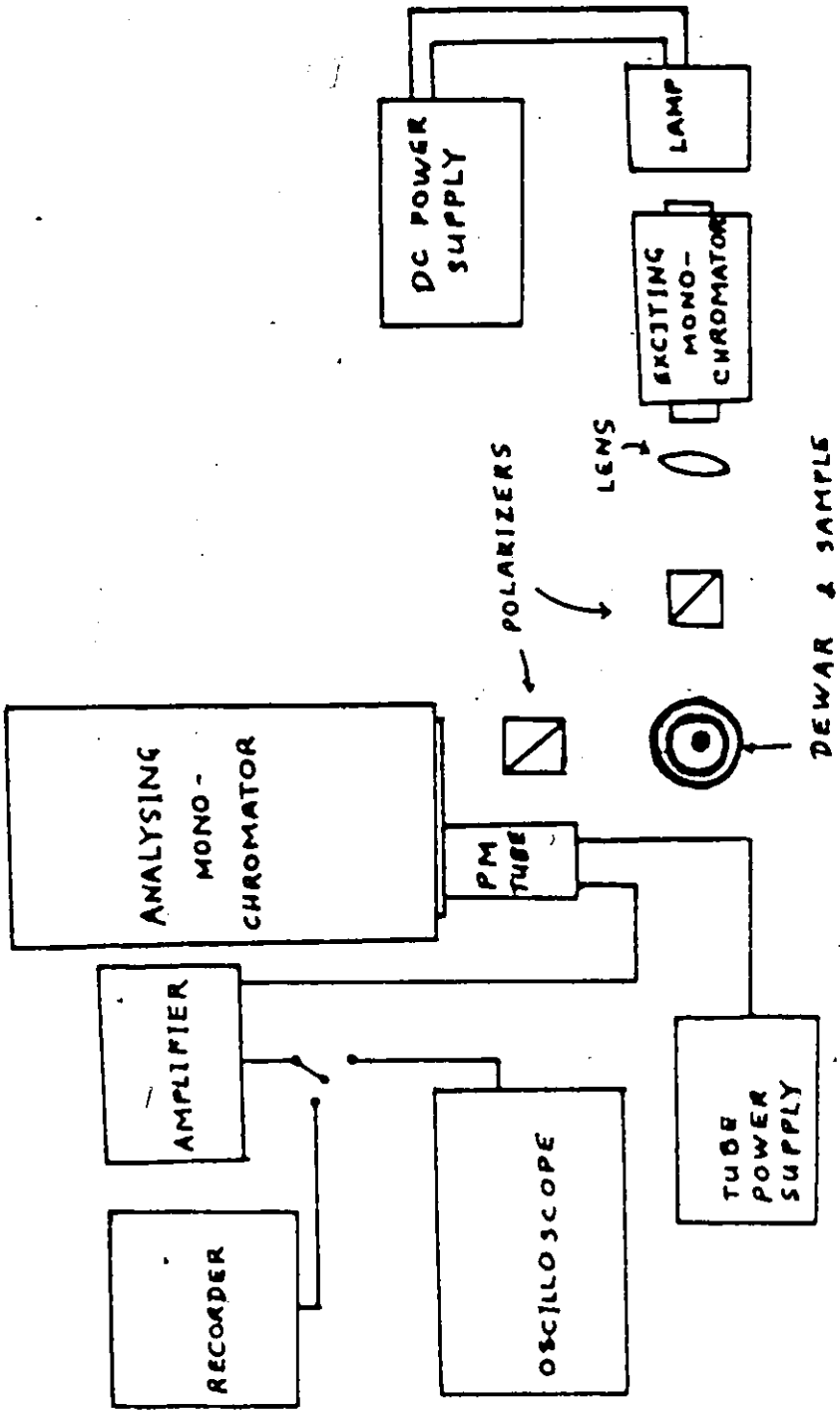

FIG 3.1 BLOCK DIAGRAM OF APPARATUS

chromator (Bausch and Lomb 0.25 m with a 1200 grooves/mm grating or a Jarrell-Ash 0.25 m Ebert with a 2360 grooves/mm, 300 nm blazed grating) followed by an appropriate UV filter. A quartz lens was used to focus this monochromated light on the sample contained in a 11 mm o.d. quartz tube immersed in a partially silvered dewar containing boiling liquid nitrogen. The emitted light was observed at right angles to the exciting light by a 0.5 m Jarrell-Ash scanning monochromator (with a 1180 grooves/mm grating, based at 400 nm) equipped with a photomultiplier (RCA type 8575). The signal from the photomultiplier was amplified by a Kiethley Model 610C Solid State Electrometer, and fed into a Varian Series G-2000 Recorder. The resulting spectra were uncorrected for instrumental response. The correction curve for the monochromator-photomultiplier combination[96] is shown in Figure 3.2.

For polarization measurements one UV polarizing Glan prism was placed between the exciting monochromator and the sample, and another between the sample and detection system. The signal was detected as above or by an Ortec photon counting system consisting of a Model 421 Integral Discriminator, a Model 441 Ratemeter, and a 9201 Photomultiplier Base used in conjunction with an Ortec Model 454 Timing Filter Amplifier.

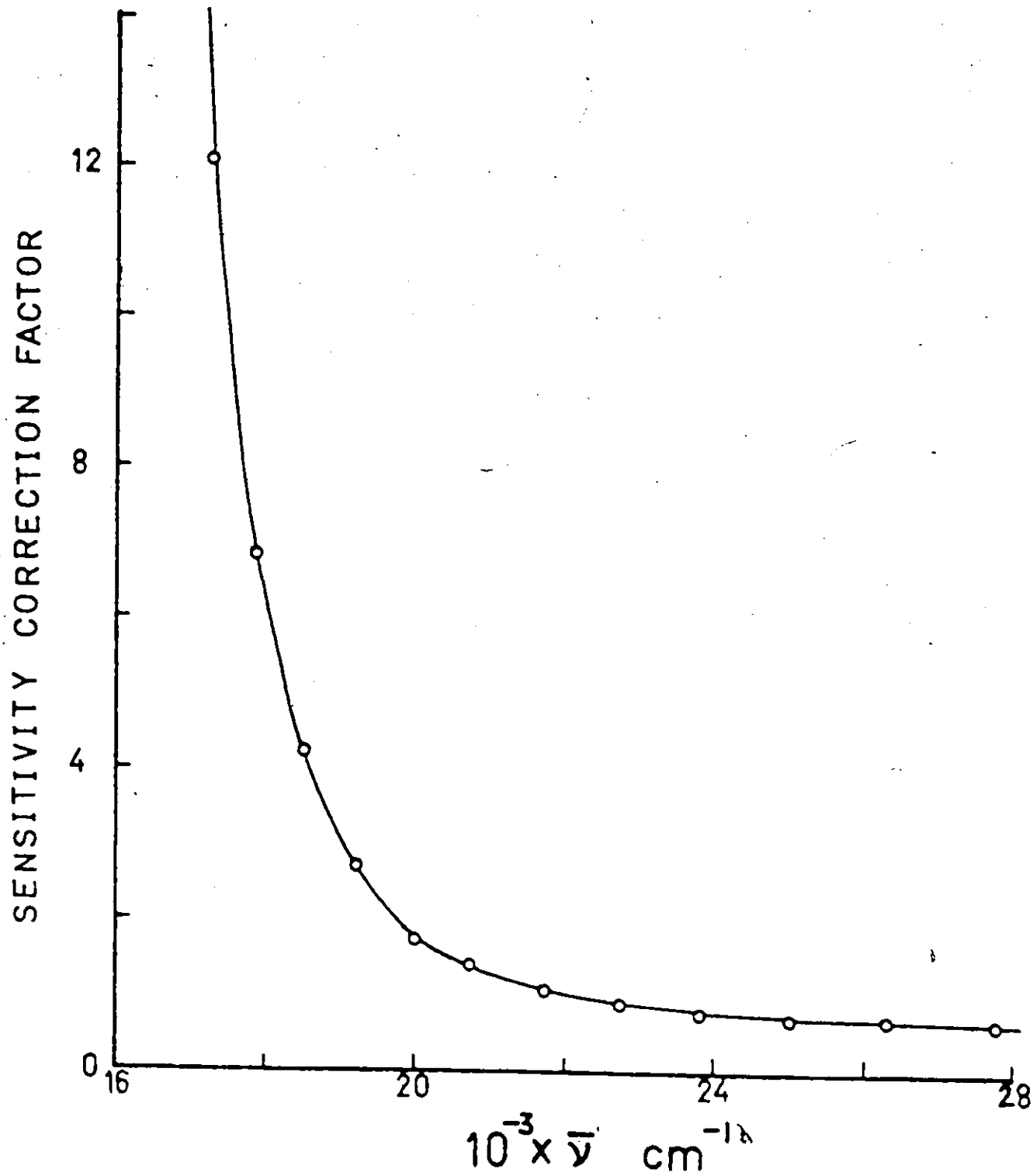

FIG 3.2 SENSITIVITY CORRECTION CURVE OF PHOTOMULTIPLIER-MONOCHROMATOR

3.5 Experimental Details

(a) Measurement of $S_0 \rightarrow S_1$ absorption spectra and $\int \epsilon d\nu$

Absorption measurements for the $S_0 \rightarrow S_1$ and $S_0 \rightarrow S_2$ transitions of the phenylacetylenes were run on a Cary 14 spectrometer at room temperature in the UV region. A pair of matched quartz cells (1 cm path length) were used. Pure solvent was placed in the reference cell while a solution of known molarity was placed in the sample cell. The values of $\int \epsilon d\nu$ were computed graphically by taking the areas under the absorption curves. Since the $S_0 \rightarrow S_2$ absorption was much more intense than the $S_0 \rightarrow S_1$, the overlap of the former was subtracted out from the tail of the latter by extrapolation.

(b) Measurement of Luminescence Spectra

The fluorescence and phosphorescence spectra for dilute solutions, 10^{-3} M or less, were obtained by exciting the $S_0 \rightarrow S_2$ transition at about 245 nm. Although both the S_0 $(A_1) \rightarrow S_1$ (B_2) and the $S_0(A_1) \rightarrow S_2$ (A_1) transitions are electric dipole allowed, the latter is about 50 times more intense (see Table 5.1). It was found that for all the lamps used the intensity of emission is greater when the excitation is into the second excited singlet band. Furthermore excitation in the first excited singlet band produced much more scattering in the region of the fluorescence spectrum. This tended to increase the back-

ground. To reduce scattering narrower slits of the exciting monochromator had to be used. This decreased the intensity of the exciting light. Several solvents were tried. The most detailed spectra for phenylacetylene-H_6, $-D_1$, $-D_5$ and $-D_6$ were in MC. For the para-derivatives the most detailed spectra were obtained in DMC while for both the meta- and ortho-derivatives MC gave the most detailed spectra; both solvents were used as polycrystalline matrices at 77°K. In the sharpest spectra half-bandwidths of about 20 cm^{-1} were obtained in these solvents. Resolution was extremely poor in the glassy form of these solvents as well as in the other solvents tried.

For polarization measurements the glass consisting of a mixture of MC and 3MP (4:1 by volume) yielded the most reproducible results.

In all cases the spectra, obtained for solutions of about 10^{-3} M solutions, started with zero background intensity and then decreased to zero again. The samples were excited ~ 250 nm and the spectra were calibrated by mercury or xenon lines.

(c) Polarization Measurements

The method of photoselection was used, with correction factors as discussed by Azumi and McGlynn[41]. From a 450 W Xe source, light was passed through a Jarrell-Ash 0.[illegible] m monochromator using 1000μ slits. The half-bandwidth of the exciting light thus obtained was about [illegible] cm^{-1} [illegible] mμ

irradiate the

(c) Measurement of Phosphorescence Lifetimes

The phosphorescence lifetimes were measured by feeding the signal directly from the photomultiplier tube (or from the electrometer) into an Hewlett-Packard 130 A Dual Beam Oscilloscope and the decay of the 0, 0 band or the most intense band was photographed by means of an Hewlett-Packard Model 196 Oscilloscope camera. For sample with relatively short lifetimes (the halo-derivatives) the oscilloscope was set on [illegible] sweep and a UV Xenon flash lamp, of lifetime 0.1 [illegible] ms, was used to excite the sample. For samples of relatively [illegible] lifetime the above method was used or the oscilloscope [illegible] for regular sweep and light from a continuous source [illegible] mechanically shuttered. Over six measurements were taken for each compound in a specific solvent and at least two samples were used.

The τ_p measurements for phenylacetylene-[illegible], -[illegible], -D_5, and -D_6 are reported for 10^{-}[illegible] M samples in [illegible] and [illegible] glasses at 77°K. The samples were subjected to [illegible] freeze-pump-thaw cycles and immersed in a quartz [illegible] containing boiling liquid nitrogen for periods ranging [illegible] hours before being excited. The decay of the [illegible] phosphorescence over two to three lifetimes [illegible]

The measured τ_p's, listed in Table [illegible], [illegible] exponential and are found to be independent [illegible] the cooling period, sample thickness, vibronic level [illegible] or second [illegible] [illegible] population. [illegible]

for $-H_6$ was measured for concentrations ranging from 10^{-3} M to 10^{-5} M and found to be independent of concentration. For 3MP the lifetimes did not change with degassing by freeze-pump-thaw treatments while in EPA they were about 5 to 10% longer if degassing was not employed. Kalantar[72] has shown that the lifetimes of toluenes varied in EPA according to the age of the EPA. These two observations are consistent with a change in the composition of the mixed solvent depending on age or degassing treatment because of the different rates of evaporation of the constituents of the mixture.

The τ_p's of the halophenylacetylenes were taken in undegassed solvents at 77°K.

The mean lives of the phosphorescence emissions were calculated from a semi-log plot of intensity (y-axis) vs. time (x-axis). All plots yielded straight lines which showed the decay curves were exponential for at least two lifetimes.

CHAPTER 4

LUMINESCENCE OF PERHYDRO AND DEUTERATED PHENYLACETYLENES

4.1 General

For all the solutions, the intensities of the fluorescence and the phosphorescence spectra were uncorrected for instrumental response. The spectra were independent of the wavelength of excitation. Furthermore, Kasha's rules were obeyed - the fluorescence originated from S_1 and the phosphorescence from T_1 i.e. the emissions were the lowest excited level of the given multiplicity.

After the molecules were excited into the S_2 state, there is internal conversion into some vibrationally excited state of S_1 ($S_2 \rightsquigarrow S_1$) followed by a vibrational relaxation into the zeorth vibrational level of S_1. The first excited triplet was populated by ISC from S_2 or S_1 either directly into some vibrationally excited state of T_1 ($S_x \rightsquigarrow T_1$) or via some intermediate triplet states. Finally, by vibrational relaxation the zeroth vibrational level of the T_1 state was populated. At 77°K, the temperature of boiling liquid nitrogen, the Boltzman factor kT is 54 cm^{-1}. Hence there was little vibrational population of S_1 and T_1 since the vibrational spacings were much larger than kT. Hence the observed emission spectra originated from the zeroth vibrational level of S_1 and T_1.

4.2 The Ground State Vibrational Modes

The ground state vibrational modes of phenylacetylene-H_6 are described in Table 4.1. The frequencies of the ground state fundamental modes of phenylacetylene-H_6, $-D_1$, $-D_5$ and D_6 are given in Table 4.2. The values listed by King and So[10, 12], are compared with those obtained from the luminescence spectra of these molecules as guests in polycrystalline KC at 77°K (similar values were obtained in other solvents). These frequencies are accurate to about $\pm$ 5 cm^{-1}. The fundamentals were labelled after Herzberg[32]. The Liffen[55] and Wilson[30] notations for substituted benzenes are also included. Some schematic diagrams of the approximate normal vibrations are shown in Figure 4.1.

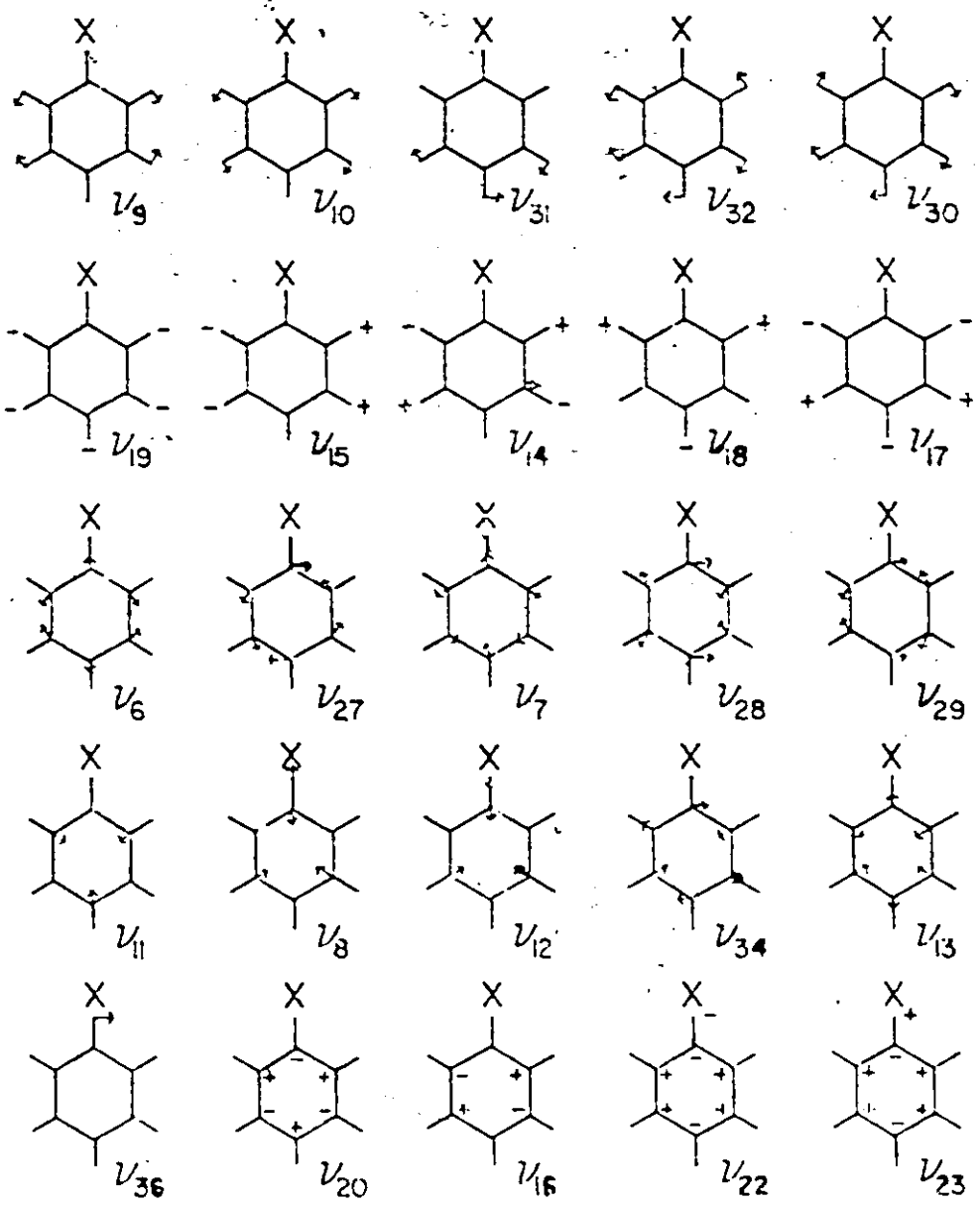

FIG. 4.1 NORMAL VIBRATIONS OF MONOSUBSTITUTED BENZENES (SCHEMATIC).

TABLE 4.1

THE SYMMETRY, DESIGNATION & APPROXIMATE DESCRIPTION OF THE NORMAL VIBRATIONAL MODES OF PHENYLACETYLENE-H_6

Symmetry	Designation[a]			Description of C_6H_5CCH Mode	
a_1	1			ν C-H	
	2			ν C-H	
	3			ν C-H	
	4		7a	ν C-H	
	5			ν C≡C	
	6	k	8a	ν C-C	
	7	m	19a	ν C-C	
	8	q	13	ν Ring-sens	(ν C-CCH)
	9	a	9a	β C-H	
	10	b	18a	β C-H	
	11	p	12	Ring	
	12	r	1	Ring-sens	(α C-C-C)
	13	t	6a	Ring-sens	(α C-C-C)
a_2	14	h	17a	γ C-H	
	15	j	10a	γ C-H	
	16	w	16a	ϕ C-C	
b_1	17	j	5	γ C-H	
	18	i	17b	γ C-H	
	19	f	11	γ C-H	

TABLE 4.1 (CONTINUED)

Symmetry	Designation			Description of C_6H_5CCH Mode
	20	v	A	ϕ C-C
	21			γ CC-H
	22	x	16b	X-sens (ϕC-C)
	23	y	10b	X-sens (γ C-CCH)
	24			γ (C-C≡C)
b_2	25			ν C-H
	26			ν C-H
	27	l	8b	ν C-C
	28	n	19b	ν C-C
	29	o	1	ν C-C
	30	e	3	β C-H
	31	c	15	β C-H
	32	d	18b	β C-H
	33			β CC-H
	34	s	6b	α C-C-C
	35			β (C-C≡C)
	36	u	9b	X-sens(β C-CCH)

a. The first column lists the i's of the ν_i designation; the second column gives the Whiffen notation for monosubstituted benzenes (Ref. 55); the third column gives the Wilson notation (Ref. 30).

b. The descriptions are:

Abbreviation	Description
νC-H	C-H stretching
βC-H	C-H in-plane deformation
γC-H	C-H out-of-plane deformation

TABLE 4.1 (CONTINUED)

Abbreviation	Description
ν C-C	C-C stretching
α C-C-C	Ring in-plane deformation
ϕ C-C	Ring out-of-plane deformation
Ring	Ring breathing
ν CC-H	C-H stretching of the acetylenic group
β CC-H	C-H in-plane deformation of the acetylenic group
γ CC-H	C-H out-of-plane deformation of the acetylenic group
ν C-CCH	C-C stretching between benzene ring and acetylenic group.
β C-CCH	C-C in-plane deformation between benzene ring and acetylenic group
γ C-CCH	C-C out-of-plane deformation between benzene ring and acetylenic group
ν C≡C	C-C stretching
β C≡C	C-C in-plane deformation
γ C≡C	C-C out-of-plane deformation
X-sens	Substituent X sensitive vibrations, in which X moves with appreciable amplitude and thus the frequencies are sensitive to the mass of X.

TABLE 4.2

FREQUENCIES (cm^{-1}) OF THE FUNDAMENTAL VIBRATIONAL MODES OF PERHYDRO- AND DEUTERATED PHENYLACETYLENES OBSERVED IN THE FLUORESCENCE (F) AND PHOSPHORESCENCE (P) SPECTRA (IN POLYCRYSTALLINE METHYLCYCLOHEXANE AT 77°K)

	$-H_6$			$-D_1$			$-D_5$			$-D_6$		
	F[b]	P[b]	K & S[c]	F	P	K & S	F	P	K & S	F	P	K & S
5		2120	2120		2005	1984		2125	2122		2010	1980
6	1615	1605	1601	1605	1600	1600		1575	1572		1575	1571
7		1470	1488		1490	1488		1385	1379		1385	1378
8	1210	1205	1192	1205	1195	1193	1150	1155	1136	1150	1145	1136
9	1185	1185	1175	1170	1175	1175		875	868		870	867
11	1010	1000	998	1005	1000	998	970	955	956	970	950	952
12	780	775	760	765	760	758	715	720	716	700	720	707
13	475	475	465	470	455	459	465	470	454	455	460	446
15		855	842		840	841			704			704
20		695	689		695	691		550	553		530	553
21		625	613		495	482		625	612		495	491
22		530	530		529	531		470	470		470	475
23		350	349		330	340		315	330		305	322
24		165	162		150	154		160	161		135	146

TABLE 4.2 (CONTINUED)

ν_i[a]	-H6-			-D_1			-D_5			-D6		
	P[b]	P[b]	K & S[c]	P	P	K & S	P	P	K & S	P	P	K & S
29	1330		1330	1325		1329	1265		1274	1280		1275
30		1280	1282		1275	1278			1034			1034
31	1160	1160	1157	1160		1157			842			841
32	1080	1065	1070	1075	1070	1070	800		822	760		821
33	645	655	649	485	495	482	675	655	648	480	495	477
34	620		613	620		623	600		602	590		601
35	510		513	535		531	505		502	515		513
36		350	350		330	349		315	340		305	322

a. [illegible] the subscript i of ν_i is listed in this column.

b. [illegible] within $\pm 10 cm^{-1}$.

c. [illegible] and [illegible], ref. 10.

4.3 Vibrational Analyses of Fluorescence Spectra

The two solvents which gave the sharpest spectra were IP and MC, the latter having the sharper bands (about 40 cm^{-1} half-width). The overall appearance of the spectra was the same for all solvents used when the concentration was 10^{-3}M or less. However in glasses (e.g. EPA or 3M) the half bandwidths were quite large ~ 300cm^{-1}. With greater concentrations, the 0, 0 region of the fluorescence was diminished due to self-absorption because of the overlapping of the emission and absorption band origins. Furthermore, a broad structureless band with a maximum intensity at around 350nm appeared. This is due to the emission of eximers. The eximer emission increased in intensity relative to monomer emission with increasing concentration. Dimers (or polymers) were also formed at concentrations greater than 10^{-2}M in MC and n-pentane. The dimer emission, which was structured, had an origin around 310nm. The analyses given below are for the solutes in MC and are also valid for IP.

In all the fluorescence spectra the intensity went down to almost zero before the 0,0 region of the phosphorescence.

(a) Phenylacetylene-H_6

The fluorescence spectrum is shown in Figure 4.2 and the vibrational analysis in Table 4.3. The 0, 0 band, which is the pure electronic transition, was observed at 35550 cm^{-1} in MC, and 35525 cm^{-1} in IP in agreement with 35500 cm^{-1} in IP, reported by Zhuravleva[3]. A very weak broad band at 190 cm^{-1}, (no $-H_6$ frequency corresponds to this) which decreased slightly in frequency with increasing deuteration, and varied slightly in shape from one experiment to another, is assigned as a lattice vibration. Similar satellite bands are seen in the fluorescence spectrum of benzene in cyclohexane matrix[56], 144 cm^{-1} for C_6H_6 and 127 cm^{-1} for C_6D_6. Leach et al.[56] observed that the activity of this band increased with temperature and suggested that this is due to a hindered rotation of the solute benzene molecule. From a vibrational analysis, this weak band does not appear to be due to solute emission from two crystalline forms of the solvent.

The first a_1 vibration appears as a medium intensity band 3 at 475 cm^{-1} and is assigned to a totally symmetric ring deformation, ν_{13}. This band was not previously reported.

There are 3 false origins in all the fluorescence spectra of phenylacetylene-H_6, $-D_1$, $-D_5$ and $-D_6$. The three b_2 vibrations responsible are ν_{35}, the acetylenic C ≡ C triple bond in-plane deformation; ν_{34}, the ring in-plane deformation; and ν_{13}, the acetylenic C-H in-plane deformation. The 0,35 and 0,34 transitions appear as the strong broad band

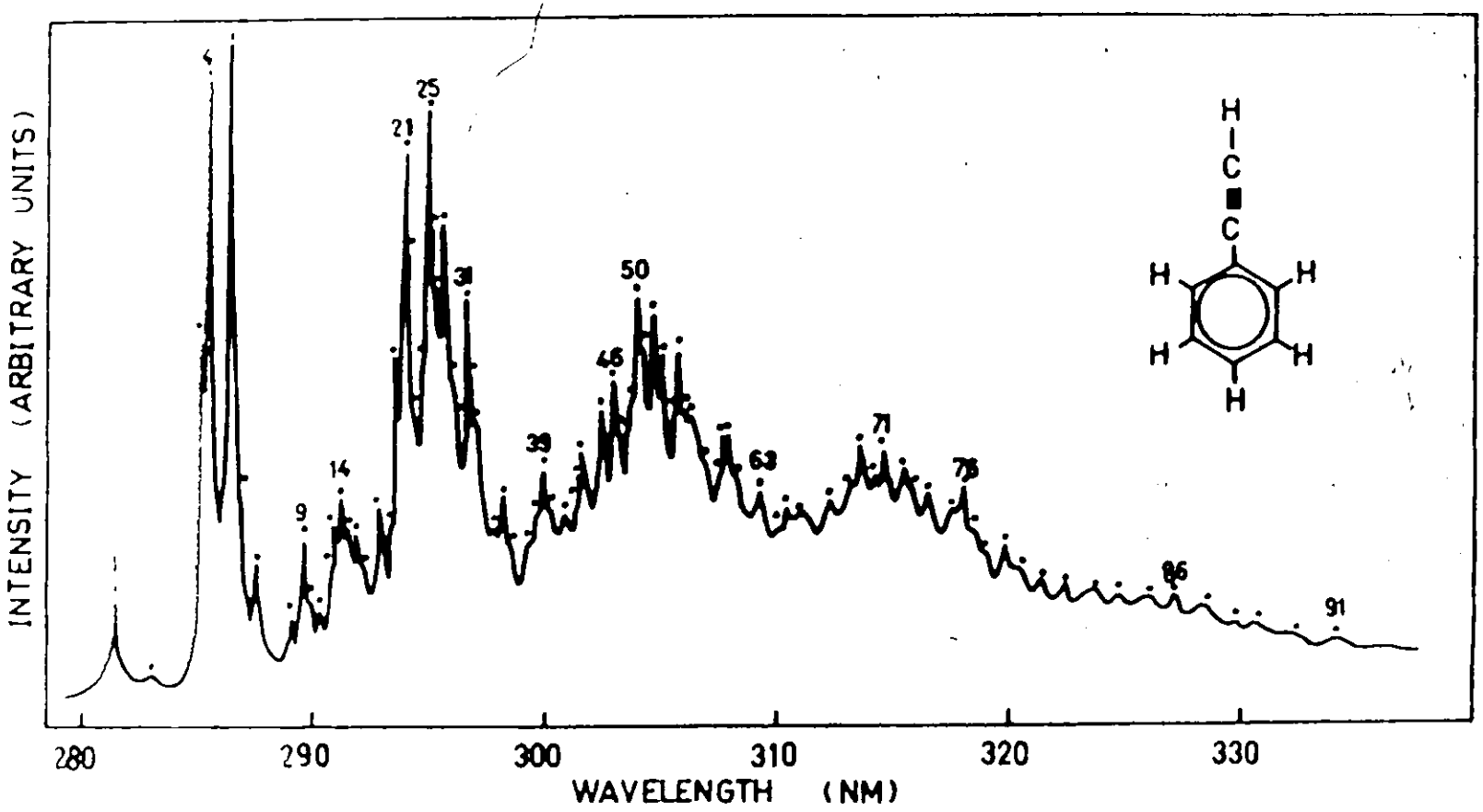

FIG. 4.2 THE FLUORESCENCE SPECTRUM OF 10^{-3}M PHENYLACETYLENE-H_6 IN POLYCRYSTALLINE METHYLCYCLOHEXANE AT 77 °K

TABLE 4.3

VIBRATIONAL ANALYSES OF THE FLUORESCENCE SPECTRA OF 10^{-3} M PHENYLACETYLENE-H6, & 10^{-4} M PHENYLACETYLENE-D_1, -D_5, -D_6, IN POLYCRYSTALLINE METHYLCYCLOHEXANE AT 77°K

Intensity[a]	Position from the 0,0 band[b] (cm^{-1})				Assignment[c]
	-H6	-D_1	-D_5	-D_6	
vw	190	185	165	140	0, Lattice
m	475	470	465	455	0,13
m		485		480	0,33
s	510	535	505	515	0,35
s	620	620	600	590	0,34
m	645*		675*		0,33
w	780	765	715	700	0,12
w			800	760	0,32; 0,34 + Lattice
vw	950	935	920	895*	0,2 x 13
w		970		930	0, 13 + 33
w	1010	1005	970	970	0,11; 0,13 + 35
vw	1080	1075			0,32
w	1105	1100	1050	1050*	0,13 + 3
w	1160	1160			0,31
m	1185	1170			0,0
m	1210	1205	1150	1150*	0,3
m	1235*	1245*	1185*	1170	0,12 + 13
		1245*		1170	0,12 + 33
m; 3(-D_1)	1280	1290	1220	1220*	0,13 + 3[illegible]
w; m(-D_5, -D_6)	1315*	1325*	1265	1280	0,2[illegible]
w; m(-D_5) -D_6	1410	1395	1315	1300	0,12 + 3[illegible]

TABLE 4.3 (CONTINUED)

Intensity[a]	Position from the 0,0 band[b] (cm^{-1})				Assignment[c]
	$-H_6$	$-D_1$	$-D_5$	$-D_6$	
		1395			0,2 x 13 + 33
w($-D_5$);s($-D_6$)			1375*	1410*	0,2 x 12
w	1465*	1465*			0,2 x 13 + 35
m; s($-D_6$)	1490	1475	1420*	1410*	0,11 + 13
m($-D_1$);s($-D_6$)		1490		1445	0,11 + 33
s	1525		1465	1465	0,11 + 35
m	1535	1525			0,2 x 12
s		1535			0,11 + 35
vw($-H_6$);m($-D_1$)	1585	1560*			0,2 x 13 + 34
vw($-H_6$);m($-D_1$)	1615*	1605			0,6
s	1630	1640	1570	1560	0,11 + 34
w	1650*				0,11 + 33
m; w($-H_6$)	1675	1650	1605*	1620*	0,8 + 13
m($-D_1$); s($-D_6$)		1685*		1620*	0,8 + 33
m; s($-D_5$)	1720	1720	1640	1655*	0,8 + 35
m; w($-H_6$)	1755*	1755	1675*	1655*	0,11 + 12
m	1755*		1675*	1655*	0,12 + 13 + 35
w	1810*	1800*			0,? + 34
w	1845*				0,8 + 33
m; w($-H_6$)	1880*	1880	1770*	1755*	0,12 + 13 + 34
w		1825			0,8 + 33
w		1925*			0,11 + ? + 13
vw; w($-D_5$); m($-D_6$)	1980	1970	1860	1825	0,8 + 12
w($-D_6$)			1860	1895	0,2 x 12 + 35

TABLE 4.3 (CONTINUED)

Intensity[a]	-H6	Position from the 0,0 band[b] (cm^{-1}) -D1	-D5	-D6	Assignment[c]
w; m(-D6)	1980	2015	1920	1965	0,12 + 13 + 35
w; m(-D6)	2005	2015	1920	1965	0,2 x 11
w		2035*			0,2 x 12 + 33
w(-H6); m (-D1)	2050*	2060*			0,2 x 12 + 35
w	2140*	2135*	1975	1995*s	0, 2 x 12 + 34
w			2065*		0,2 x 13 + 8
w	2170*	2150*			0,9 + 11
w; m(-D1)	2170*	2180*	2090*	2100*	0,8 + 13 + 35
m; w(-D6)	2205	2215	2120	2100*	0,8 + 11
w; m(-D1,-D5)	2230*	2240*	2155*	2100*	0,11 + 12 + 13
m(-D1); w(-D6)		2240*		2145*	0,11 + 12 + 33
w; m(-D5,-D6	2205	2280	2180	2190	0,11 + 12 + 35
w	2285	2280	2225*	2225*	0,8 + 13 + 34
vw	2350*	2360*			0,8 + 31
w	2370*	2360*			0,8 + 9
w; m(-D5,-D6)	2405	2390	2280	2265	0,11 + 12 + 34
w; m(-D1,-D5)	2405	2390	2300*	2290*	0,2 x 8
m		2470			0,2 x 11 + 33
w	2480	2490	2380*	2355*	0,8 + 12 + 35
m	2535	2535			0,2 x 11 + 35
w; m(-D5)	2545*		2400	2355*	0,11 + 2 x 1[illegible]
m				2390	0,2 x 11 + 13; 0,2 x 11 + 33
vw	2590*				0,11 + 2 x 13 + 35
m			2445	2410	0,2 x 11 + 35

TABLE 4.3 (CONTINUED)

Intensity[a]	-H_6	Position from the 0,0 band[b] (cm^{-1}) -D_1	-D_5	-D_6	Assignment[c]
m; w(-H_6)	2625*	2590	2445	2460	0,8 + 12 + 34
m(-D_5);w(-D_6)			2490*	2465*	0,11 + 2 x 13 + 34
m	2645	2645	2510	2510	0,2 x 11 + 34
m; w(-H_6)	2675*	2665	2590*	2535*	0,8 + 11 + 13
m		2700		2590	0,8 + 11 + 33
m	2720	2730	2610	2620*	0,8 + 11 + 35
m; w(-D_5)	2765	2750	2655*	2620*	0,2 x 11 + 12
m; w(-D_1,-D_5)	2765	2775	2655*	2710	0,11 + 12 + 13 + 35
w	2815*	2805*			0,9 + 11 + 34
m	2825	2825	2720	2710	0,8 + 11 + 34
m(-D_1);w(-D_6)		2870		2740*	0,2 x 8 + 33
m; w(-D_6)	2850*	2870	2775	2740*	0,2 x 8 + 13
m; w(-D_6)	2915*	2910*	2775	2785	0,2 x 8 + 35
w; m(-D_5)	2955*	2955*	2815	2830	0,8 + 11 + 12; 0,8 + 12 + 13 + 35
w(H_6);m(-D_1)	3010	3020			0,3 x 11
m	3030				0,8 + 9 + 34
m	3060	3060	2860	2860	0,2 x 8 + 34
w			2905*	2905	0,3 x 11
w; vw(-D_1)	3145*	3145	2990	2945*	0,11 + 2 x 12 + 34
w; m(-D_1)	3210	3210	3030*	3065	0,8 + 2 x 11
w; m(-D_6)	3290	3240	3125	3140	0,8 + 11 + 13 + 34
w; m(-D_6)	3290	3306	3125	3140	0,2 x 11 + 13 + 35
w; m(-D_6)	3335*	3300	3125	3140	0,8 + 2 x 13 + 34
w; m(-D_5, -D_6)	3405	3395*	3235	3235	0,2 x 8 + 11

TABLE 4.3 (CONTINUED)

Intensity[a]	$-H_6$	Position from the 0,0 band[b] (cm^{-1}) $-D_1$	$-D_5$	$-D_6$	Assignment[c]
			3360*		0,2 x 8 + 13 + 34; 0,2 x 11 + 2 x 12
m($-D_1$);w($-D_6$)		3490		3370*	0,3 x 11 + 33
m; w($-H_6$)	3526	3530	3400	3420	0,3 x 11 + 35
m; w($-H_6$)	3600	3580	3430	3455	0,3 x 8; 0,8 + 11 + 12 + 34
m	3650	3630	3455	3455	0,3 x 11 + 34
m		3660		3535	0,3 + 2 x 11 + 33
m($-H_6$);w($-D_1$)	3765	3775*			0,3 x 11 + 12; 0,2 x 11 + 12 + 13 + 35
m	3835	3835	3660	3650	0,8 + 2 x 11 + 34
m		3845*			0,2 x 8 + 11 + 13
w		3905*		3720*	0,2 x 8 + 11 + 33
m; w($-D_1$, $-D_6$)	3915*	3945*	3700	3760	0,2 x 8 + 11 + 35
w	3955*		3740*		0,8 + 2 x 11 + 12; 0,8 + 11 + 12 + 13 + 35
w	4035	4005*	3845	3835	0,4 x 11
m; w($-D_5$, $-D_6$)	4065	4065	3845	3835	0,2 x 8 + 11 + 34
m		4095			0,3 x 8 + 33
w	4115*	4145	3925*	3965	0,3 x 8 + 35
w; vw($-H_6$)	4200	4220	3985	4055	0,8 + 3 x 11
w	4250	4250	3985	4055	0,3 x 8 + 34
w	4340		4095		0,8 + 11 + 2 x 12 + 34
vw	4405				0,2 x 8 + 2 x 11
w			4195	4165	0,2 x 8 + 11 + 13 + 35

TABLE 4.3 (CONTINUED)

Intensity[a]	Position from the 0,0 band (cm^{-1}) $-H_6$	$-D_1$	$-D_5$	$-D_6$	Assignment[c]
vw				4225	0,8 + 2 x 11 + 12 + 33
w; vw($-D_5$)	4485		4295	4265	0,8 + 2 x 11 + 35
vw		4475			0,4 x 11 + 33
w; vw($-D_1$)	4525	4475	4390	4360	0,4 x 11 + 35
w; vw($-D_1$)	4605	4600	4490	4420	0,4 x 11 + 34
w; vw($-D_1$)	4755	4675	4655	4490	0,8 + 3 x 11 + 35
vw				4595	0,4 x 8
w; vw($-D_1$)	4845	4820			0,8 + 3 x 11 + 34
vw($-D_1$); w($-D_6$)		4875		4700	0,2 x 8 + 2 x 11 + 33
w; vw($-D_1$)	4970	4960	4740	4700	0,2 x 8 + 2 x 11 + 35
w; vw($-D_1$)	5060	5050	4835	4790	0,2 x 8 + 2 x 11 + 34
vw				4875	0,3 x 8 + 11 + 33
w; vw($-D_1$, $-D_6$)	5165	5130	4910	4875	0,3 x 8 + 11 + 35
w; vw($-D_1$, $-D_6$)	5260	5255	5015	5025	0,3 x 8 + 11 + 34
vw			5110	5120	0,4 x 8 + 35
vw	5485	5440	5210	5200	0,4 x 8 + 34
vw			5325	5325	0,5 x 11 + 35
vw	5635	5620	5470		0,5 x 11 + 34
vw				5515	0,16 + 4 x 11 + 35
vw			5670	5635	0,8 + 4 x 11 + 34
vw				5750	0,5 x 8

* Denotes shoulder

a. Uncorrected for instrumental response; s = strong, m = medium, w = weak, v = very

b. Error of about $\pm$ 10cm^{-1} or less

c. Numbering of the normal modes follows Herzberg from Ref. 10.

5, found at 510 cm^{-1} and 620 cm^{-1}, respectively. The 0,33 transition, band 6, appears as a shoulder at 645 cm^{-1}. This band is best seen in $-D_1$ and $-D_6$, where its frequency is much smaller. Zhuravleva reported the band at 510 cm^{-1} but did not designate it as an in-plane deformation of the triple bond.

The 620 cm^{-1} band was interpreted as in this work, i.e. as of e_{2g} (606 cm^{-1}) parentage in benzene. This vibration removes the forbiddeness of the benzene $S_0 - S_1$ transition. The band at 645 cm^{-1} was not previously reported.

Bands 7 and 9, weak bands at 780 cm^{-1} and 1010 cm^{-1}, are assigned as due to two fundamentals, a totally-symmetric substituent sensitive skeleton deformation 0,12(a_1) and the ring breathing mode 0,11(a_1). The ring breathing mode is prominent in the fluorescence of benzene, where it appears in progressions built on one quantum of the 606 cm^{-1}, and in substituted benzenes such as toluene, benzonitrile and phenylisocyanide.

In the region between 1000 cm^{-1} and 1600 cm^{-1} six more fundamentals are assigned. The very weak band 10 at 1080 cm^{-1} is due to 0,32(b_2). Any progressions based on one quantum of this fundamental are masked by the more intense bands. This also holds for the weak shoulders, band 12 at 1160 cm^{-1}, which is assigned to 0,31(b_2) and band 17, at 1315 cm^{-1}, assigned to 0,29(b_2). The bands 13 and 14 at 1185 cm^{-1} and 1210 cm^{-1} are interpreted as the C - H in-plane

deformation $\nu_9(a_1)$ and the totally symmetric stretching between the ring and the substituent $\nu_8(a_1)$. Zhuravleva reported bands at 1190 cm^{-1} in both the fluorescence and phosphorescence spectra. This analysis of the fluorescence spectrum assigns this band to 0,8.

This is supported by deuterium shifts (see below) and by the assignments in benzonitrile. A very weak shoulder, band 24, appears at 1615 cm^{-1} and is assigned to 0,6 one component of the degenerate e_{2g} 1585 cm^{-1} mode in benzene. Zhuravleva assigned fundamentals at 1390 cm^{-1} and 1490 cm^{-1}. These are most likely band 18, at 1410 and band 20, at 1490 cm^{-1}, in this study. If the frequencies of the fundamentals listed by King and So[10, 12] are correct, then this earlier assignment is incorrect.

The remainder of the spectrum is assigned up to 5635 cm^{-1}. (Zhuravleva recorded the spectrum to 3040 cm^{-1}). The prominent progressions are based on progressions of ν_{11} built on one quantum of a b_2 vibration, i.e., 0, nx11 + 35, and 0, nx11 + 34 for n running from one to five. In Figure 4.2 these are bands 21, 46, 67, 82 and 25, 50, 69, 83, 91. The other long series is multiples of ν_8, based on the same false origins, i.e. 0, nx8 + 35 and 0, nx8 + 34, where n is one to four. These are bands 28, 57, 77 and 31, 61, 79, 90. Bands based on combinations of ν_8 and ν_{11} with themselves and on one quantum of ν_{34} or ν_{35} (0, nx8 + mx11; 0, nx8 + mx11 + 34; and 0, nx8 + mx11 + 35) make up most of the spectrum.

(b) Phenylacetylene-D_1

When the acetylenic hydrogen is replaced by deuterium the position of the 0, 0 band of the fluorescence is blue shifted only slightly, by 10 cm^{-1} in MC (Figure 4.3). This is comparable to the vapor absorption results of 13 cm^{-1}. No observable shift was seen in IP. The vibrational analysis of $-D_1$ (Table 4.3) is essentially the same as $-H_6$. The same six a_1 fundamentals appear at bands 3, 7, 10, 14, 15, 26, at 470 cm^{-1}, 765 cm^{-1}, 1005 cm^{-1}, 1170 cm^{-1}, 1205 cm^{-1}, 1605 cm^{-1}. These are the 0,13, 0,12, 0,11, 0,9, 0,8, 0,6 transitions. The b_2 fundamentals, ν_{35}, ν_{34}, ν_{33}, ν_{32}, ν_{31}, ν_{29} appear as bands 5, 6, 4, 11, 13, 18 at 535, 620, 485, 1075, 1160, 1325 cm^{-1}, respectively.

As in $-H_6$ the strongest bands are the 0,35 and 0,34 transitions and these act as false origins. The main difference between the fluorescence spectra of $-H_6$ and $-D_1$ is that now an extra well-resolved band is seen at 485 cm^{-1} which is assigned as 0,33. (This band was a shoulder in $-H_6$). The presence of this band in the spectrum results in the resolved false origins. This is seen in $-D_6$ also. Several additional bands can now be identified in the spectrum, due to progressions and combinations based on one quantum of ν_{33} (0, nx8 + 33 with n ranging from one to three, and 0, nx11 + 33 with n from one to four). Since the other fundamentals assigned in $-H_6$ are

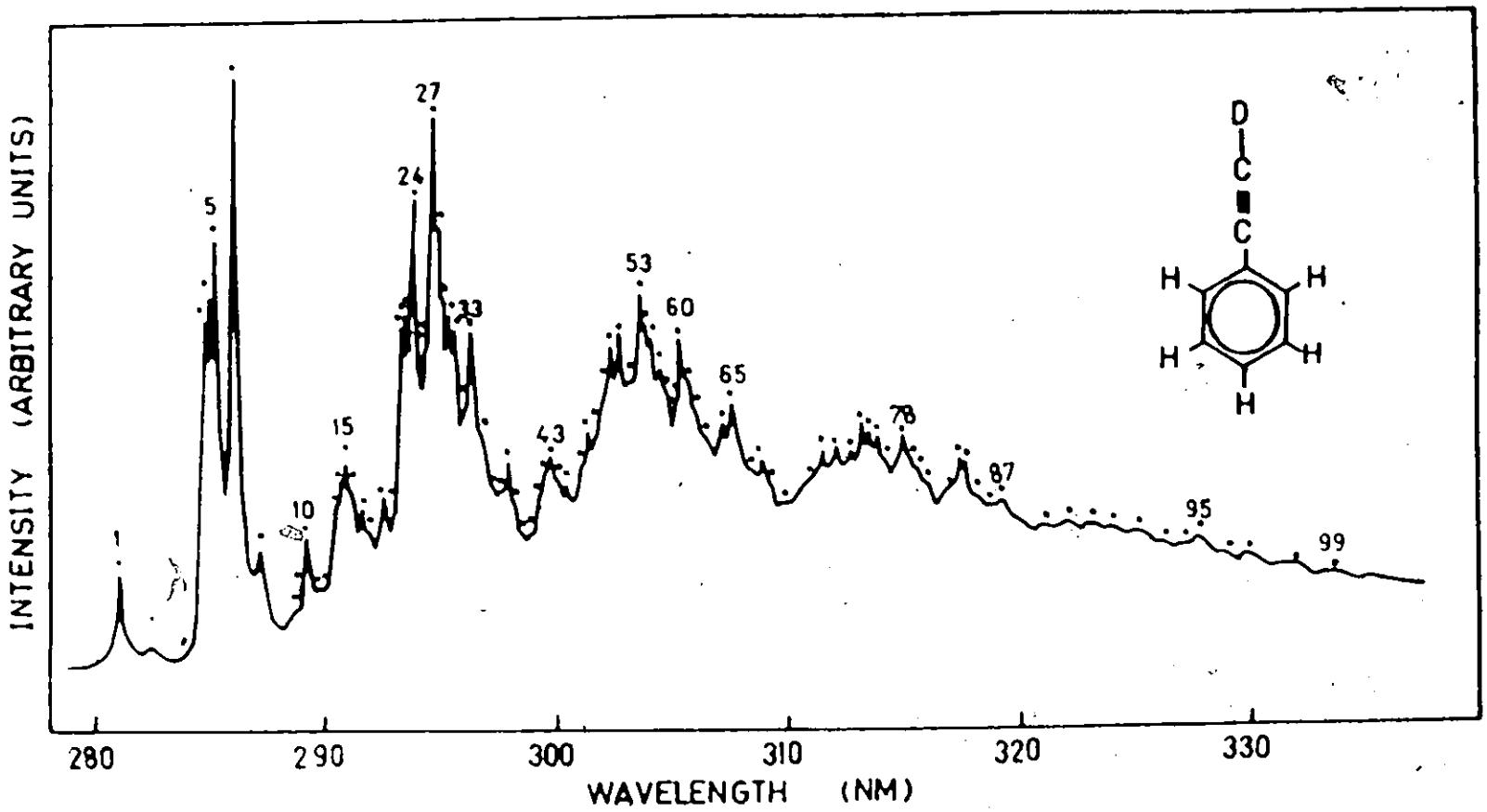

FIG. 4-3 THE FLUORESCENCE SPECTRUM OF 10^{-4}M PHENYLACETYLENE-D_1 IN POLYCRYSTALLINE METHYLCYCLOHEXANE AT 77 °K

not very sensitive to the deuteration of the acetylenic group very many bands in $-D_1$ have nearly identical positions as in $-H_6$. Progressions and combinations in ν_{11} and ν_8, built on one quantum of a non-totally symmetric vibration form the dominant part of the spectrum.

(c) Phenylacetylene - D_5

Ring deuteration has a much greater effect than acetylenic deuteration in changing the position of the 0, 0 band. In Table 4.3 the 0, 0 is now 35690 cm^{-1}, blue shifted by 140 cm^{-1} in comparison to $-H_6$. Absorption measurements[10] show a similar shift of 155 cm^{-1}. In LP the 0, 0 band is at 35670 cm^{-1}, i.e. not very much different from that in MC. The general appearance of the spectrum, shown in Figure 4.4, is very similar to that for $-H_6$, though not as sharp. Again, the two false origins 0,35 and 0,34 are strong bands, 4 and 5, at 505 cm^{-1} and 600 cm^{-1}. Transitions due to other b_2 fundamentals 0,33, 0,32, 0,29 found are bands 6, 8, 15, at 675, 800, 1265 cm^{-1}. In this spectrum and that of $-D_6$ the 0,31 transition does not appear. The transitions 0,33 and 0,29 are sensitive to ring deuteration. The weak band 8 at 800 cm^{-1}, assigned as 0,32, seems to follow the shape of band 2, the lattice vibration at 165 cm^{-1}. This is also seen with band 8 at 760 cm^{-1} in $-D_6$. Therefore the alternative assignment, of 0,33 coupled to a lattice mode is equally possible. The frequency of this band is slightly too

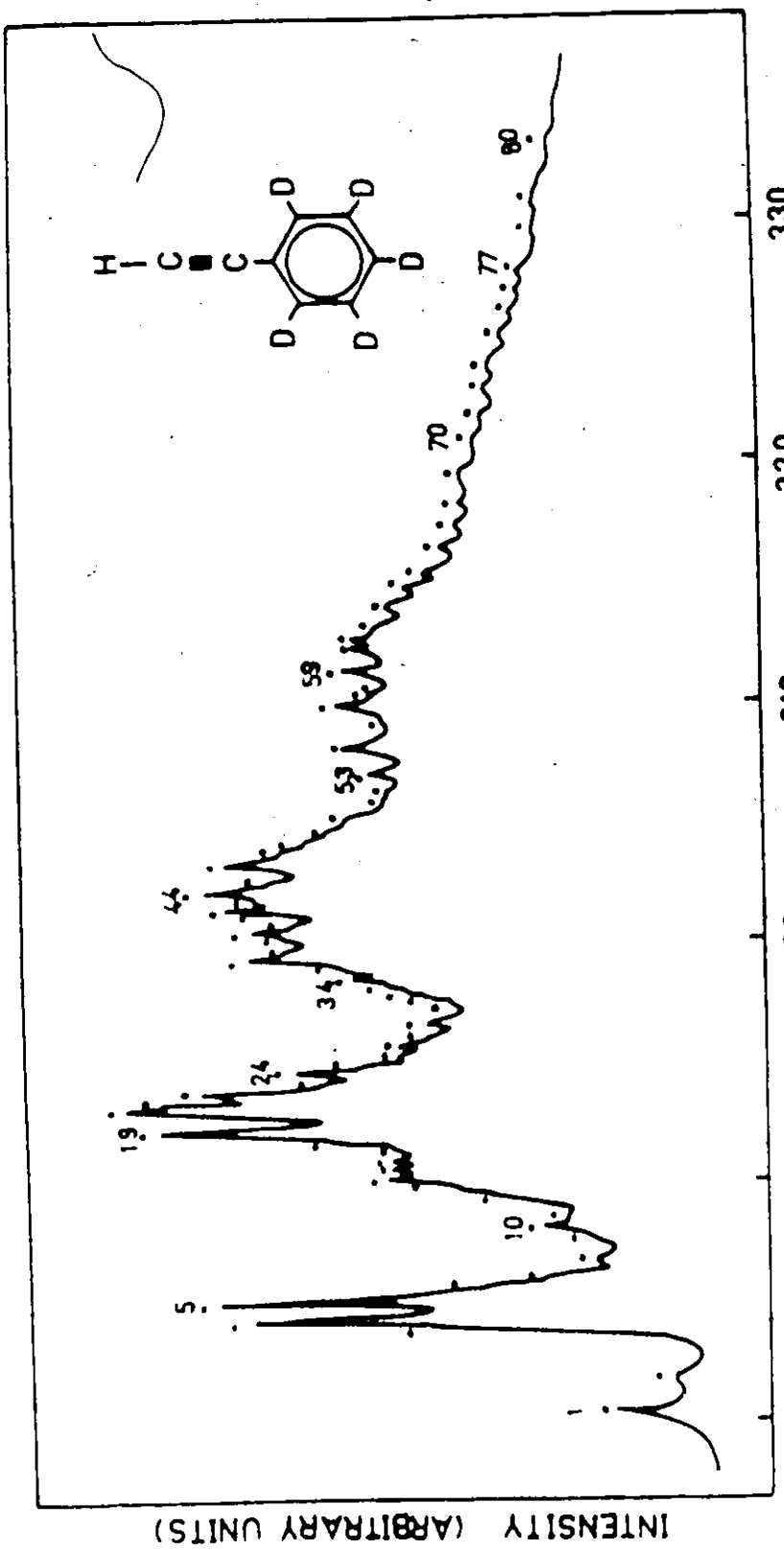

FIG. 4.4 THE FLUORESCENCE SPECTRUM OF 10^{-4}M PHENYLACETYLENE-D_6 IN POLYCRYSTALLINE METHYLCYCLOHEXANE AT 77 °K

low for the former and slightly too large for the latter assignment. The transitions 0,12, 0,11 and 0,8 are sensitive to ring deuteration and the assignments for bands 7, 10, and 12 at 715, 970 and 1150 cm^{-1} are consistent with the expected shifts. Both the 0,9 and the 0,6 transitions are absent in $-D_5$ and $-D_6$. If band 14 in $-H_6$ were assigned as 0,9 rather than 0,8, then a very large shift, of about 300 cm^{-1}, would be expected in the position of the band in going to $-D_5$. Because of the similarity of the spectra of $-H_6$ and $-D_5$, band 12 in $-D_5$ is associated with band 14 in $-h_6$. The small deuterium shift observed fits a 0,8 assignment. Again, the most prominent progressions are in ν_{11} (up to five quanta) and ν_8 (up to four quanta), based on one quantum of ν_{35} or ν_{34}

(d) Phenylacetylene -D6

The 0, 0 band of the fluorescence spectrum of completely deuterated phenylacetylene is at 35690 cm^{-1} (Table 4.3) in both MC and IP. The basic spectrum (Figure 4.5) remains the same as for all the phenylacetylenes. The a_1 fundamentals appear bands 3, 7, 11, 13, at 455, 700, 900, 1150 cm^{-1} which correspond to 0,13, 0,12, 0,11, 0,8. The b_2 fundamentals are bands 5, 6, 4, 8, 16 at 515, 590, 480, 760, 1280 cm^{-1} which correspond to 0,35, 0,34, 0,33, 0,32, 0,27. Again, ν_{35} and ν_{34} act as false origins with up to five quanta of ν_{11} and four quanta of ν_8.

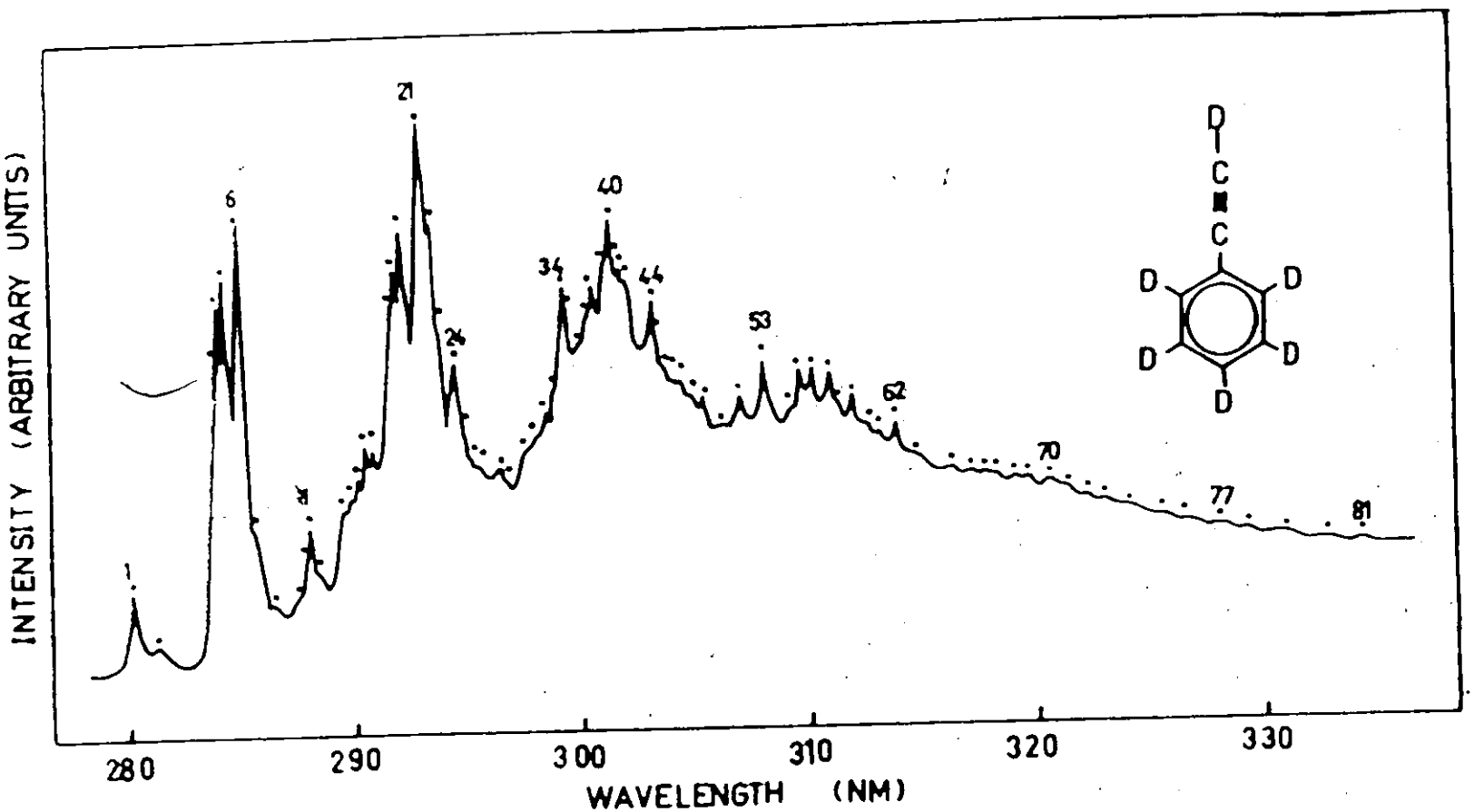

FIG. 4.5 THE FLUORESCENCE SPECTRUM OF 10^{-4}M PHENYLACETYLENE-D_6 IN POLYCRYSTALLINE METHYLCYCLOHEXANE AT 77 °K

As in $-D_1$, the third strong false origin, band 4, is resolved. Consequently, progressions based on one quantum of ν_{33} can be identified with up to three quanta of ν_{11} and two quanta of ν_8. Otherwise the spectrum and assignments follow those of $-D_5$ very closely. Like the spectrum of $-D_5$, that of $-D_6$ is not as sharp as those of $-D_6$ and $-D_1$.

4.4. Discussion of the Fluorescence of Phenylacetylene

The vibrational analyses the fluorescence spectra are very similar for all four phenylacetylenes. The majority of bands arise from a large forbidden component of the fluorescence spectrum. The false origins are formed by one quantum of a non-totally symmetric b_2 fundamental and account for about 95% of the spectral intensity in phenylacetylene-H_6.

The vibrational analyses are consistent with both combining states having C_{2v} symmetry. In absorption, the $S_o \rightarrow S_1$ ($^1A_1 \rightarrow {}^1B_2$ in C_{2v}) transition is short axis in-plane (y) polarized; the $S_o \rightarrow S_2$ ($^1A_1 \rightarrow {}^1A_1$ in C_{2v}) transition is long axis in-plane (z) polarized. The b_2 vibrations coupled to the electronic transition mix in a large amount of the long axis in-plane transition.

It is interesting to compare the $S_o \rightarrow S_1$ transition of phenylacetylene with those of benzonitrile (C_6H_5CN) and phenylisocyanide (C_6H_5NC) since these three molecules form an isoelectronic series. It is found that the spectra of phenylacetylene and phenylisocyanide are essentially very similar, while that of benzonitrile is different. The near-ultraviolet absorption spectra of these molecules are very similar to the fluorescence spectra observed in the present work for phenylacetylene, and for phenylisocyanide[47, 48] and benzonitrile[59, 60]. In phenylacetylene the 0, 0 band of the $S_o \rightarrow S_1$ transition is weak

and most of the spectral intensity involves non-totally symmetric vibrations. Benzonitrile, however, has a strong 0, 0 band and most of the spectral intensity is due to totally symmetric vibrations. In the absorption spectrum of phenylacetylene[10] the ratio of forbidden to allowed components in the $S_0 \rightarrow S_1$ absorption is about three to one. In the fluorescence this ratio is even higher.

The amount of forbidden component in the fluorescence spectra is ~95% for C_6H_5CCH, ~90% C_6H_5C[57] and less than 10% for C_6H_5CN[59]. These observations are correlated below by various approaches.

The mixing coefficients in equation 2.7 are given by:

$$C_{mk} = \sum \frac{\langle \psi_n^0 | \frac{\partial}{\partial Q_i} | \psi_m^0 \rangle}{E_m^0 - E_n^0} Q_i \qquad (2-1)$$

Hence the forbidden component is inversely proportional to the energy difference between the perturbing states m and n. If this difference is less than 1e.v. the forbidden component may have comparable or even larger spectral intensity than the allowed component.[61] In phenylacetylene the energy difference between the first excited singlet state $S_1(^1B_2)$ and the second excited singlet state $S_2(^1A_1)$ is 0.37 ev[10]. This is consistent with large amount of forbidden component in the absorption and emission spectra. Similarly, the energy difference in benzonitrile this value is 0.83 ev[7]. For benzonitrile this value is

forbidden component is very weak. Thus there is a good correlation between the amount of forbidden intensity and the inverse of the energy gap between the perturbing states.

From equation 4.1, the amount of mixing between the two states m and k depends linearly on the perturbation matrix element $\langle \psi_k^o | \frac{\partial H}{\partial Q} | \psi_m \rangle$. In a detailed treatment, Albrecht[63] correlated the magnitude of the perturbation matrix element with the nature of the electronic wavefunctions within the Herzberg-Teller framework for substituted benzenes. His approach led to the conclusion that the matrix element is large when both of the states, m and k, are largely non-charge-transfer in character. If either one of the states is entirely a charge-transfer type state while the other has no charge-transfer character the matrix element is small and little forbidden intensity is seen. No simple predictions can be made when both states are charge-transfer. A tentative conclusion based on the amount of forbidden character observed is that both the S_1 and S_2 states have little or no charge-transfer in phenylacetylene.

It was found[62] that the change in dipole moment $\Delta\mu$ upon excitation is a sensitive measure of the effect of the substituent on the benzene π system. It is a direct measure of the extent of intramolecular charge transfer occurring on excitation, and depends almost entirely on the π electron distribution in the molecule. The values of $\Delta\mu$ for phenylacetylene

and phenylisocyanide, each with 25% allowed character, are 0.14D and 0.13D respectively compared with 0.31D for benzonitrile which has 80% allowed character in the absorption spectrum. These authors concluded that the change in dipole moment is directly proportional to the percentage of allowed character in the vibronic transitions. Their results are consistent with the treatment of Albrecht[63], on the assumption that the perturbing $^1A_1$ does not have large amounts of charge-transfer character and does not vary from compound to compound. For phenylacetylene and phenylisocyanide the amount of charge-transfer in the $^1B_2$ state is small, whereas it is large in benzonitrile.

Brand and Knight[64] have estimated charge-transfer in substituted benzenes in terms of changes in the moments of inertia. From their measurements of the $^1A_1 \rightarrow {}^1B_2$ transition of benzonitrile, they suggest that the B_2 state has charge-transfer from the ring to the -CN group. The charge-transfer component partially transfers a mildly antibonding aromatic electron to a strongly antibonding orbital of the -CN group. This same argument could be used for the -CCH and -NC group. Recently, King and van Putten[65] examined the $^1A_1 \rightarrow {}^1B_2$ transition for benzonitrile and phenylacetylene by looking in detail at the molecular orbitals involved in the charge-transfer between ring and substituent. They confirmed that the -CN substituent has a large perturbing influence on the benzene ring while the -CCH substituent does not.

Microwave studies by Diel et al[6] had established that the ground singlet state of phenylacetylene is planar, probably

with a regular hexagon ring. An analysis of the Franck-Condon envelope of the flourescence spectrum of phenylacetylene yields some information about the geometry of the first excited singlet state. According to the Franck-Condon principle (Section 2.5), if the geometry of the first excited singlet state is significantly different from the ground state, long progressions in those normal modes converting one state into the other are expected in the spectrum. From the vibrational analyses, given in Section 4.2, the absence of prominent progressions in out-of-plane fundamentals rules out major deviations from a planar excited singlet state. The only moderately long progressions are in totally symmetric modes of ring breathing and ring-acetylenic group stretch. The first of these suggests either a slightly expanded or a slightly contracted ring which is still a regular hexagon.

The sharpness of the spectra achieved in the present study does not warrant reduced intensity measurement on the progressions, as has been done for toluene by Nieman[17] who found a 0.037Å increase for the average C - C bond distances in the ring for the first excited state compared to the ground state. (The sharpness achieved in the present study was limited by the temperature broadening, and not by instrumental resolution; hence a study at a lower temperature, say 4°K, may yield the required information). From a rotational band contour analysis in the neighborhood of the $S_o \rightarrow S_1$ absorption origin, King and So[10,11] suggest that the ring is expanded in the first excited state by 0.032Å for the average C - C bond distance. The results pre-

sented here are consistent with that study. The other progression, in ν_8, suggests that the ring-substituent group C - C distance is slightly changed upon electronic excitation. This qualitative observation fits well with the estimated changes from band contour studies.[10, 11]

4.5 Vibrational Analyses of Phosphorescence Spectra

The phosphorescence spectra of the phenylacetylenes were studied in polycrystalline matrices (Ir and MC) and in rigid glasses (EPA and 3MP). Again, the overall appearance of the spectra were the same in all four solvents for concentrations of 10^{-3}M or less of solute. The spectra were sharpest in the polycrystalline matrices. The sharpest spectra was obtained in MC, where the half-bandwidth of the 0, 0 of the phosphorescence was about 25 cm^{-1}. The phosphorescence was a blue long-lived emission (with lifetime about 2s) occuring in the region between 390 nm and 550 nm. All four phenylacetylenes exhibited very strong 0, 0 bands of phosphorescence, indicating the orbital allowedness of the triplet-singlet transition. The 0, 0 energy gap was slightly blue-shifted with deuterium substitution. The assignments given in the vibrational analyses are consistent with all four of the phenylacetylene spectra, although alternate assignments are possible for some bands only those which are common features are given. Overall, the phosphorescence spectrum of phenylacetylene -H_6 was the sharpest of the four. The sharpness of the spectra decreased with increasing deuteration.

(a) Phenylacetylene-H_6

The strong 0, 0 band was at 25230 cm^{-1} in 3MP, 25285 cm^{-1}

in EPA, 25320 cm^{-1} in MC, and 25240 cm^{-1} in IP. The values are in good agreement with that previously reported[3], 25213 cm^{-1} in IP.

The assignment of the 0, 0 band of the phosphorescence supported by Evans[13] who reported a value of 25100 cm^{-1} for the 0, 0 band of the $S_0 \rightarrow T_1$ oxygen enhanced absorption spectrum of phenylacetylene-h_8 in chloroform. (Phenylacetylene in this solvent yielded a broad, almost structureless, $T_1 \rightarrow S_0$ emission spectrum; hence it was not possible to confirm that the 0, 0 of the $S_0 \rightarrow T_1$ absorption and emission overlapped).

This study, which was carried out for $\Delta\nu$ up to 3000 cm^{-1}, is more detailed than that of Shuravleva[3]. Table 4.4 contains the analysis of the MC spectrum shown in Figure 4.6. Here the spectrum is rich in vibrational structure about 15 fundamentals are observed.

A shoulder, observed at 55 cm^{-1} to the red of the 0, 0, is assigned to a lattice mode. This mode does not appear to be coupled with any of the vibrations seen in the spectrum. Furthermore, the intensity of this mode did not vary from sample to sample and was independent of the method of cooling. From these observations emission from more than one site can be ruled out.

Most of the spectral intensity is due to the appearance of a_1 fundamentals, which appear in the region between 0 and 2130 cm^{-1}. Fundamentals of a_2, b_1 and b_2 symmetry also appear,

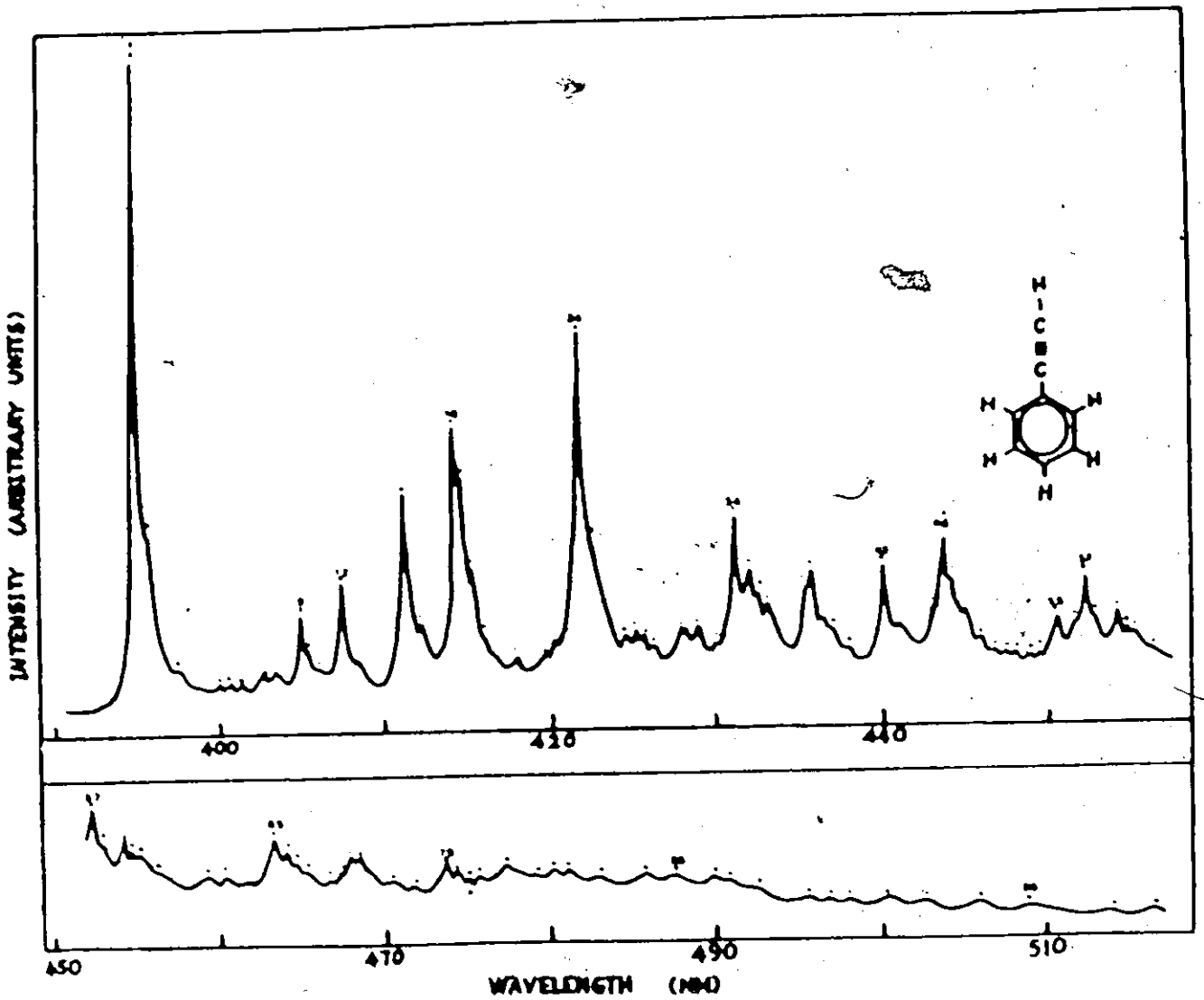

FIG.4.6 THE PHOSPHORESCENCE SPECTRUM OF 10^{-3}M PHENYLACETYLENE-H_6 IN POLYCRYSTALLINE METHYLCYCLOHEXANE AT 77°K

TABLE 4.4

VIBRATIONAL ANALYSES OF THE PHOSPHORESCENCE SPECTRA OF 10^{-3}M PHENYLACETYLENE-H_6, & 10^{-4}M PHENYLACETYLENE-D_1, $-D_5$, $-D_6$, IN POLYCRYSTALLINE METHYLCYCLOHEXANE AT 77°K

Intensity[a]	Position from the 0,0 band[b] (cm^{-1})				Assignment
	$-H_6$	$-D_1$	$-D_5$	$-D_6$	
m	55*	45[sh]			0, Lattice
w	165	150	160*	135*	0,24
w; vw($-H_6$)	330	305	315	30[illegible]	0,2 x 24
w	350	330	31[illegible]	30[illegible]	0,30; 0,23
vw	400	390	345*		0,16
w	475	455[sh]	470*	460*	0,13
w		495			0,21; 0,33
w	530	530	470*	460*	0,23
w		560[sh]	515		0,16 + 24
w	625			495	0,21
w	655*			495	0,33
vw; w($-D_6$)	685	695	660	630*	0,20
w			625		0,21
w			655*		0,33
w				64[illegible]	0,21 + 24
w	775	760	720	720	0,1[illegible]
w			790*		0,21 + 24
m			875	870	0,9
w	855*	840*			0,15
m		970*			0,2 + 53; 0,2 x 21

Intensity[a]	Position from the 0,0 band[b] (cm^{-1})				Assignment
	$-H_6$	$-D_1$	$-D_2$	$-D_6$	
m	1000	1000	955	950	0,11
w		1025*			0,10
w	1065	1070*			0,32
m	1185	1175			0,9
m; w($-D_5$, $-D_6$)	1205*	1195*	1155	1145	0,8
m	1240		1240		0,2 x 21
w		1240*		1180	0,13 + 21
w	1280*	1275*			0,30
vw			1320		0,9 + 13
vw	1310*		1320		0,2 x 33
w; vw($-D_5$)	1305		1320		0,13 + 21
w		1445		1390	0,13 + 20
w	1470	1490	1385	1385	0, 7
w	1535	1515	1445	1450	0,2 x 13
w			1500		0,9 + 21
m	1605	1600	1575	1575	0,6
m		1645*			0,9 + 21; 0,9 + 33
m	1645*	1645*			0,9 + 13
m			1630*	1635*	0,9 + 30
w	1775	1760	1675*	1690*	0,11 + 12
w	1800				0,9 + 21
w	1825				0,9 + 33
w			1750	1740	0,2 x 7
w			1830	1830	0,9 + 11
w; vw($-D_5$)	1855	1845			0,9 + 20

TABLE 4.4 (CONTINUED)

Intensity[a]	Position from the 0,0 band[b] (cm^{-1})				Assignment
	$-H_6$	$-D_1$	$-D_5$	$-D_6$	
w	1955	1930			0,9 + 12
w	1975*		1860		0,8 + 12
w; m($-D_1$)	2010	2005	1910	1920	0,2 x 11
w			2045*	1985*	0, 8 + ?
m		2005		2010	0,5
vw; w($-D_5$, $-D_6$)	2085	2055	2045*	2045*	0,6 + 13
w		2090		2045*	0,6 + 21
w; m ($-H_6$)	2120	2135	2045*	2045*	0,6 + 2?
m	2120		2125		0,5
w	2180	2170			0,9 + 11
w		2195*			0,9 + 10
w; m($-D_5$)	2210	2195*	2125	2095*	0,8 + 11
w	2235	2230*			0,9 + 32
w	2235		2195		0,6 + 21
w	2360*	2355			0,2 x 9
vw				2365	0,2 x 9 + 20
w	2380	2355	2295	2295	0,6 + 12
w	2415*	2390*			0,? + 9
vw			2330*		0,2 x 9 + 20
vw			2330*	2330*	0,7 + 9
w	2445*	2435			0,6 + 13
w			2440	2440	0,6 + 9
w	2485	2480			0,7 + 11
w		2570*			0,6 + 2 x 21; 0,6 + 2 x 33

TABLE 4.4 (CONTINUED)

Intensity[a]	Position from the 0,0 band[b] (cm^{-1}) -H6	-D_1	-D_5	-D_6	Assignment
w	2605	2600	2545	2495	0,6 + 11
w; m(-D6)			2545	2535	0,9 + 11 + 12
w	2660	2650*			0,6 + 32
w	2760*	2680*	2590*	2600*	0,3 x 11 + 12
w	2780	2775			0,6 + 9
w	2810*	2800*	2720	2705	0,6 + 8
w			2720	2705	0,3 x 9 + 11
w	2850				0,6 + 9 x 21
w	2895				0,6 + 3 x 33
w		2835*			0,3 x 9 + 21; 0,3 x 9 + 33
w			2740*	2750	0, 9 + 2 x 11
w				2750	0,6 + 12 + 21
w			2825		0,6 + 9 x 21
vw; w(-D_1)	2945	2950			0,9 + 11 + 12
vw; w(-D_1)	2990	2950			0,3 x 9 + 21
w; vw(-H6)	2990	2995	2865*	2870	0,3 x 11
vw	3010		2905*		0,6 + 12 + 21
vw	3010				0,3 x 9 + 33
vw			2905*		0,6 + 9 + 13
vw	3050		3065		0,3 x 9 + 21
w; vw(-H_6)	3085	3110	2960*	2955	0,6 + 7
w	3135	3110	3000	3015*	0,6 + 3 x 12
w		3155*	3000		0,5 + 9
w	3185*	3175			0,9 + 3 x 11

TABLE 4.4 (CONTINUED)

Intensity[a]	Position from the 0,0 band[b] (cm^{-1})				Assignment
	$-H_6$	$-D_1$	$-D_5$	$-D_6$	
w; m($-D_5$, $-D_6$)	3215	3190	3150	3140	0,2 x 6
w	3235*	3220*			0,6 + 9 + 13
w	3315				0,5 + 9
w		3270			0,6 + 9 + 21
w; m($-D_6$)	3330			3140	0,5 + 8
w	3345	3350			0,2 x 9 + 11
w			3190*	3185*	0,2 x 9 + 2 x 12
w; vw($-D_1$)	3410	3430			0,2 x 9 + 32
w	3410				0,6 + 9 + 21
w	3550	3535			0,3 x 9
vw			3320	3305	0,6 + 2 x 9
w			3400	3400	0,6 + 9 + 11
w	3605	3600			0,6 + 2 x 11
w	3740	3600			0,5 + 6
w	3740	3665*			0,9 + 11 + 2 x 12
w		3665*			0,2 x 6 + 21
w			3470	3465	0,3x 9; 0,6 + 2 x 11
w	3780	3770			0,6 + 9 + 11
vw; w($-D_6$)			3600	3575	0,6 + 8 + 9
w				3575	0,5 + 6
w				3610*	0,2 x 6 + 21
vw	3795*		3700	3660*	0,6 + 8 + 11
w	3835				0,2 x 6 + 21
vw; w($-D_5$)	3895	3880	3700	3660*	0,2 x 6 + 20
vw			3700		0,5 + 6

TABLE 4.4 CONTINUED

Intensity[a]	Position from the 0,0 band (cm^{-1})				Assignment
	$-\nu_6$	$-D_1$	$-D_5$	$-D_6$	
vw				3745	0,5 + 2 x 9; 0,8 + 3 x 9
w, vw($-D_1$)	3930*	3880			0,2 x 9 + 2 x 12
w			3765		0,2 x 6 + 21
vw			3780*		0,4 x 11; 0,8 + 3 x 9
w; vw($-D_6$)	3950	3950*	3855	3840	0,2 x 6 + 12
w	3950	3950*			0,6 + 2 x 9
w			3855		0,5 + 2 x 9
w	3980	3980			0,4 x 11; 0,6 + 8 + 9
w		3980			0,2 x 5
vw	4060	4085			0,2 x 6 + 15
vw	4130				0,5 + 2 x 11
w		4180			0,5 + 8 + 11
w	4205	4195			0,2 x 6 + 11
w	4245			4000	0,2 x 5
vw; w($-D_1$)	4265	4245			0,2 x 6 + 32
w	4305				0,5 + 8 + 11
w			3970*		0,6 + [illegible] + 11 + 20
w		4355			0, [illegible]
w	4380	4355	4020	4000	0,2 x [illegible]
vw; w($-D_6$)	[illegible]			4000	0,6 + [illegible] + 11 + [illegible]
w			[illegible]	[illegible]	[illegible] + 11
w	4500				[illegible]
w	[illegible]				0,4 x [illegible] + 11
vw				[illegible]	[illegible]

TABLE 4.4 (CONTINUED)

Intensity[a]	Position from the 0,0 band[b] (cm^{-1})				Assignment
	$-H_6$	$-D_1$	$-D_5$	$-D_6$	
w			4250		0,2 x 5
w; vw($-D_6$)			4300	4260	0,6 + 2 x 9 + 11
vw; w($-D_1$)	4605	4590			0,6 + 3 x 11
w	4725	4590			0,5 + 6 + 11
w; vw($-D_1$)	4725	4675			0,4 x 9
w			4375		0,2 x 6 + 2 x 21
vw			4445	4445	0,2 x 6 + 3 x 11
vw		4710			0,8 + 3 x 9
w	4805	4780			0,3 x 6
w	4905	4780	4565	4445	0,5 + 6 + 9
w			4650	4530	0,5 + 6 + 11
w	4935			4710	0,5 + 6 + 9
w			4710	4710	0,3 x 6
w; vw($-D_5$, $-D_6$)	5005	4950	4740*	4780*	0,5 x 11
w		4985			0,8 x 5 + 11
vw			4830		0,5 + 6 + 8
vw		5040			0,6 + 2 x 9 + 32
vw	5120	5125			0,6 + 3 x 9
vw	5185	5165	4920	4870	0,2 x 6 + 2 x 9
vw			4950	4970	0,2 x 6 + 9 + 11
vw	5240		5215	4970	0,2 x 5 + 11
vw				5030	0,2 x 6 + 2 x 11
vw	5330	5200	5255	5140	0,5 + 2 x 6
vw	5410	5360			0,2 x 6 + 9 + 11

TABLE 4.4 (CONTINUED)

Intensity[a]	Position from the 0,0 band[b] (cm^{-1})				Assignment
	$-H_6$	$-D_4$	$-D_5$	$-D_6$	
vw	5540	5540			0,2 x 6 + 2 x 9
vw-	5675	5540			0,5 + 3 x 9
vw	5845	5595			0,2 x 5 + 6
vw		5780			0,3 x 6 + 11
vw			5410	5410	0,3 x 6 + 12
vw	5965	5955	5575	5565	0,3 x 6 + 9
vw				5565	0,2 x 5 + 6
vw			5630	5640	0,3 x 6 + 11
vw			5800		0, 2 x 5 + 6
vw			5800	5805	0,2 x 6 + 2 x 9 + 11
vw			6030	6000	0,2 x 6 + 3 x 11
vw			6110	6000	0,5 + 2 x 6 + 9
vw			6255	6265	0,4 x 6

* Denotes shoulder

a. Uncorrected for instrumental response; s = strong, m = medium, w = weak, v = very

b. Error about ± $10cm^{-1}$

c. Numbering of the normal modes from Ref. 10.

but with weak spectral intensity. The non-totally symmetric vibrations show very little vibronic activity.

The transitions due to a_1 modes are 0,13, 0,12, 0,11, 0,9, 0,8, 0,7, 0,6 and 0,5 which appeared at 475, 775, 1000, 1185, 1205, 1470, 1605 and 2130 cm^{-1} are bands 7, 12, 14, 16, 17, 22, 24 and 34, respectively. All of these fundamentals, with the exception of ν_5 (the acetylenic C ≡ C triple bond stretch) and ν_7 appear in the fluorescence spectrum. Not all of the bands were previously reported. The band at 775 cm^{-1} seems to fit best with ν_{12}, a totally symmetric C-CCH vibration and lies in a region, where excitation source interference was reported by Zhuravleva. The band at 475 cm^{-1} is assigned to a substituent sensitive ring in-plane deformation. Both of the bands are at the same positions and given the same assignments in the phosphorescence of benzonitrile[59, 60, 66] and phenylisocyanide[57, 58]. Since these molecules are isoelectronic with phenylacetylene it is reasonable to expect that the normal modes of vibration common to all three have similar frequencies and description. Similarly, band 14 at 1000 cm^{-1} corresponds to the ring-breathing motion ν_{11}(992 cm^{-1} in benzene). At about 1200 cm^{-1} there are two bands which are assigned as 0, 9 (band 16 at 1185 cm^{-1}) and 0,8 (the shoulder, band 17, at 1205 cm^{-1}). This assignment is confirmed in $-D_5$ and $-D_6$ where there is a large interval between them. The substituent sensitive C - C stretching between the ring and the substituent (ν_8) is observed in the phosphorescence of both benzonitrile and phenyl-

isocyanide. In the phosphorescence of benzene[56], where a ν_8 type vibration is not possible, a strong band at 1178 cm^{-1} was attributed to an in-plane hydrogen bonding (ν_9 in the phenylacetylenes). The contribution of ν_8 to the spectral intensity of phosphorescence is negligible; this is in contrast to the fluorescence where the main contribution is from ν_8. The weak band 22 at 1470 cm^{-1} is assigned to the C - C stretching mode ν_7. Band 24 at 1605 cm^{-1} is the most intense (other than the 0, 0) in all four phenylacetylenes, and is assigned to ν_6, which is one component of the degenerate e_{2g} 1585 cm^{-1} mode in benzene. Zhuravleva reported at band 1964 cm^{-1} and assigned it to a 1960 cm^{-1} fundamental. In this study 3 bands, 30, 31, 32 are seen in this region at 1955 cm^{-1}, 1975 cm^{-1}, 2010 cm^{-1} respectively. On the basis of the normal mode assignments by King and So, Zhuravleva's assignment seems incorrect. Here the bands are assigned as 0, 9+12, 0, 8+12 and 0, 2×11.

A number of non-totally symmetric vibrations occur with spectral intensity much less than that of the totally symmetric vibrations. None of these were previously reported. On the basis of the spin-orbital mixing of singlet and triplet states given in Table 2.1, if the emitting triplet state is a $^3A_1$ state vibronic perturbation will involve both b_1 and b_2 vibrations, but no a_2 vibrations. Therefore the very weak shoulder, band 13, at 855 cm^{-1} and assigned as the a_2 fundamental ν_{15}, a C - H out-of-plane deformation is anomalous. Its appearance in the

phosphorescence spectrum may be due to solvent perturbation of the triplet geometry. Since its intensity is very weak this perturbation is not very great. Therefore, it can be assumed that triplet state geometry of the phenylacetylenes has essentially C_{2v} symmetry. The appearance of b_2 fundamentals contribute a slight amount of long axis in-plane (x) polarization to the spectrum. These are bands 5, 10, 16, 19, and 20 at 350, 655, 1065 and 1280 cm^{-1} which are assigned to 0,36, 0,33, 0,32, and 0,30 respectively. These bands are very weak in intensity and most occur as shoulders. An alternative assignment to band 5 is 0,23, a b_1 fundamental. Both ν_{23} and ν_{36} are deformations between the phenyl group and the acetylenic group. The fact that these have the same frequency (Table 4.2) prevents the distinction between an in-plane or out-of-plane mode. The b_1 modes contribute an out-of-plane component to the polarization. Four possible b_1 fundamental modes can be assigned for bands 3, 8, 9 and 11, at 165, 530, 625 and 685 cm^{-1}, namely 0, 24, 0,22, 0,21, and 0,20 respectively. Although their spectral intensity is small compared to that of the a_1 modes their contribution is greater than that of the b_2 modes.

Most of the other bands are built on ν_5, ν_6, or ν_8, with the greatest contribution based on ν_6. In MC bands 57 and 85 are interpreted as a ν_6 progression. In In a progression of up to four quanta of ν_6 can be seen.[57] In contrast to the fluorescence, the totally symmetric acetylenic stretch ν_5, is fairly active in the phosphorescence spectrum. The observations are found in the other phenylacetylenes.

(b) Phenylacetylene-D_1

The phosphorescence spectrum of phenylacetylene-D_1 in MC is shown in Figure 4.7 and the vibrational analysis is presented in Table 4.4. As in the case of phenylacetylene-H_6, the strongest band is the 0, 0 band observed at 25280 cm^{-1} (3MP), 25325 cm^{-1} (EPA); 25360 cm^{-1}(MC), and 25290 cm^{-1} (IP). A lattice mode is observed as the shoulder, band 2 at 45 cm^{-1} to the red of the 0, 0 band. The same fundamentals are observed in $-D_1$ as in $-H_6$. Transitions due to a_1 modes are 0,13, 0,12, 0,11, 0,9, 0,8, 0,7, 0,6 and 0,5 are observed as bands 7, 12, 15, 18, 19, 23, 25 and 30, at 455, 760, 1000, 1175, 1195, 1490, 1600 and 2005 cm^{-1} respectively. These modes appear with about the same relative intensity compared to the 0, 0 band as in $-H_6$, the most intense being 0,6. The fundamental ν_8 occurs as a poorly resolved shoulder to the red of ν_9. By reference to Table 4.2, it can be seen that acetylenic hydrogen substitution by deuterium lowers ν_5 considerably, but has a negligible effect on all the other a_1 modes observed in the phosphorescence spectrum. The a_2 mode, ν_{15}, is unaffected and appears as a weak shoulder at 855 cm^{-1} as band 14. The b_2 transitions 0,36, 0,33 0,32 and 0,30, are seen at 330, 495, 1070 and 1275 cm^{-1} as bands 5, 8, 17 and 21. These bands appear with very weak intensity as in $-H_6$, with the exception of band 8, which will be discussed again. Only ν_{33} of the b_2 modes is considerably lowered by acetylene deuterium substitution. Making a greater contribution to the spectral intensity are the transitions due to b_1 modes

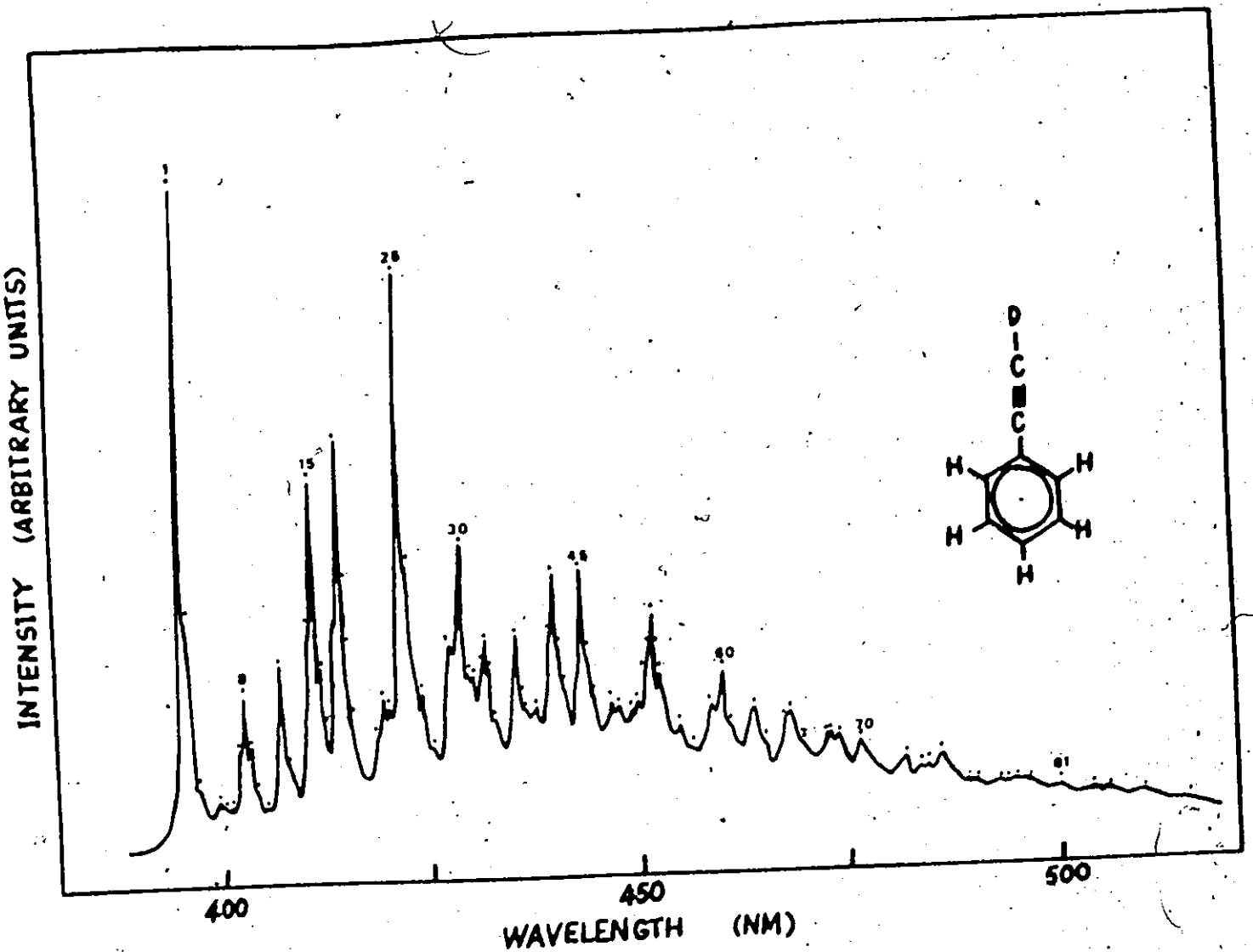

FIG.4.7 THE PHOSPHORESCENCE SPECTRUM OF 10^{-4}M PHENYLACETYLENE-D_1 IN POLYCRYSTALLINE METHYLCYCLOHEXANE AT 77°K

0,24, 0,22, 0,21 and 0,20 which are seen as bands 3, 9, 8 and 11 at 150, 530, 695 and 695 cm^{-1} respectively. These appear with the same relative intensities as in $-H_6$. Therefore the main contribution to band 8 is from the ν'_{21} mode which is also seen as band 8 in $-H_6$. This is the only b_1 mode which is affected by deuterium substitution in $-D_1$. The overall appearance of the spectrum of phenylacetylene-D_1 is the same as that of $-H_6$, with the effects of deuteration seen by the lowering of ν_5 and ν_{21}. All other modes in the 0 - 2000 cm^{-1} region are relatively unaffected. The assignments in Table 4.4 reflect these deuteration effects. Most of the assignments follow those for $-H_6$. The progressions in ν_6 appear as bands 54 and 74.

(c) Phenylacetylene-D_5

Figure 4.8 gives the phosphorescence spectrum of the ring deuterated phenylacetylene-D_5 in MC (containing about 2% 3MP); the vibrational analysis is found in Table 4.3. Here the overall appearance of the spectrum is the same as $-H_6$ and $-D_1$ with frequency shifts compatible with ring deuteration. The 0,0 band, which is blue shifted, is still the strongest band in the phosphorescence spectrum at 25305 cm^{-1} (3MP), 25365 cm^{-1} (EPA) 25415 cm^{-1} (MC) and 25325 cm^{-1} (IP). For $-D_5$ and $-D_6$ no lattice modes are resolved, though the lower third of the 0, 0 band is

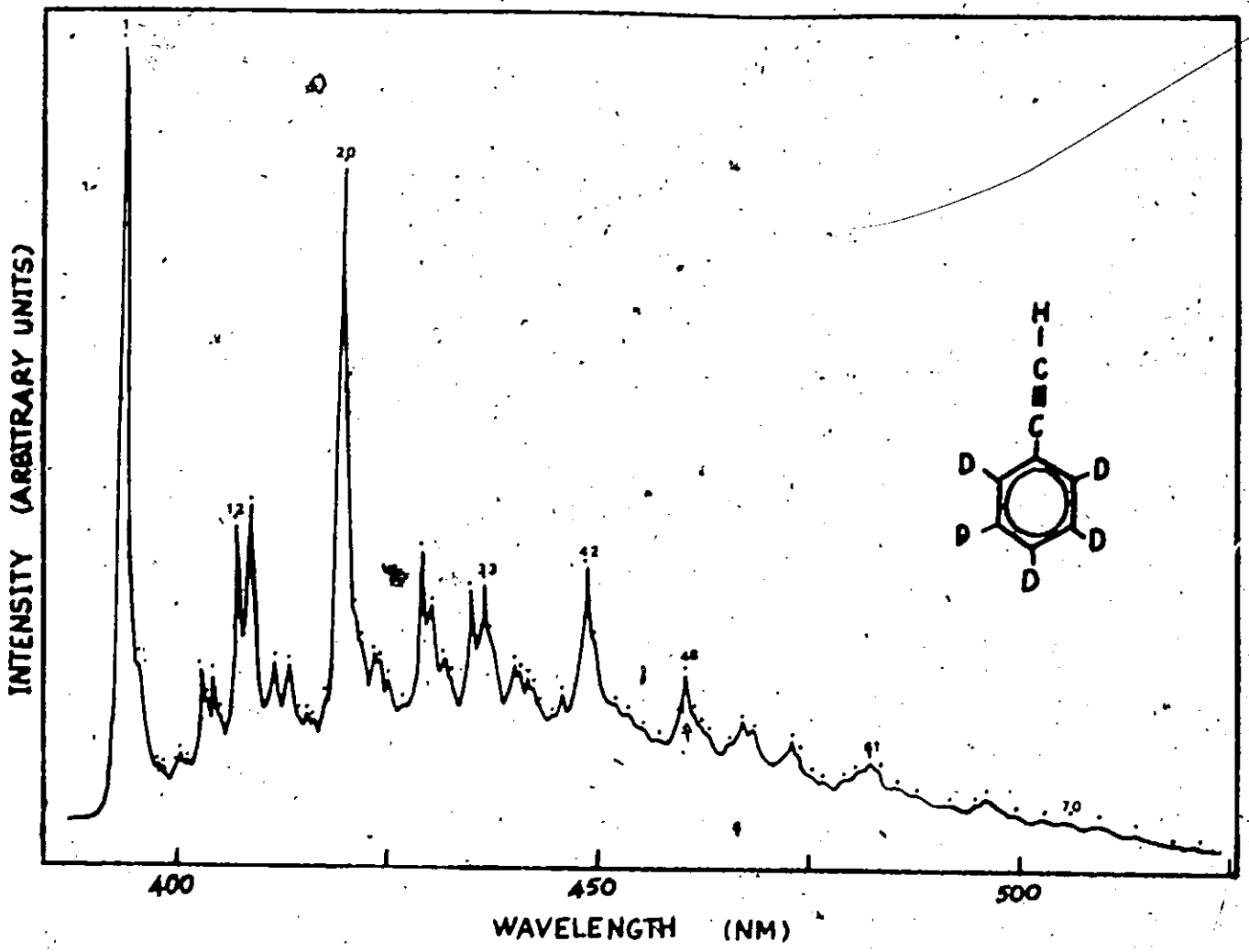

FIG.48 THE PHOSPHORESCENCE SPECTRUM OF 10^{-4} M PHENYLACETYLENE-D_5 IN POLYCRYSTALLINE METHYLCYCLOHEXANE AT 77°K

broadened on the red side. All the a_1 modes seen in $-H_6$ and $-D_1$ are also seen here again, with about the same relative intensities compared to the 0, 0 band. All except ν_{13} and ν_5 are shifted to lower frequencies on ring deuteration. The broad band 4 at 465 cm^{-1} is made up partly by 0,13 and partly by 0,22. Band 25, at 2130 cm^{-1} has shifted away from the 0,0 band with respect to band 30 of $-D_1$, back to the position of band 35 of $-H_6$, all compatible with ν_5, the C ≡ C stretching mode. Band 9 at 720 cm^{-1} shifts towards the 0, 0 (band 8 in $-D_6$) compared to $-H_6$ and $-D_1$, strongly suggesting it is associated with the substituent sensitive ring in-plane deformation ν_{12}. Band 14 moves about 320 cm^{-1} from the position of band 16 in $-H_6$ and band 18 in $-D_1$ to 875 cm^{-1}; it is also seen as band 9 in $-D_6$. This band is consistent with its assignment to a C - D in-plane deformation, ν_9. Band 13, at 955 cm^{-1}, also present in $-D_6$ as band 11, is obviously the ring breathing vibration, ν_{11}. In benzene, the 992 cm^{-1} ring breathing is lowered to 945 cm^{-1} on complete deuterium substitution. Band 14, at 1145 cm^{-1}, (1135 cm^{-1} in $-D_6$ band 16) was a shoulder in $-H_6$ (band 17) and $-D_1$ (band 19) is now seen distinctly as ν_8, a C - C stretch between the phenyl and the acetylenic groups. Because its frequency is close to that ν_9 in $-H_6$ and $-D_1$, weak contributions from ν_8 might possibly be masked by much more intense ν_9. The very weak band 17 at 1385 cm^{-1} is shifted towards the 0, 0 by about 110 cm^{-1} compared with $-H_6$ (band 22)

and $-D_1$ (band 23) and is consistent with the C - C stretch ν_7. The very intense band 20, at 1575 cm^{-1}, is slightly lower than the 1600 cm^{-1} bands of $-H_6$ and $-D_1$; complete deuterium substitution is known to lower the 1585 cm^{-1} C - C stretching frequency in benzene to 1559 cm^{-1}. Thus a ν_6 assignment is strongly indicated.

Most of the non-totally symmetric modes which appear in $-H_6$ and $-D_1$ are not easily and unambigiously assigned in the phosphorescence spectra of $-D_5$ and $-D_6$. This is because in $-D_5$ and $-D_6$ the background in the spectra is greater and many of these very weak peaks are washed out. The a_2 mode ν_8 is probably hidden under band 10 in $-D_5$, where the main contribution is from ν_{12}. Among the b_2 modes, ν_{36}, the C - C in-plane deformation between the ring and the C ≡ CH group, probably contributes to the very broad band 3 at 315 cm^{-1}. The acetylenic C - H in-plane deformation, ν_{33}, is the weak shoulder band 9, at 655 cm^{-1}. This band shifts away from the 0, 0 band compared with band 8 in $-D_1$ (where it is swamped by the contribution from the ν_{21} mode), back to its position in $-H_6$ (weak shoulder band 10). The contribution of ν_{32} to band 12 at 875 cm^{-1} is negligible. The weak contributions of the b_1 modes to the spectral intensity are again stronger than those of the b_2 modes. Band 2, 5, 7, are at 160, 470 and 550 cm^{-1} and are assigned to 0,24, 0,22 and 0,20 respectively. Band 8 at 625 cm^{-1} is clearly due to 0, 21 since this band also shifts away from the 0,0 when compared with band 8 of $-D_1$ back to its position in $-H_6$ (band 9).

Of the remaining bands, the most important feature is the presence of a ν_6 progression, assigned to bands 42, 61, and 74.

(d) Phenylacetylene-D_6

Figure 4.9 depicts the phosphorescence spectrum of the completely deuterated phenylacetylene-D_6 in MC (containing about 2% 3MP); the corresponding analysis is presented in Table 4.3. The intense 0, 0 band is further blue shifted and appears at 25340 cm^{-1} (3MP), 25390 cm^{-1} (EPA), 25460 cm^{-1} (MC), and 25370 cm^{-1} (IP). The overall similarities between the $-H_6$ and $-D_1$ spectra are also evident in a comparison of $-D_6$ and $-D_5$. The transitions due to a_1 modes are 0,12, 0,11, 0,9, 0,8, 0,7, 0,6 and 0,5 as bands 8, 11, 9, 12, 15, 17 and 24 at 720, 950, 870, 1145, 1385, 1575 and 2010 cm^{-1}. The 0,13 transition is swamped out by 0,21. The only b_2 mode enters as the weak broad band 3 at 305 cm^{-1} due to 0,36. The b_1 modes are seen as bands 5 and 6 at 495 cm^{-1} and 530 cm^{-1} and assigned as 0,21 and 0,20. Therefore the number of non-totally symmetric modes observed in $-D_6$ is less than in $-D_5$. The important features in $-D_6$ are the shifts in bands 5 and 24, showing sensitivity to deuteration of the acetylenic group in accord with the 0,21 and 0,5 interpretations. Progressions in ν_6 are bands 39, 55 and 66.

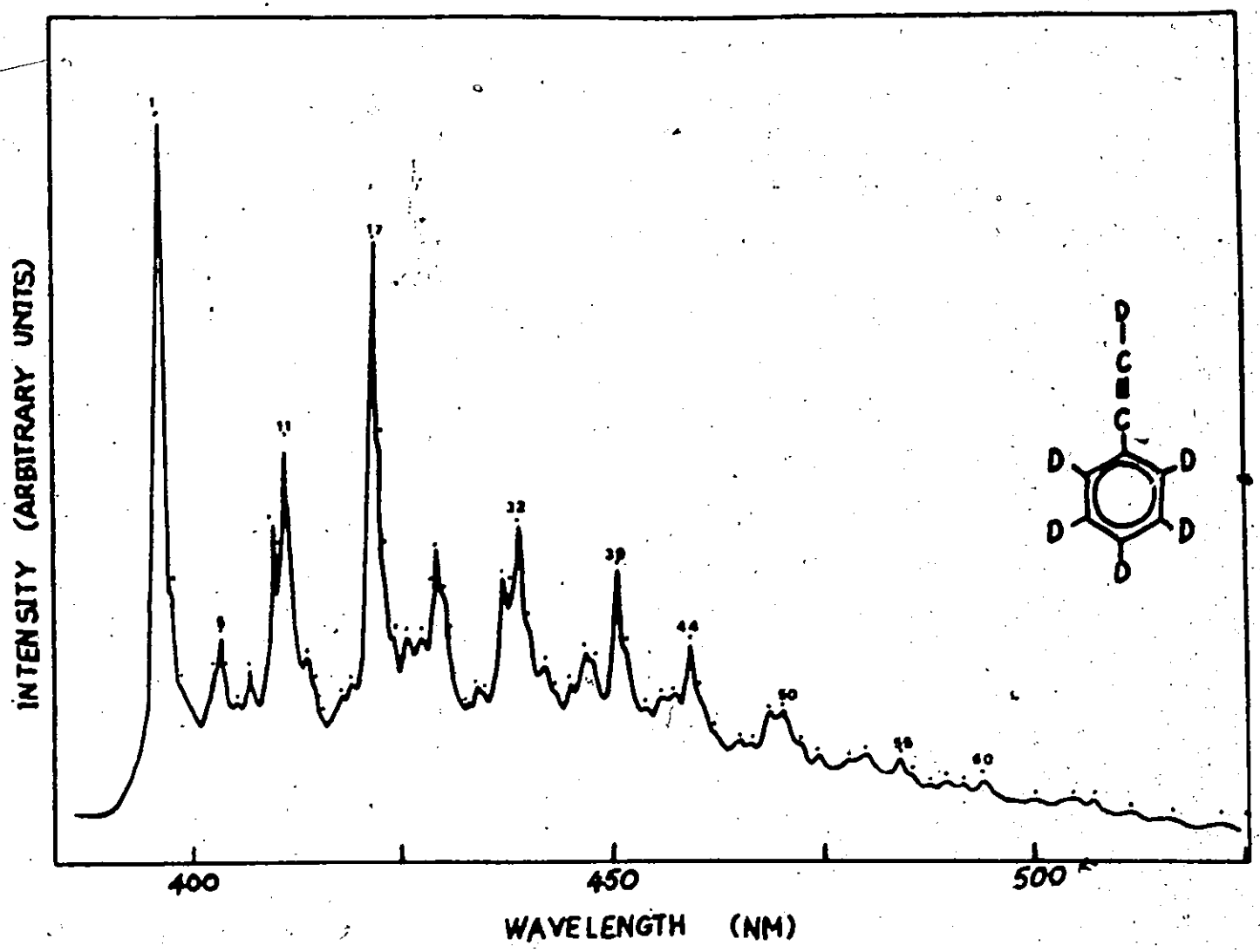

FIG.4.9 THE PHOSPHORESCENCE SPECTRUM OF 10^{-} M PHENYLACETYLENE-D_6 IN POLYCRYSTALLINE METHYLCYCLOHEXANE AT 77°K

4.6 Discussion of the Phosphorescence of Phenylacetylene

From the vibrational analyses of the phosphorescence spectra, a few comments can be made about the geometry of the lowest triplet state of the phenylacetylene. According to the Franck-Condon principle, if the lowest triplet state geometry differs markedly from that of the planar, regular hexagon ring of the ground state, then long progressions of the vibrations converting one into the other should be apparent in the phosphorescence.

A moderately long progression in ν_6 occurs for all four spectra in MC (Table 4.4) and IP[67]. (A moderately long progression is also seen in ν_9, but this mode is concerned primarily with the hydrogen atoms, and not with the ring). If this C-C stretching mode carries the triplet state geometry into that of the ground state, then these results suggest a planar, non-regular hexagonal ring geometry of the triplet state of the phenylacetylenes in both MC and IP matrices. From the vibrational analysis it can be concluded that the geometry of the lowest triplet state is a hexagon consisting of either four long bonds and two short bonds (quinoidal) or two long bonds and four short bonds (antiquinoidal).

From phosphorescence intensity measurements, Nieman[17] has concluded that the triplet state of toluene has an antiquinoidal geometry. Similar calculations were done for phenyl-

acetylene-H_6 by measuring the reduced intensities of the ν_6 and ν_{11} progressions in the phosphorescence spectra. The difference between the long and short bonds of the ring is found to be roughly 0.07 ^{o}A, as for toluene. If there is an overall expansion of the ring in the lowest triplet state compared to the ground state, of about the same magnitude as for benzene, then these results imply that the triplet state of phenylacetylene is also antiquinoidal.

The phosphorescence spectrum of phenylacetylene is very similar to that of the isoelectronic molecules phenylisocyanide and benzonitrile. In all three molecules the 0, 0 band is very strong, the most intense modes are the totally symmetric vibrations, while a few b_1 and b_2 modes appear with weak intensity. In all three molecules the vibrational spectra have the same features with the main progression in the totally symmetric C-C stretching mode around 1600 cm^{-1}, suggesting a planar, non-regular hexagonal ring for the lowest triplet state. The absence of long progressions of out-of-plane vibrational modes support a planar geometry.

The progressions seen in the flourescence are different from those in the phosphorescences, where ν_6 and ν_9 are evident. Several other monosubstituted benzenes also have progressions in the fundamentals equivalent to ν_6 (one component of the degenerate e_{2g} mode of benzene at about 1600 cm^{-1}) in phosphorescence, and equivalent to ν_{11} (the a_{1g} mode of benzene at about

1000 cm^{-1}) in fluorescence. The luminescence of benzene has progressions in the ring breathing mode in both fluorescence and phosphorescence. The progression in 1600 cm^{-1} is not seen in the phosphorescence. Chemical perturbation affect the first excited singlet state geometry of benzene only minimally since the fluorescence spectra of benzene and several monosubstituted benzenes are similar. On the other hand, the phosphorescence spectrum of benzene is quite different from those of most benzene derivatives, thus indicating the great extent to which chemical perturbation affects the lowest triplet state geometry.

4.7 Polarization of the Luminescence of Phenylacetylene-H_6

(a) General

The method of photoselection[40, 41] was used to measure the degree of polarization of 10^{-3}M phenylacetylene-H_6 in a mixture MC and 3MP (4:1 by volume). Measurements were also taken in two other glasses, EPA and 3MP. The results in these two glasses indicated the same trend as in the above glass, but fluctuated greatly from sample to sample. The wavelengths of excitation were 282 nm and 246 nm, which corresponded to the 0, 0 absorption region of the $S_0 \rightarrow S_1$ transition ($^1A_1 \rightarrow {}^1B_2$, ^1L_b band in the Platt[61] notation) and the $S_0 \rightarrow S_2$ transition ($^1A_1 \rightarrow {}^1A_1$, ^1L_a band) respectively. Because of the drastic cutting down of the ultra-violet light intensity when transmitted through the polarizers, the slits of the exciting monochromator was 1000 μ. This fairly large band-pass decreased the spectral purity of the exciting light. The polarization of the 0, 0 band of the fluorescence could not be obtained for the $S_0 \rightarrow S_1$ excitation because of interference from the exciting light. This is a common problem for most aromatic compounds.

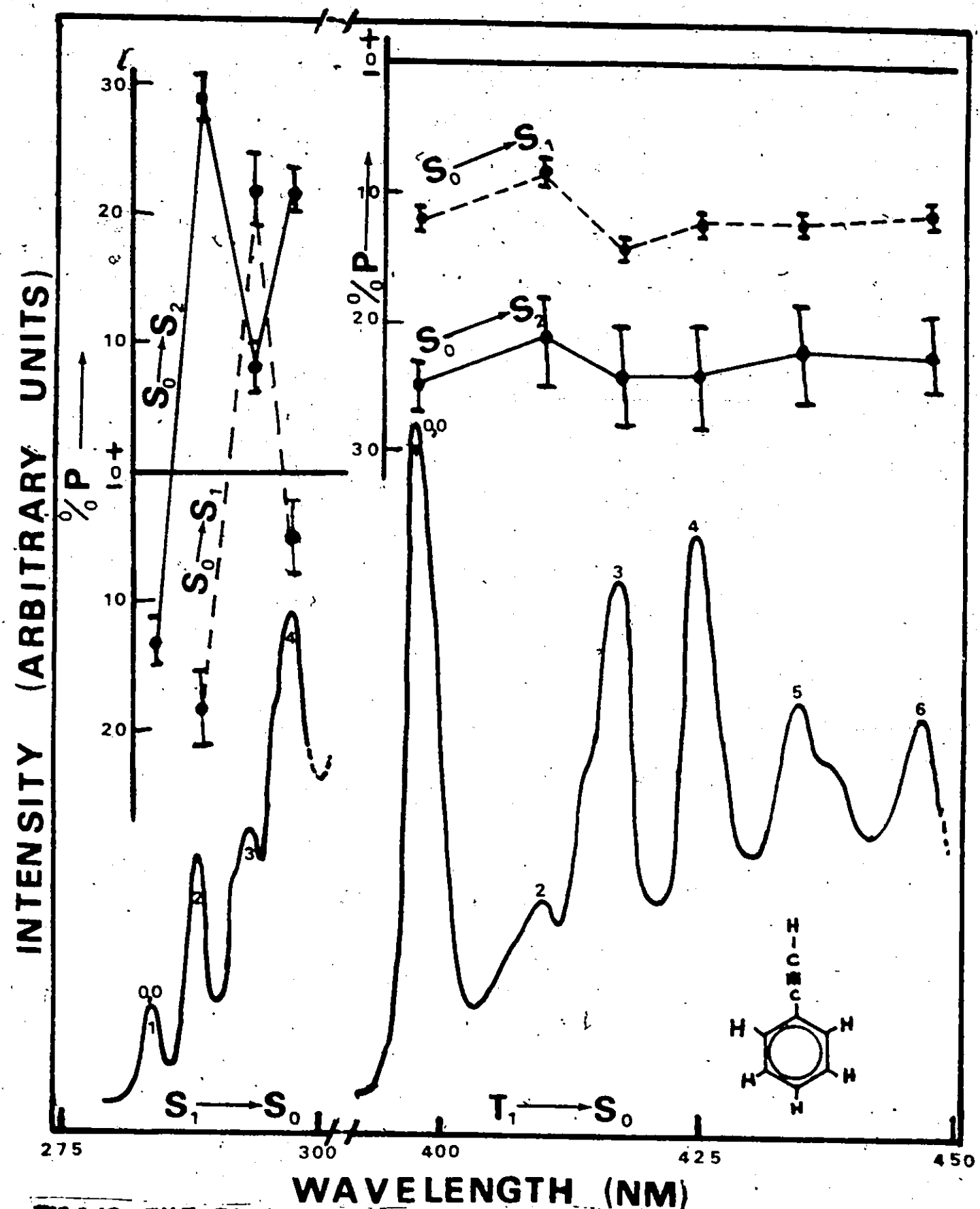

FIG 4.10 THE POLARIZATIONS OF THE FLUORESCENCE AND PHOSPHORESCENCE OF PHENYLACETYLENE IN A RIGID GLASS AT 77 °K

(b) Polarization of the Fluorescence

The fluorescence spectrum of phenylacetylene in the glassy solvent at 77°K is shown in Figure 4.10. Band 1 is the 0, 0 of fluorescence; band 2, of b_2 symmetry, consists of the unresolved b_2 vibrational modes ν_{35} and ν_{34}; band 3 consists mainly of the totally symmetric ring breathing mode ν_{11}; band 4, of b_2 symmetry, is a combination of ν_{11} with ν_{35} and ν_{34}. For both $S_0 \rightarrow S_1$ (^1L_b) and $S_0 \rightarrow S_2$ (^1L_a) excitations a distinct vibrational structure appears in the spectrum. In the ^1L_a state, the degree polarization of the 0, 0 band is moderately negative (-0.13). The remaining bands are polarized in an oscillatory fashion, but are all still positively polarized. Bands 2 and 4 are strongly positive (0.2[illegible] and 0.22 respectively), while band 3 is weakly positive (0.08). Ideally, band 3 should be negatively polarized, but overlap with bands 2 and 4 may have a strong influence on the degree of polarization. The oscillation of the polarization is usually interpreted as due to the coupling of vibrations of different symmetry. The negative value for the 0, 0 band shows that the absorbing and emitting dipoles are at right angles in C_{2v}. This is consistent with the assignment of S_2 being an A_1 state (long-axis polarized) and S_1 being a B_2 state (short-axis polarized). Also, vibrations of b_2 symmetry should be positively polarized while those of a_1 symmetry should be negatively polarized (here, less positive than b_2).

For $S_o \rightarrow S_1$ excitation the absorbing and emitting dipoles are parallel. Therefore, the 0, 0 band should be positively polarized, but this could not be observed. Here the oscillatory pattern is in the opposite sense of than obtained from the $S_o \rightarrow S_2$ excitation. Band 2 is negatively polarized (-0.11); band 3 is positively polarized (0.14); while band 4 is essentially unpolarized, but less positive than band 3. Band 3 was shown to be polarized like the 0, 0 band for $S_o \rightarrow S_2$ excitation. Therefore, it seems reasonable to assume that the 0, 0 band, after $S_o \rightarrow S_1$ excitation is also positively polarized i.e. the emitting and absorbing dipoles are parallel. This again is consistent with the B_2 symmetry of the S_1 state.

(c) Polarization of Phosphorescence

Polarization measurements on the 0, 0 band of the phosphorescence spectrum is used to assign the orbital symmetry of the lowest emitting triplet state of phenylacetylene. The theory is discussed in Section 2.9.

The degree of polarization of the major bands in the phosphorescence spectrum is shown in Figure 4.10. The main feature is that the peaks are polarized negatively for both ^1L_a (-0.25) and ^1L_b (-0.12) excitation, with that for ^1L_a excitation being more negative. It is seen that all the major peaks have about the same degree of polarization as the 0-0 band. There is no clearly defined vibronic structure. The weak band 2 is less negatively polarized than its immediate neighbours especially for ^1L_b excitation. This is due partly to the contribution from scattered light becoming more noticeable in a low spectral intensity region (this effect is greater in the longer wavelength excited spectrum), and partly to con-

tributions from the non-totally symmetric vibrations which contribute significantly in this region (as is seen the more detailed spectrum obtained in the polycrystalline matrix). Thus the phosphorescence spectrum is made up almost entirely of Subspectrum I.

The values obtained for the 0, 0 band are similar to those reported for phenylisocyanide (in nC - 3-MP) and benzonitrile (in 3-MP). The polarization of the major band agrees with those obtained by Friedrich et al[35], who offer an alternative interpretation, which attributed most of the spectrum to be of vibronic origin.

These results enable the orbital symmetry of the lowest triplet state of phenylacetylene to be assigned (see Table 7.1). In group theoretical language, because phenylacetylene belongs to the C_{2v} point group, the orbital symmetry of triplet $\pi\pi^*$ states that have orbitally-allowed dipole transitions to the ground state are $^3A_1$ and $^3B_2$. Since the spin wavefunctions transform as axial rotations ($R_x \rightarrow B_2$, $R_y \rightarrow B_1$, $R_z \rightarrow B_2$), and the total (orbit plus spin) wavefunction transforms as the direct product of orbital and spin functions, for a $^3A_1$ orbital wavefunction two spin components, B_1 (x-polarized) and B_2 (z-polarized), can be dipole emissive, while for $^3B_2$, $B_1(x)$ and $A_1(z)$ are allowed. The degree of phosphorescence polarization results indicate that there is a minor contribution from a y-axis transition, in addition to the predominance of the out-of-plane component, suggesting a $^3A_1$ orbital symmetry (^3L_a, $^3B_{1u}$ in D$_{6h}$).

The high contribution of the out-of-plane polarized component is in agreement with the results of other workers[37]. The usual interpretation of this result is that the lowest triplet state is perturbed by out-of-plane $\sigma\,\pi^*$ or $\pi\,\sigma^*$ states. A recent calculation of the radiative triplet lifetime of naphthalene[47] indicates that $\sigma\,\pi$ involvement can explain the spin orbit coupling in that molecule.

The strong bands in the phosphorescence spectrum were polarized very nearly like that of the (0, 0) band, both with $^1B_2$ and $^1A_1$ excitation. This is consistent with the assignment of these peaks as a_1 vibrations. The weak bands were not resolved in the glass, and were essentially unpolarized in the polycrystalline IP and MC matrices. Hence expected variations in the degree of polarization in this region could not be confirmed.

the $T_1 - S_0$ transition is space allowed, with very little vibronic activity. Here, the deuterium effect is almost entirely on k_i. This is substantiated by the theoretical calculations of Friedrich et al[36] (discussed below) and by examination of the ratios of the intensities of certain vibrational progressions compared to the 0,0 bands of the phosphorescence spectra. In Table 4.5 these ratios are compared from the detailed spectra in EP (upper values) and in MC (lower values), for four a_1 modes and one b_1 mode. For the series $-H_6$, $-D_1$, $-D_5$ and $-D_6$ there is no significant trend towards a decrease in intensity ratios. The fact that there is a general increase instead is explained in terms of decrease in sharpness of the $-D_5$ and $-D_6$ spectra.

From the observed phosphorescence lifetimes, given in Table 4.6, deuteration increases the lifetimes. It is noted that deuteration of the acetylenic hydrogen produces the same increase in τ_p as deuteration of all five ring hydrogens. Complete deuteration yields the largest lifetime in both solvents. The lifetimes in EPA are all considerably longer than in 3MP, as has been reported for benzene[48] and other molecules. The energy gap between the zeroth vibrational level of the triplet state and that of the ground state, $\Delta E(T_1 - S_0)$ is also given in Table 4.6. For both 3MP and EPA, small blue shifts occur in proceeding through the series $-H_6$, $-D_1$, $-D_5$, $-D_6$. Although the energy gap for a particular phenylacetylene is larger in EPA than in 3MP the differences in the two solvents are not very

TABLE 4.5

RATIOS OF THE INTENSITIES OF THE MAIN VIBRATIONAL PROGRESSIONS COMPARED TO THE 0,0 BAND IN THE PHOSPHORESCENCE SPECTRA OF PHENYLACETYLENES AT 77°K

Assignment	Solvent	Molecule -H_6	-D_1	-D_5	-D_6
0,0		1.00	1.00	1.00	1.00
0,11(a_1)	IP*	0.41	0.54	0.55	0.67
	MC	0.31	0.52	0.34	0.40
0,9 (a_1)	IP	0.64	0.57	0.58	0.52
	MC	0.40	0.58	0.34	0.40
0,6 (a_1)	IP	0.76	0.77	0.94	0.94
	MC	0.51	0.84	0.78	0.65
0,5 (a_1)	IP	0.43	0.48	0.48	0.51
	MC	0.24	0.44	0.32	0.25
0,21(b_1)	IP	0.10	0.17	0.23	0.14
	MC	0.14	0.20	0.06	0.20

* IP = isopentane, MC = methylcyclohexane

large. Hence the much greater lifetimes observed in EPA are attributed to the greater polarity[73] of EPA compared to 3MP.

By using the usual assumption that k_c is constant and the values in Table 4.6 it is possible to calculate, from equation 2.9, the added contribution to the radiationless decay of the triplet state of phenylacetylene in 3MP when $-D_6$ is protonated on the acetylenic group, Δk_i ($-D_6 \rightarrow -D_5$), or on the ring, Δk_i ($-D_6 \rightarrow -D_1$). Both are found to be 0.09 s^{-1}. For EPA, Δk_i ($-D_6 \rightarrow -D_5$) is 0.07 s^{-1} and Δk_i ($-D_6 \rightarrow -D_1$) is 0.09 s^{-1}. The near equality of the contributions in these acetylene-substituted benzenes is in sharp contrast to the results reported in toluene[73, 74], where the methyl-substituent has a relatively small effect on Δk_i, but in 2 - naphthaldehyde[49], in which the aldehydic-[illegible] greatly alters Δk_i.

Recent developments in the theory of radiationless transitions show that the most important mechanism for the non-radiative deactivation of T_1 for planar aromatics is via π-σ vibronic coupling[31]. The radiationless rate constant depends mainly on the integrals of the matrix elements of the electronic wavefunctions for the two electronic states involved and of the FC factor for the overlap of the initial vibrational state with each of the energetically accessible vibrational levels of the final electronic state.

The unusual deuterium isotope effect in phenylacetylene is explained in terms of π-σ vibronic coupling by Friedrich et al[36] who evaluated the electronic matrix element, R', and the FC factor for the S_0 - T_1 transition (see Table 4.6). It was

TABLE 4.6

SOME PROPERTIES OF THE $S_o - T_1$ AND $S_o \rightsquigarrow T_1$ TRANSITIONS FOR PROTONATED AND DEUTERATED PHENYLACETYLENES

	-H_6	-D_1	-D_5	-D_6	
$\Delta E^a_{T_1S_o}$ (3MP)	25230	25280	25305	25340	cm^{-1}
τ_p (3MP)	1.75	2.16	2.14	2.67	s
τ_p^{-1} (3MP)	0.57	0.46	0.46	0.37	s^{-1}
$\Delta E^a_{T_1S_o}$ (EPA)	25285	25325	25365	25390	cm^{-1}
τ_p (EPA)	2.40	2.94	3.22	3.93	s
τ_p^{-1} (EPA)	0.42	0.34	0.31	0.25	s^{-1}
$(R^2)^b$	0.354	0.358	0.207	0.217	cm^{-1}
$(2\pi/3\hbar)FC^c$	1.48	1.12	0.51	0.30	
E_1^d (νCC-H)	14	4	27	8	%
E_3 (νC-H)	36	42	13	29	%
E_5 (νC - C)	31	33	38	40	%
$E_6 + E_8$	16	16	16	18	%
E_{oop}	4	5	5	6	%

a. Experimental lifetime, the average of 10 measurements, with about 1% error.
b. Total electronic matrix element for the S_o-T_1 transition, from Ref. 36.
c. Franck-Condon factor, from Ref. 36.
d. E_i is the energy (as a % of the total) accepted by mode ν_i from Ref. 36.

shown that both integrals change considerably on ring deuteration for phenylacetylene. Whereas in most unsaturated hydrocarbons about 60% of the total electronic energy is accepted by C-H stretching modes and about 20% by out-of-plane (oop) and skeletal modes[27], Table 4.6 shows that in $-d_3$ and $-d_1$ the C-H stretching mode (ν_2) together with the acetylenic C-H (C-D) stretch (ν_1) accepts no more than 30% of the total electronic energy to be converted. Of the remainder, 20% is accepted by oop and skeletal modes and 30% by the acetylenic triple-bond stretching mode (ν_5); which is in competition with the C-H stretching mode as an energy sink. In the electronically excited state the triple bond has a great FC factor because of its large coupling constant and great reduction in bond order. On ring deuteration the energy accepted by the triple-bond is increased further (to about 40%) while the total energy accepted by the C-D stretching modes is reduced to less than 40%. In benzene[28] about 70% of the energy is accepted by a C-H stretching mode and about 20% by the e_{2g} skeletal deformation at 1580 cm^{-1} for C_6H_6 while about 60% is accepted by the C-D stretching mode and about 30% by the e_{2g} deformation for C_6D_6. Hence for both benzene and phenylacetylene the C-H (C-D) bending modes do not contribute significantly as energy sinks. Furthermore the deuterium effect by way of CD stretching modes accounts only partially for changes in the FC factor. The larger changes in the FC factor are due to the modifying effect on other vibrations which play a significant role - namely, the e_{2g} deformation in benzene and the triple bond stretch in

phenylacetylene. Both of these modes involve changes in geometry in the excited state (T_1).

In conclusion, it must be emphasised that, unlike the exocyclic single bonds of toluene[73, 74], the exocyclic multiple bond is a very effective energy sink when its bond order changes strongly upon excitation.

CHAPTER 5

LUMINESCENCE OF THE HALOPHENYLACETYLENES

5.1 General

The great interest shown in the luminescence of heavy-atom* substituted aromatic molecules has been reviewed by Lower and El-Sayed[37]. Only a few detailed phosphorescence spectra of substituted benzenes have been published. Most of the spectra in rigid solutions are poorly resolved, probably because suitable solvents for the solute molecules have not been used. The halo-substituted phenylacetylenes provide suitable systems for the investigation of the effect of heavy-atom substituents on benzene both as a function of the mass of the heavy-atom and of its position on the ring. For this purpose the following seven halo-derivatives of phenylacetylene were prepared: para-fluoro (p-F), -chloro (p-Cl), -bromo (p-Br), -iodo (p-I), meta-chloro (m-Cl), -bromo (m-Br) and ortho-chloro (o-Cl). Furthermore, since the para-derivatives belong to the C_{2v} point group (as phenylacetylene itself) while the ortho- and meta- derivatives belong to the C_s point group, it is interesting to find out what effects formal destruction of the C_{2v} π-electron cloud has on the phosphorescence spectra, especially on the allowedness of the 0, 0 band and on the geometry of the emitting triplet state.

* A heavy-atom has an atomic number greater than 14.

5.2 The Effect of Heavy-Atom Substitution on $\int \epsilon \, d\bar{\nu}$

For a spectroscopic transition the $\int \epsilon \, d\bar{\nu}$ is the integrated intensity of the absorption from the lower to the upper state[33]. Here ϵ is the molar decadic extinction coefficient. The limits of the integration extend over the complete contour of the series of vibronic bands at energy ν cm^{-1} associated with the transition. The values of $\int \epsilon \, d\bar{\nu}$ (Table 5.1) were computed graphically by replotting the absorbance versus the calculated wavenumber of the specific region of the transition and taking the areas under the absorption curves by counting squares. Since the $S_0 \rightarrow S_1$ transition is of much less intensity than the $S_0 \rightarrow S_2$ transition, the overlap of the latter was subtracted out by graphical extrapolation of this transition.

The value of $\int \epsilon \, d\bar{\nu}$ [illegible] of both the $S_0 \rightarrow S_2$ (^1L_a) and the $S_0 \rightarrow S_1$ (^1L_b) transitions do not change radically on substitution. The greatest increase of the intensity of the $S_0 \rightarrow S_1$ transition is by a factor of 2 or 3 (o-Cl and p-Br). In m-Cl, m- and p-Cl the intensity of the $S_0 \rightarrow S_2$ transition is about half that of phenylacetylene. The intensity of the p-F transition decreases by factors of two (^1L_b) and four (^1L_a) compared with the parent. This decrease helps significantly to result in the observed phosphorescence lifetimes (Section 5.3). Since the effects in intensities are not drastic it is concluded that heavy-atom substitution has very little effect on the allowedness of the

TABLE 5.1

SOME TRIPLET AND SINGLET PARAMETERS

OF THE HALOPHENYLACETYLENES

Molecule	τ_p (ms)[a] in 3MP	in MC/3MP	$\frac{\tau_p(Cl)}{\tau_p(h)}$[b]	$\frac{\zeta^2(h)}{\zeta^2(Cl)}$[e]	$\frac{(\phi_p/\phi_f)h}{(\phi_p/\phi_f)\phi CCH}$[c]	$\int \epsilon d\nu \times 10^{-6}$[d] $S_o \rightarrow S_1$	$S_o \rightarrow S_2$
øCCH	1750	1810			1	1.9	100
p-F	2220	2500	0.1	0.2	18	1.0	25
p-Cl	249	247	1	1	120	2.5	110
p-Br	9.3	8.9	27	18	1300	5.6	91
p-I	0.86	0.76	290	74	>10,000*	2.2	95
m-Cl	727	718	1	1	14	1.8	57
m-Br	26.4	25.0	28	18	110	2.0	47
o-Cl	539	551			8	4.5	57

*No detectible fluorescence from p-I; fluorescence from a photoproduct detected (see text)

a) All values are within 1% error, for solvents at 77°K.
b) In 3MP.
c) h denotes halo-substituted phenylacetylene; values are for 3MP at 77°K.
d) In MC/3MP at Room temperature.
e) From Ref. 19.

singlet-singlet $\pi\pi^*$ transitions of these phenylacetylenes. These results are important in considering the enhancement of S - T transitions for the halophenylacetylenes (Section 5.3).

5.3 Phosphorescence Lifetimes

The observed phosphorescence lifetimes (τ_p's) of phenylacetylene and its halo-derivatives (in glassy solvents at 77°K) are shown in Table 5.1. For lifetimes less than 1 s. a Xenon flash of half-time 0.15 ms was used. Thus all observed lifetimes were greater than that of the flash.

From the phosphorescence lifetimes in pure 3MP and in MC /3MP at 77°K it is seen that there is not much difference for an increase in viscosity[106] by a factor of 10^6. The greatest effect of the heavy-atom is for the substituent in the para-position. These lifetimes are comparable to those obtained for the corresponding α-substituted halonaphthalenes. As expected the lifetime of the $S_o \leftarrow T_1$ transition decreases with the increasing mass of the heavy-atom i.e. becomes more allowed. For the p-F there is a slight increase in lifetime, showing that the heavy-atom effect of the F-atom is not very great. The meta- compounds shows a similar effect with increasing mass of the heavy-atom. However the decrease in the τ_p's of the meta- and ortho-derivatives is not as great as for the corresponding para- halophenylacetylenes. The τ_p's of phenylacetylene and the halophenylacetylenes correspond

quite closely to those reported by McClure[93] for naphthalene, 1-fluoro-, 1-chloro-, 1-bromo- and 1-iodonaphthalene of 2300, 1500, 300, 18 and 2.5 ms, respectively, in EPA at 77°K.

The observed phosphorescence lifetimes, τ_p's, are rationalised[19] in simple spinorbit coupling through equation 2.16;

$$\tau_p^{-1} = (\tau_p^{o})^{-1} + k_i \qquad (5.1)$$

where τ_p^{o} is the radiative phosphorescence lifetime of the triplet state and k_i is the first order rate constant for radiationless deactivation of this state. For any given series of molecules (e.g. the <u>para</u>- halophenylacetylenes) the radiative lifetime $\tau_p^{o}(k)$ is related to the atomic spinorbit coupling factor ζ_h for heavy-atom h by the equation[19];

$$\frac{\tau_p\ (h)}{\tau_p^{o}\ (Cl)} = \left(\frac{\zeta(Cl)}{\zeta(h)}\right)^2 \qquad (5.2)$$

Equation 5.2 is used in calculating column five in Table 5.1, where typical values of ζ are substituted.

From Table 5.1, fourth column, the ratios of the observed phosphorescence lifetimes of the halophenylacetylenes in rigid glasses follow closely the ratios predicted, from equation 5.2, for the radiative lifetimes. This is also found for the 1-halonaphthalenes[19]. Hence, from equations 5.1, it is concluded that since k_i is generally greater than $(\tau_p^{o})^{-1}$, the probability of the radiationless deactivation $T_1 \longrightarrow S_o$ process is proportional to ζ^2 in a similar way as the radiative $T_1 \rightarrow S_o$ process[19].

The results also support the assertion that spinorbit coupling is dominated by one atomic center, since equation 5.2 was derived with this assumption.

The increase in τ_p for p-F is rationalized by the lowering of the electric dipole moment of equation 2.12, which is proportional to $\int \epsilon \, d\vec{v}$. This dilutes the slight heavy-atom enhancement.

The dependence of the τ_p's on the position of the substituent is portrayed by the p-, m-, and o-chlorophenylacetylene results in Table 1. Chlorine in the para position results in a 2 to 3 times shorter lifetime than for the ortho or meta species. Such an observation can be rationalized on the basis of a variation of spin orbit coupling due to a changing MO coefficient at the carbon atom adjacent to the chlorine atom, since the MO coefficient on the carbon governs the delocalization of the electron at the chlorine[69]. The results indicate the absence of a significant ortho effect, as was observed for the halobiphenyls[91]. There the ortho halobiphenyls exhibited a much shorter τ_p than the corresponding meta and para derivatives, since presumably ortho substitution destroyed the coplanarity of the two phenyl rings. Like the halophenylacetylenes, the fluorobenzonitriles[104] show the order:

$$\tau_{p(para)} < \tau_{p(ortho)} < \tau_{p(meta)}.$$

The positional dependence of the observed phosphorescence lifetimes of the halo-phenylacetylenes are consistent with the observations of Roy[92] for the $T_1 \leftarrow S_o$ absorption of some halo-toluenes. Roy found that the $T_1 \leftarrow S_o$ absorption intensity is greater for p-fluorotoluene than for o-fluorotoluene. Now τ_p^o is inversely proportional to the probability (and, hence, spectroscopic intensity) of the $T_1 \leftarrow S_o$ absorption. The increased allowedness of the $T_1 \leftarrow S_o$ absorption and its consequent smaller τ_p^o for <u>para</u>-halo-substituted benzenes can be rationalised on the basis of vector diagrams constructed by Platt[61]. The spectroscopic moment of a substituent is a vector in the plane of the benzene ring and is perpendicular to the bond axis. For singlet-singlet transitions the $-C \equiv CH$, $-CH_3$ and halogen groups have the same vector sign. Assuming this holds for singlet-triplet transitions, the transition moments for <u>para</u>-substituted halophenylacetylenes and halotoluenes should be larger than those of the corresponding <u>ortho</u>- and <u>meta</u>- derivatives. Also the <u>ortho</u>- and <u>meta</u>- derivatives should have about the same transition moments. By relating changes in τ_p as due mainly to changes in τ_p^o Table 5.1 shows that there is very little difference in the <u>ortho</u>- and <u>meta</u>-halophenylacetylenes lifetimes while the greatest effect is in the <u>para</u>-halophenylacetylenes.

5.4 Relative Ratios of the Phosphorescence to Fluorescence Yields

The ratios of the Intersystem Crossing yields, that is $(\phi_p/\phi_f)_h/(\phi_p/\phi_f)\phi CCH$ are presented in column 6 of Table 5.1; the 4:1 MC:3MP solvent system was used. For the para derivatives, this ratio increases rapidly as the mass of the substituent increases. Part of the increase is due to a decrease in the fluorescence quantum yield ϕ_f, where

$$\phi_f = \frac{k_f}{k_F + k_{ISC}} \qquad (5.3)$$

where k_f is the radiative rate constant for fluorescence and internal conversion from S_1 to S_0 is assumed to be not important. Qualitatively ϕ_f must be decreasing, since greater instrumental detection sensitivities are required to record the fluorescences as the mass of the halogen increases. This decrease is due to an increasingly larger value of k_{ISC}, the Intersystem Crossing rate constant, in the RHS of equation 5.3; this is accompanied by only a small variation in k_f, as the results of column 7 of Table 5.1 indicate. Another factor to be considered in the ratio of the Intersystem Crossing yields is the change in ϕ_p with increasing heavy atom. Certainly the triplet quantum yield ϕ_T is increasing, where

$$\phi_T = \frac{k_{ISC}}{k_f + k_{ISC}} \qquad (5.4)$$

and from instrumental sensitivity variations needed to record the phosphorescence spectra, ϕ_p is also increasing, where

$$\phi_D = \phi_T \frac{r_D}{r_D^0} \qquad (2.5)$$

For p-iodophenylacetylene no fluorescence was detected, and the entry in column 6 for that molecule is an estimated lower limit. A photochemically produced impurity was detected for p-iodophenylacetylene, which luminesced in a region 2,500 cm^{-1} to the red of the expected position for fluorescence of p-iodophenylacetylene. The impurity is most likely formed from intramolecular photochemical cleavage of the I-$C_{(sp)}$ bond; such reactions were found for p-bromo- and p-iodobiphenyl in a rigid glass at 90°K.[105] The excitation spectrum obtained by monitoring the fluorescence spectrum is different from that obtained by monitoring the phosphorescence spectrum of p-I, showing that the two emissions are from different molecules. The impurity has a long lived phosphorescence emission (about 0.1 sec) in the green region, showing that this impurity is not a hydrocarbon radical or an iodobenzene derivative. A substituted phenyl radical[95] should fluoresce below 20,000 cm^{-1}.

The Intersystem Crossing yield also increases with heavy atom for the meta-substituted halophenylacetylenes, although here the effect is not as dramatic as in the para position. In the fluorobenzonitriles a similar result was found for the para versus meta-derivatives, and mirrors the phosphorescence lifetime trends.

5.5 Vibrational Analysis of the Phosphorescence Spectra of the Halophenylacetylenes

(a) Fundamental Vibrational Modes

Like phenylacetylene, the halophenylacetylenes have 36 fundamental vibrational modes. For purposes of detailed comparison these modes are given the same ν-notation as phenylacetylene, with appropriate changes in the approximate descriptions to take in account the introduction of the halogen atom. Replacement of a ring H-atom by a halogen atom (h) changes an in-plane bending mode, β C-H, to β C-h, an out-of-plane bending mode, γC-H, to γC-h and a stretching mode, ν, C-H, to ν C-h.

The literature lacks data on the frequencies of the ground state fundamentals of the halophenylacetylenes. However, assignments were made by comparison with other disubstituted benzenes and by the polarizations of certain bands (which helped in the assignment of symmetries). The assignments of the expected ranges given in the comprehensive text by Varsanyi[70], and references therein, proved useful. Also, for the meta- and ortho-derivatives the work on substituted styrenes[71] was used. Comparison of the phosphorescence spectra of the halophenylacetylenes reveals great similarities in vibrational activity. This strengthened the case for the assignments. Some frequencies are expected to remain relatively unchanged (mainly those related to the ring stretching modes and the acetylenic mode), while others are expected to decrease significantly as the mass of the heavy atom increases (mainly the C-h

modes). Nearly all the fundamentals which appear in the phosphorescence spectra that are of benzene parentage can be identified. Also, those related to the substituents are identified.

(b) Para-halophenylacetylenes

The phosphorescence spectra of the para-halophenylacetylene in DMC are shown in Figure 5.1(A) - 5.4(A). The polarized spectra in a glass are shown in Figure 5.1(B) - 5.4(B). Table 5.2 shows a listing of the assigned ground state fundamentals. The vibrational analyses are shown in Table 5.3. In general the same modes which appear in phenylacetylene are observed in the phosphorescence spectra of the para-halophenylacetylenes. However, there are some significant changes in intensities, related to the greater vibrational activity as Subspectrum II becomes of greater importance, relative to Subspectrum I.

The positions of the origin or 0,0 bands in DMC are 27480 (p-F), 24485 (p-Cl), 24475 (p-Br) and 24240 (p-I) cm^{-1}. Compared with phenylacetylene (in MC), para-substitution by fluorine blue shifts the $S_o \leftarrow T_1$ transition by 2160 cm^{-1} while there is a red shift by about the same energy in the cases of p-Cl (835 cm^{-1}), p-Br (845 cm^{-1}) and p-I (1080 cm^{-1}). The intensity of the 0, 0 band relative to the most intense band of the spectrum is less as the mass of the heavy atom increases. The sharpest spectrum is that of p-Br, the next sharpest is p-Cl, and the least sharp is p-F (this seems related to solvent fit).

TABLE 5.2

FUNDAMENTALS OBSERVED IN THE PHOSPHORESCENCE SPECTRA OF THE PARA-HALOPHENYLACETYLENES

Symmetry	Designation[a]		Description		Frequency (cm^{-1})[b] p-F	p-Cl	p-Br	p-I
a_1	4	7a	ν	C-h	1180 (1159)	360 (349)	315 (270?)	295
	5		ν	C≡C	2145	2135	2130 (2104)	2120
	6	8a	ν	C-C	1595 (1608)	1595 (1599)	1585 (1582)	1575
	7	19a	ν	C-C	1490 (1506)	1475	1465	1465
	8	13	ν	C-CCH	1280 (1293)	1225 (1191)	1190 (1185)	1200
	9	9a	β	C-H	1130 (1129)	1175 (1170)	1175 (1171)	1160
	11	1		Ring	835 (846)	1095 (1083)	1065 (1067)	1050
	12	12(6a)		Ring	690 (677)	785 (775)	775 (763)	790
	13	6a(12)	α	C-C-C	480 (496)	500 (512)	495	475
b_1	17	5(10b)	γ	C-H	950	1010	1005	970
	18	17b(11)	γ	C-H		830	825	815
	19	11(17b)	γ	C-h		155	105	105
	20	4	ϕ	C-C	710	710	700	690
	21		γ	CC-H	620	620	615	610

TABLE 5.2 (CONTINUED)

Symmetry	Designation[a]	Description	Frequency (cm^{-1})[b] p-F	p-Cl	p-Br	p-I
	22 16b	ϕ C≡C	445	405	390	375
	23 10b(5)	γ C-H	305	230	210	190
	24	γ C-C≡C			155	
b_2	32 18b	β C-H		1150	1105	1090
	33	β CC-H	650 (635)	640 (633)	650 (632)	
	36 9b	β C-CCH	400 (378)	320	224 (270)	

a. First column gives i's of ν_i, second gives Wilson notation for substituted benzenes (Ref. 30); designation in brackets holds for p-F only i.e. when both substituents are light. (Less than 25 amu, from Ref. 70).

b. Values in brackets are for peaks observed in the Raman spectra at -35°C.

To the blue of the 0, 0 band side bands appear in p-Cl (145 cm^{-1}), p-Br (115 cm^{-1}) and p-I (90 cm^{-1}). As in phenylacetylene no band appear in p-F. These bands are discussed later in Chapter 6.

The eight a_1 fundamentals, which make up most of the phosphorescence spectrum of phenylacetylene appear in the phosphorescence spectra of the para-halophenylacetylenes. In addition, ν_4, now a C-h stretch, appears. In <u>para</u>-disubstituted benzenes both triangles of the David's star are loaded[70], hence the frequencies of both ν_{11} (1, in the Wilson notation) and ν_{12}(12) are substituent sensitive. In p-F, both substituents are light, therefore, the ring breathing mode, ν_{11}, decreases in frequency. When at least one of the substituents is heavy the frequency increases. Hence the 0,11 transition is found at 835 cm^{-1} in p-F (a strong peak), 1095 cm^{-1} in p-Cl (a medium-weak peak), 1065 cm^{-1} in p-Br (a weak peak) and 1050 cm^{-1} in p-I (a very weak peak). Since the masses of the substituents are different, ν_{12} (12) also has breathing character and is assigned at 690 cm^{-1} in p-F (weak peak), 785 cm^{-1} in p-Cl (medium intensity peak), 775 cm^{-1} in p-Br (weak shoulder). In p-F the intensity of the 0,11 transition, relative to the 0, 0 band is greater than that of phenylacetylene or the other halo-

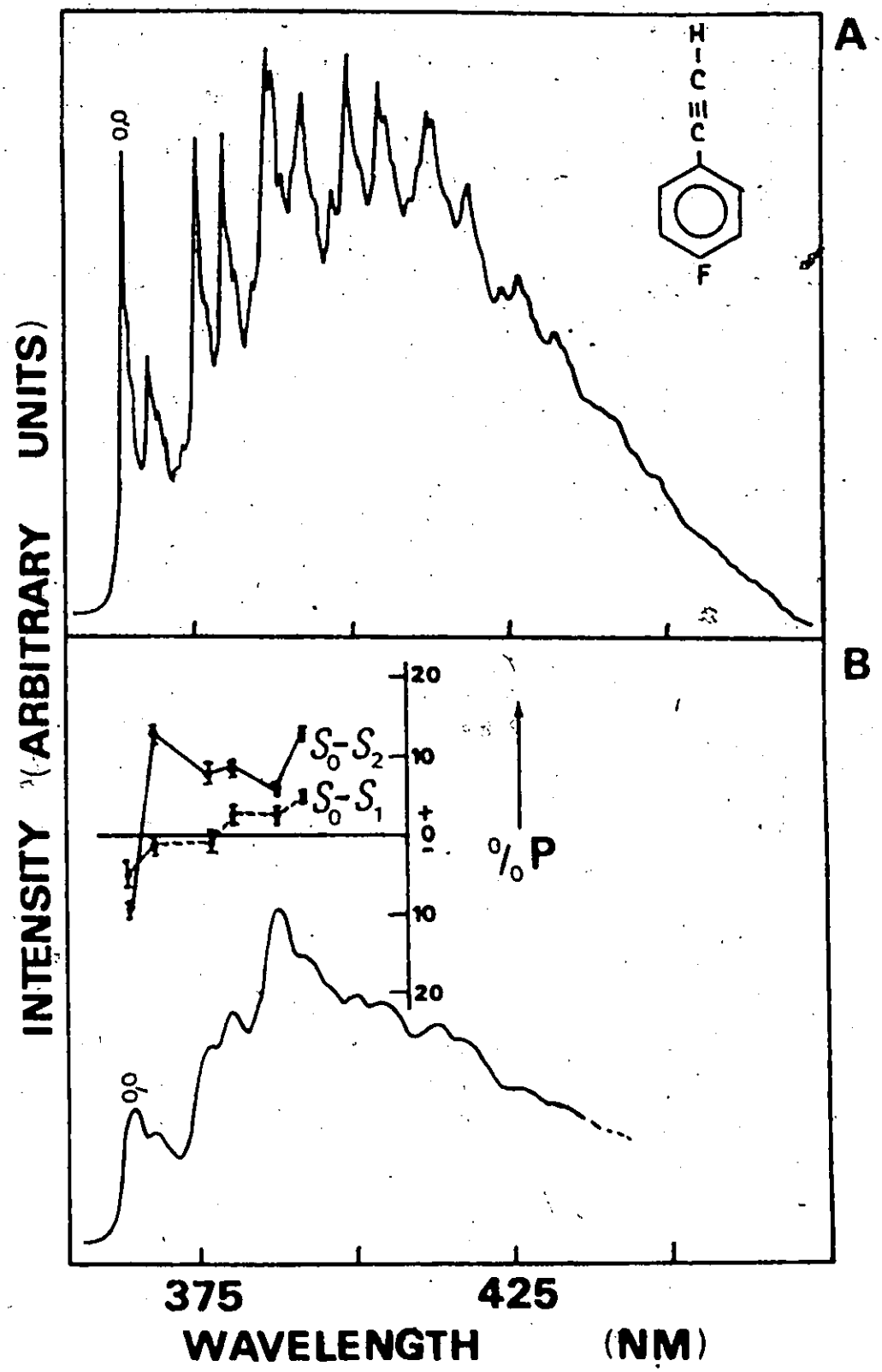

FIG.5.1 THE PHOSPHORESCENCE SPECTRUM OF 10^{-3}M p-F ϕCCH AT 77°K (A) IN TRANS-1,4-DIMETHYLCYCLOHEXANE (B) IN A RIGID GLASS

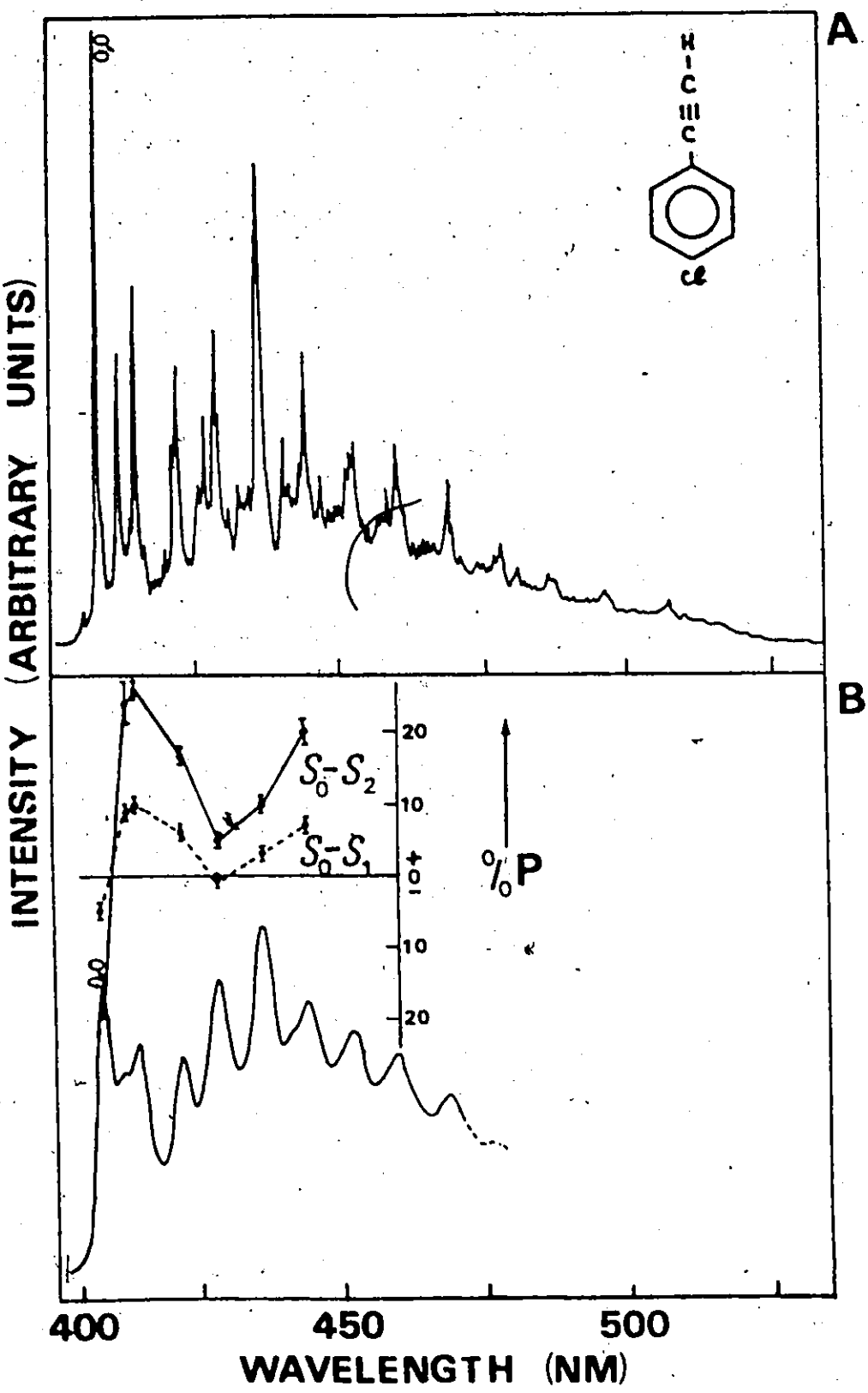

FIG.52 THE PHOSPHORESCENCE SPECTRUM OF 10^{-3}M p-ClϕCCH AT 77°K (A) IN TRANS-1,4-DIMETHYLCYCLOHEXANE (B) IN A RIGID GLASS

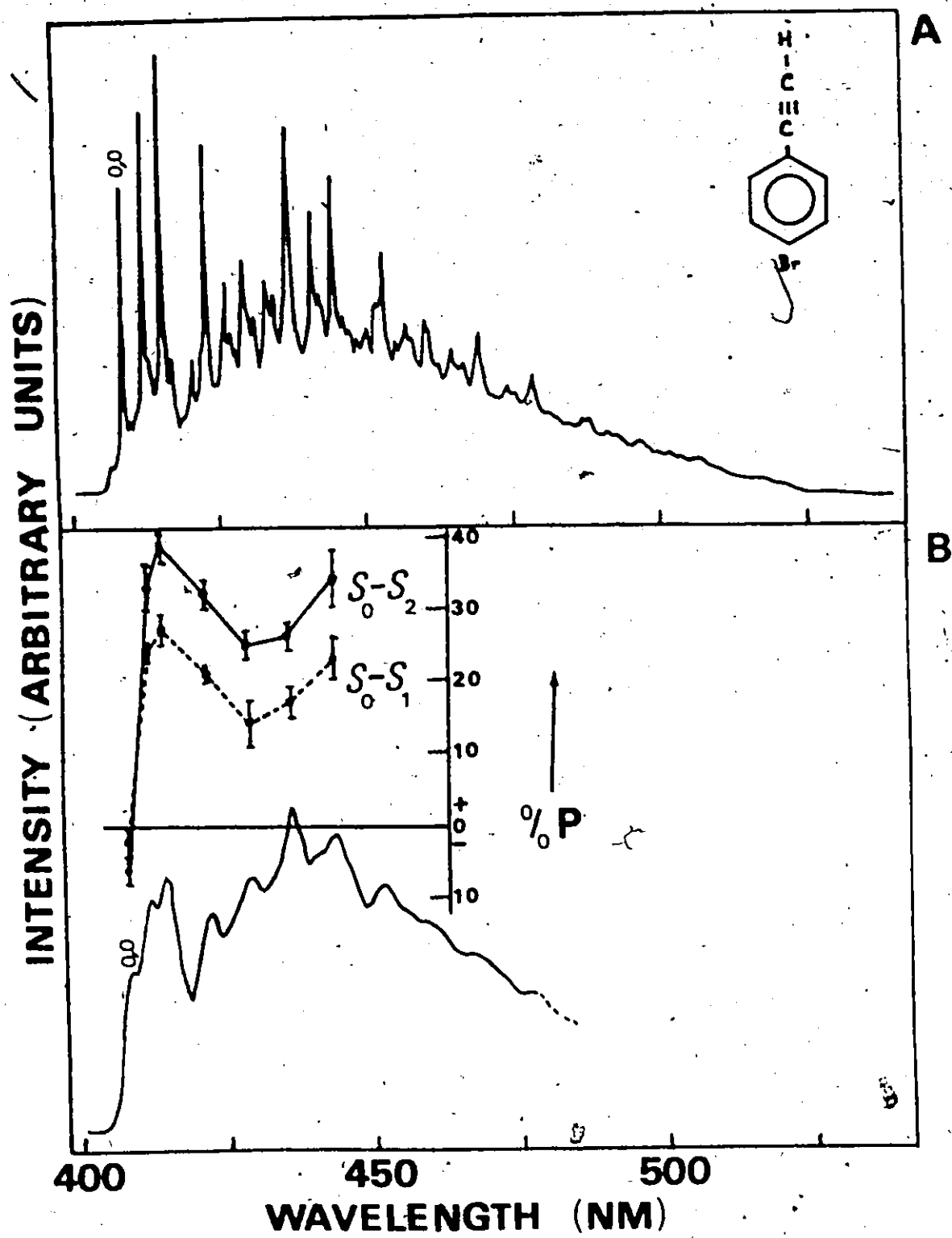

FIG.5.3 THE PHOSPHORESCENCE SPECTRUM OF 10^{-3}M p-BrφCCH AT 77°K (A) IN TRANS-1,4-DIMETHYLCYCLOHEXANE (B) IN A RIGID GLASS

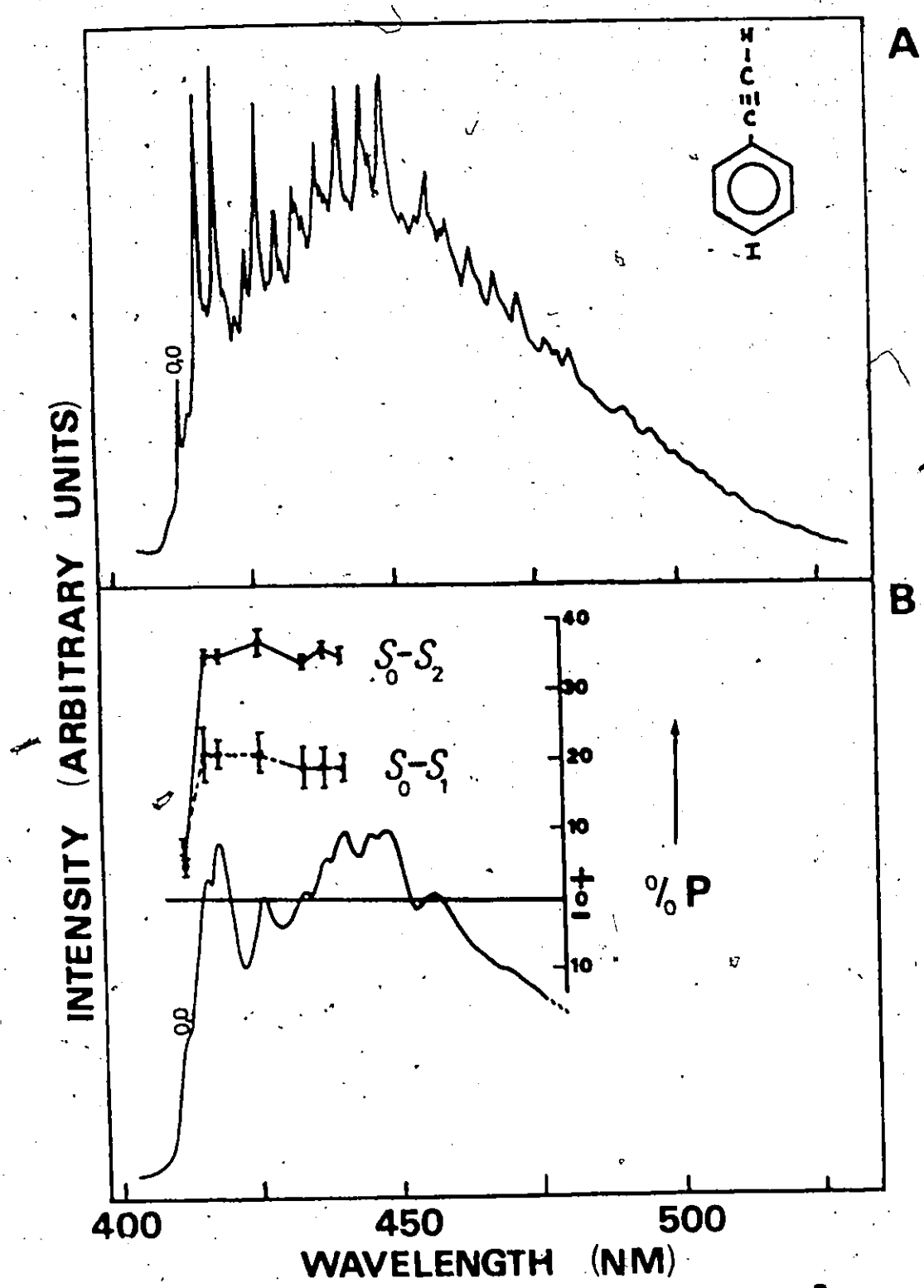

FIG.5.4 THE PHOSPHORESCENCE SPECTRUM OF 10^{-3}M p-I ϕCCH AT 77°K (A) IN TRANS-1,4-DIMETHYLCYCLOHEXANE (B) IN A RIGID GLASS

TABLE 5.3

VIBRATIONAL ANALYSES OF THE PHOSPHORESCENCE SPECTRA OF 10^{-3}M PARA-FLUORO-, -CHLORO-, -BROMO- AND -IODOPHENYLACETYLENE IN TRANS-1, 4-DIMETHYLCYCLOHEXANE AT 77°K

Frequency (cm^{-1})[a]				Assignment[b]
p-F	p-Cl	p-Br	p-I	
				0, Lattice
100	75			
	155	105	105*	0,19 (II)
		155*		0,24 (II)
305	230	210	190	0,23 (II)
400	320	280*		0,36
	360	315	295	0,4 (I)
445*	405	390	375	0,22 (II)
480	500	495	475	0,13 (I)
	590	550*	475	0,4 + 23 (II)
620*	620	615	610	0,21 (II)
650	640	650*		0,33
	680			0,4 + 36
		675		0,22 + 36
	710	700	690	0,20 (II)
690	785	775*	790*	0,12 (I)
	830	825	815	0,18 (II)
835				0,11 (II)
	865*			0,4 + 13 (I)
	910*	900	830	0,13 + 22 (II)
	945			0,2 x 4 + 23 (II)

TABLE 5.3 (CONTINUED)

Frequency (cm^{-1})[a]				Assignment[b]
p-F	p-Cl	p-Br	p-I	
950*	1010	1005	970	0,17 (II)
	1045			0,22 + 33
	1095	1065	1050	0,11 (I)
1130	1175	1175	1160	0,9 (I)
1180*				0,4 (I)
1280	1225	1190	1200	0,8 (I)
	1320	1285	1245	0,11 + 33 (II)
		1335	1265	0,4 + 17 (II)
1445	1405	1390	1380	0,9 + 23 (II)
	1430			0,4 + 11 (I)
	1460	1390	1380	0,8 + 33 (II)
		[illegible]	1435	0,11 + 22 (II)
1490*	1475	1465	1465	0,7 (I)
			1555	0,8 + 22 (II)
1595	1595	1585	1575	0,6 (I)
1655				0,2 x 11 (I)
1785	1685*	1680*	1675	0,7 + 33 (II)
	1805*	1760*		0,11 + 20 (II)
1910	1830	1800	1775	0,6 + 23 (II)
	1880	1830*	1810*	0,11 + 12 (I)
	1925	1885*	1825*	0,9 + 20 (I)
	1960	1945	1875	0,9 + 12 (I)
			1875	0,11 + 18 (II)
	2005	1990	1965	0,6 + 22 (II)
			1980	0,9 + 18 (II)
	2100	2065*	2020	0,11 + 17 (II)
2060*	2100	2075	2045*	0,6 + 13 (I)

TABLE 5.3 (CONTINUED)

Frequency (cm^{-1})[a] p-F	p-Cl	p-Br	p-I	Assignment[b]
		2130	3095*	0,2 x 11 (I)
2145*	2135	2130	2120*	0,5 (I)
	2190			0,2 x 11 (I)
	2190	2195	2165	0,9 + 17 (II)
	2225		2195	0,6 + 21 (II)
2285				0,6 + 12 (I)
	2275	2245	2195	0,9 + 11 (I)
	2300	2285	2270	0,6 + 20 (II)
	2360	2360		0,2 x 9 (I)
	2380		2345*	0,8 + 9 (I)
	2430	2415	2395	0,2 x 8 (I)
	2490	2470	2445	0,7 + 17 (II)
	2535	2525	2510	0,5 + 22 (II)
	2615	2605	2560	0,6 + 17 (II)
2430	2675	2645		0,6 + 11 (I)
	2735*	2695		0,2 + 2 x 12 (I)
2745	2765	2780	2760	0,6 + 9 (I)
2860*	2790*	2795	2760	0,6 + 8 (I)
	2845	2815		0,5 + 20 (II)
	2890	2840		0,2 x 9 + 13 (I)
	2920	2870	2830	0,6 + 11 + 23 (II)
	2970	2895*		0,2 x 11 + 12 (I)
		2950*		0,2 x 9 + 21 (II)
	3015	2975	2960	0,6 + 12 + 21 (II)

TABLE 5.3 (CONTINUED)

Frequency (cm^{-1})[a]				Assignment[b]
p-F	p-Cl	p-Br	p-I	
3060	3070	3055	3020*	0,6 + 7 (I)
	3140*	3065*	3055	0,4 + 6 + 9 (I)
3210	3190	3180	3165	0,2 x 6 (I)
	3225*			0,6 + 12 + 18 (II)
3280				0,6 + 2 x 11 (I)
	3265*	3250*	3200*	0,6 + 9 + 13 (I)
3395				0 6 + 9 + 12 (I)
	3305	3280*	3260*	0, 6 + 7 + 23 (II)
		3305		0,9 + 2 x 11 (I)
3510	3420	3380*	3340*	0,2 x 6 + 23 (II)
	3470	3395		0, 6 + 11 + 12 (I)
	3520			0,3 x 9 (I)
		3460	3450	0,6 + 9 + 20 (II)
	3550			0,6 + 9 + 12 (I)
3595	3580	3585	3545*	0,2 x 6 + 22 (II)
	3630	3605	3570	0,6 + 8 + 18 (II)
3660	3700*	3670	3630	0,2 x 6 + 13 (I)
	3725	3690	3695	0,5 + 6 (I)
	3780	3715		0,6 + 2 x 11 (I)
	3810	3765	3750	0,2 x 6 + 21 (II)
	3895	3875	3830*	0,2 x 6 + 20 (II)
	3945	3950	3860*	0,6 + 2 x 9 (I)
3890	3965			0,2 x 6 + 12 (I)
	4010	4000	3935	0,2 x 6 + 18 (II)
	4075	4065*	3995	0,6 + 7 + 17 (II)
	4125	4120		0,5 + 6 + 22 (II)

TABLE 5.2 (CONTINUED)

Frequency (cm^{-1})[a]				Assignment[b]
p-F	p-Cl	p-Br	p-I	
	4215	4185	4150	0,2 x 6 + 17 (II)
	4240			0,3 x 9 + 20 (II)
4040	4270	4235	4205*	0,2 x 6 + 11 (I)
	4360	4340	4345	0,2 x 6 + 9 (I)
4355	4495	4450		0,6 + 2 x 9 + 13 (I)
	4540	4585	4410	0,2 x 6 + 11 + 23 (II)
	4580	4545	4455	0,6 + 9 + 11 + 20 (II)
4720	4780	4730	[illegible]	0,3 [illegible] (I)
5185	5170	5170	5115	0,3 x 6 + 23 (II)

* Denotes shoulder.

a. Error about ± 10cm^{-1}

b. The i of ν_i is listed (see Table 5.1); I denotes Subspectrum I; II denotes Subspectrum II.

phenylacetylenes, and shows a decrease in intensity with increasing mass of the heavy atom. On the other hand ν_{13} (6a) shows very little intensity changes and is assigned to the weak peak at 480 (p-F), 500 (p-Cl), 495 (p-Br) and 475 cm^{-1} (p-I). In p-I the intensity of the 0, 13 transition is pushed up by the 0, 4 + 23 combination band.

The two totally symmetric C-C stretches ν_6 (8a) and ν_7 (19a) appear at approximately the same frequencies as in phenylacetylene. There is only a slight decrease in frequency with increasing mass of heavy atom. As in phenylacetylene 0,6 is the most intense a_1 vibrational transition and is found at 1595 cm^{-1} in p-F (very strong peak), 1595 cm^{-1} in p-Cl (strong peak), 1585 cm^{-1} in p-Br (strong peak) and 1575 cm^{-1} in p-I (medium intensity peak). Appearing as weak peaks are 0,7 at 1490 (shoulder, p-F), 1475 (p-Cl), 1465 (p-Br), and 1465 cm^{-1} (p-I).

The C-H in-plane deformation transition, 0,9 appears with medium intensity at 1180 (shoulder, p-F), 1175 (peak, p-Cl), 1175 (peak, p-Br) and 1160 cm^{-1} (peak, p-I).

The two C-X stretches (13 and 7a, Wilson notation) cannot be discussed separately since these modes couple with the C-C stretching modes, 1 and 12 of benzene. Here ν C-CCH is defined as 13 and νC-h as 7a. For two light substituents the C-X stretches are both above 1100 cm^{-1}. If at least one of the substituent is heavy the distinction between the C-X stretching vibration and the C-C-C in-plane bend is not easy to justify. Here 7a couples to 6a and is found below 400 cm^{-1}, while 13 couples to 12 and is found above 1100 cm^{-1}. Thus the 0,8 and 0,4 transitions occur at 1280 and 1180 cm^{-1}, respectively in p-F. For the heavier substituents, 0,8 occurs at 1225 (p-Cl), 1190 (p-Br) and 1200 cm^{-1} (p-I), while 0,4 is found at 360 (p-Cl), 315 (p-Br) and 295 cm^{-1} (p-I). The 0,8 peaks are of medium intensity, less than the 0,9 peaks, except in p-Br where 0,8 increases to about the same intensity as 0,9.

The in-plane acetylenic stretching mode is seen as the 0,5 transition at 2140 (weak shoulder, p-F), 2135 (weak peak, p-Cl), 2130 (weak peak, p-Br) and 2120 cm^{-1} (very weak shoulder, p-I).

As in phenylacetylene the contribution to the phosphorescence spectrum from b_2 modes is very weak. One in-plane C-H deformation mode is seen as 0,30 at 1150 (p-Cl) 1105 (p-Br) and 1090 cm^{-1} (p-I); it is absent in p-F. The acetylenic C-H in-plane deformation occurs as the 0,33 transition at 650 (shoulder, p-F), 640 (p-Cl) and 650 cm^{-1} (p-Br). The 0,36 transition due to the substituent-sensitive in-plane deforma-

tion, between ring and substituent is seen at 350 (p-F), 310 (p-Cl) and 280 cm^{-1} (p-Br).

In phenylacetylene, five b_1 modes are identified. In the halo-phenylacetylenes additional b_1 modes arise. Unlike phenylacetylene, the out-of-plane deformation between the acetylenic group and the benzene ring, ν_{24}, does not contribute to the vibronic coupling scheme except in p-Br, where it occurs as the very weak shoulder at 155 cm^{-1}.

In p-Cl, p-Br and p-I, two out-of-plane C-H deformations, ν_{17} (5) and ν_{18} (17b) now appear. The more intense transition of the two, 0,18 occurs at 1010 (moderately strong peak, p-Cl) 1005 (strong peak, p-Br), and 970 cm^{-1} (strong peak, p-I); the less intense, 0,17 is seen at 830 (weak peak, p-Cl), 825 (moderately strong peak, p-Br) and 815 cm^{-1} (moderately strong peak, p-I). In p-F the weak shoulder at 950 cm^{-1} is assigned to 0,17.

The acetylenic out-of-plane C-H deformation remains essentially unchanged in frequency with the 0,21 transition at 620 (very weak shoulder, p-F) 620 (weak peak, p-Cl), 615 (weak peak, p-Br), and 610 cm^{-1} (weak peak, p-I).

Of the two out-of-plane C-X deformations appearing, ν_{19}(11) is very weak at 155 (p-Cl), 105 (p-Br) and 105 cm^{-1} (shoulder, p-I); the substituent-sensitive ν_{23} (10b) is found at 305 (p-F), 230 (p-Cl), 210 (p-Br) and 190 cm^{-1} (p-I), with intensity increasing from moderately strong to strong as the mass of the heavy-atom increases.

The substituent-sensitive ring out-of-plane deformation, ν_{22} (16b), also increases greatly in intensity at 445 (shoulder, p-F), 405 (p-Cl), 390 (p-Br), and 375 cm^{-1} (p-I). The other ring out-of-plane deformation, ν_{20}(4) shows very little frequency change as weak peaks at 710 (p-Cl), 700 (p-Br) and 690 cm^{-1} (p-I). It is absent or hidden by the 0,12 transition in p-F.

The symmetry assignments of the major bands of the phosphorescence spectra are supported by the polarizations of the peaks (see Figure 5.1 - 5.4(B). In-plane modes (here of a_1 symmetry) are negatively polarized while out-of-plane modes are positively polarized. The mixed polarizations obtained are consistent with the vibrational assignments. Peaks 2, 3, and 4 are more positively polarized than their neighboring peaks supporting their assignments as the b_1 mode transitions 0,23, 0,22, and 0,18. Peaks 5 and 6 (5 and 7 in p-I) are less positive than the neighboring peaks, but never become actually negative (because of the strong positive contributions of overlapping peaks); this supports the assignments of peak 5 as ν_9 (and ν_8) and peak 6 (peak 7 in p-I) as 0,6. All other major peaks are a combination 0, b_1 + a_1 vibrations, giving a net b_1 symmetry; hence they are in-plane polarized. For the p-F, Figure 5.1(B), peaks 2 and 6 are more positively polarized than their neighbors in conformity with the assignments of 0,23 (b_1) and 0, 6 + 23. Peaks 3, 4 and 5 are consistent with 0, a_1 assignments (0,11, 0,9 and 0,6, mainly).

Peaks observed in the Raman spectra of solid p-F, p-Cl and p-Br at -35°C correspond very closely to most of the a_1 and

b_2 (in-plane) modes observed in the phosphorescence spectra of these compounds (Table 5.2). Confidence in these assignments is strengthened by comparison of their relative intensities with the 0, 0 band. In general, all modes of a_1 and b_2 symmetries are in the same ratio to the 0,0 as they are in phenylacetylene for p-Cl, p-Br and p-I. As the mass of the heavy-atom increases, the b_1 modes increase in spectral importance in about the same ratio to each other.

Furthermore, the assigned modes have frequencies in the range given by Varsanyi[70]. More specifically vibrational assignments for the para-halofluorobenzenes[27, 99] and para-diethynylbenzene[29] support these assignments.

The vibrational analyses of Subspectrum I in the para-derivatives are similar to that of phenylacetylene. For Subspectrum II one quantum of b_1 vibration is coupled to the assignments of Subspectrum I. As in phenylacetylene the most active a_1 vibration is ν_6, with moderate activity in ν_9 and ν_{11}.

(c) Meta-chloro- and -bromophenylacetylenes

The phosphorescence spectra of 10^{-3} M meta-chlorophenylacetylene (m-Cl) and meta-bromophenylacetylene (m-Br) in methylcyclohexane at 77°K are shown in Figure 5.5(A) and 5.6(A). The polarized spectra in the glass consisting of methylcyclohexane and 3-methylpentane (4:1 by volume) are shown in Figure 5.5(B) and 5.6(B). Table 5.4 lists the ground state frequencies while Table 5.5 gives the vibrational analyses of the phosphorescence spectra in polycrystalline methylcyclohexane.

The 0, 0 bands, assigned at 25040 cm^{-1} (m-Cl) and 25015 cm^{-1} (m-Br), are red-shifted compared with phenylacetylene by 280 cm^{-1} and 305 cm^{-1}, respectively.

There are three side bands to the blue side of the origin band at 275, 180, 125 cm^{-1} (m-Cl) and 195, 130, 90 cm^{-1} (m-Br).

Like the para-halophenylacetylenes the phosphorescence spectra of m-Cl and m-Br can be resolved into Subspectrum I and Subspectrum II, with both subspectra of about the same intensity. The vibrational analyses is similar for both m-Cl and m-Br.

Meta-substitution reduces the symmetry to C_s, with the in-plane modes, a_1 and b_2 (C_{2v}), becoming a'(C_s) and the out-of-plane modes, a_2 and b_1 (C_{2v}) becoming a'' (C_s). For purposes of

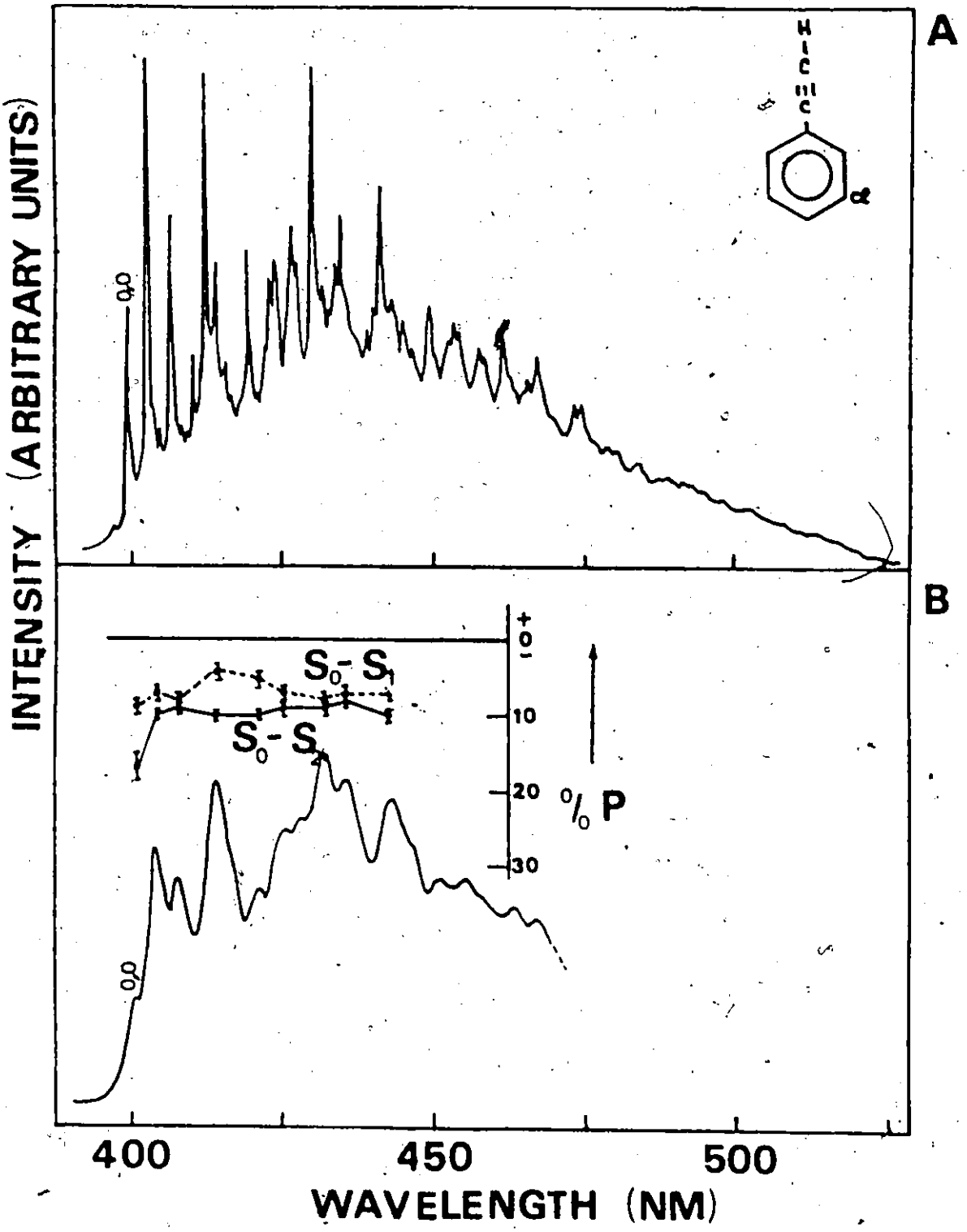

FIG. 5.5 THE PHOSPHORESCENCE SPECTRUM OF 10^{-3} M m-ClØCCH AT 77 °K (A) IN METHYLCYCLOHEXANE (B) IN A RIGID GLASS

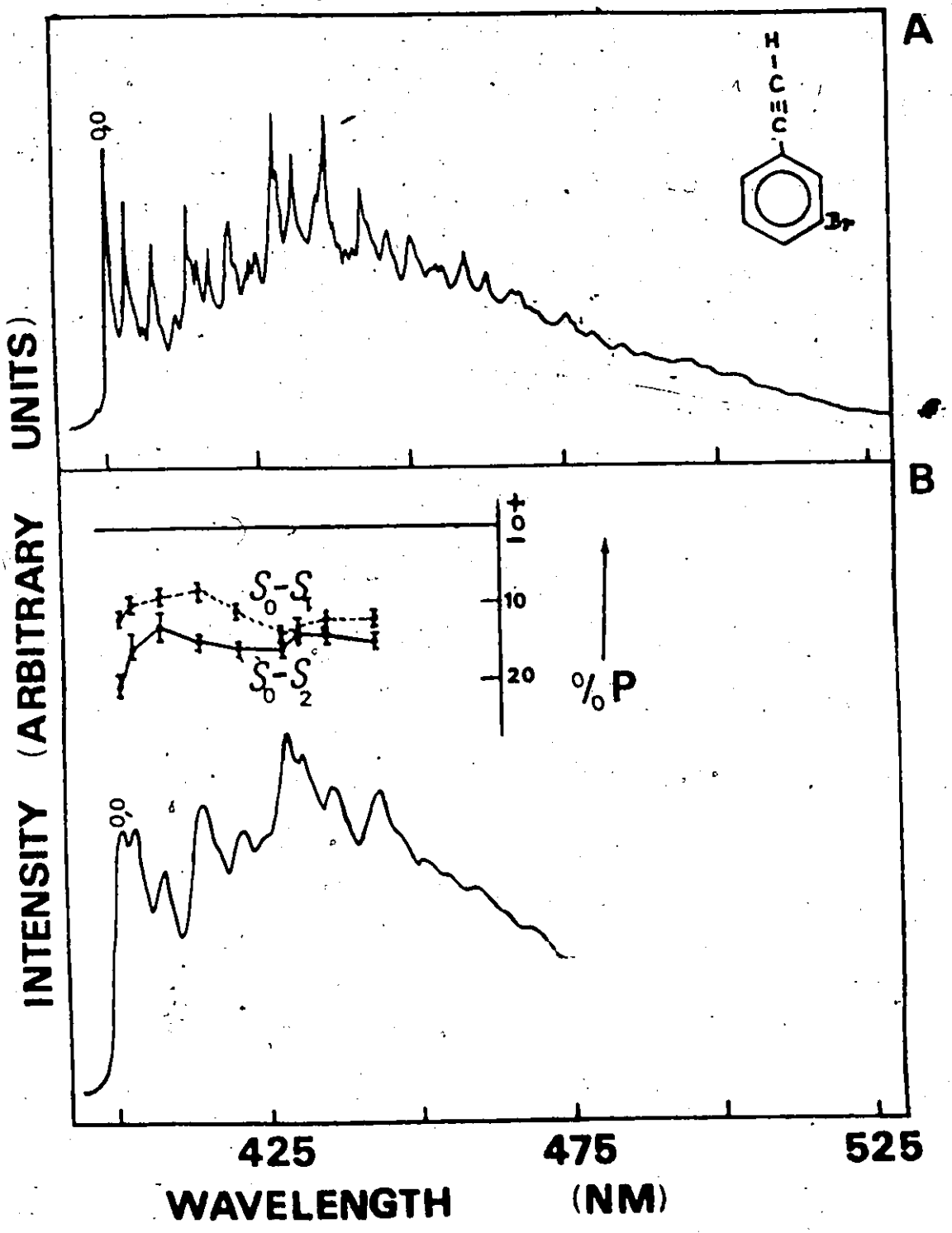

FIG. 5.6 THE PHOSPHORESCENCE SPECTRUM OF 10^{-3} M m-BrØCCH AT 77 °K (A) IN METHYLCYCLOHEXANE (B) IN A RIGID GLASS

comparison the designations and numbering of the vibrational modes are kept the same as for phenylacetylene.

The a' fundamentals occur with greater and the a'' with less intensities in m-Br than in m-Cl, consistent with the ratio of Subspectrum II to Subspectrum I. Two in-plane aromatic C-C stretches, ν_6 (8a) and ν_7 (19a), occur at 1610, 1415 cm^{-1} (m-Cl and 1605, 1385 cm^{-1} (m-Br), respectively. The frequency of ν_6 (moderately strong peak in m-Cl and very strong peak in m-Br) is essentially unchanged compared with phenylacetylene; there is a slight decrease in frequency for ν_7 (the moderately intense peaks). The ring breathing mode ν_{11} (12) occurs with no change in frequency at 1000 cm^{-1} in both (medium-weak peak in m-Cl and moderately intense peak in m-Br). The C-H in-plane deformation, ν_{32} (18b), is seen as the very weak peaks at 1095 (m-Cl) and 1105 cm^{-1} (m-Br). The acetylenic C-X in-plane deformation occurs at 655 cm^{-1} (m-Cl and 625 cm^{-1} (m-Br) with very weak intensity. Two in-plane C-X deformations, ν_9 (9a) and ν_{31} (15), show a great drop in frequency compared with the corresponding C-H modes in phenylacetylene; ν_9 occurs at 295 cm^{-1} (m-Cl) and 255 cm^{-1} (m-Br) as weak shoulders; ν_{31} is seen only in m-Br as weak shoulder at 295 cm^{-1}. Three in-plane substituent-sensitive modes are assigned; ν_8 (13), the stretch between the ring and substituent occurs as a weak shoulder at 1245 cm^{-1} (p-Cl) and the moderately strong peak at 1200 cm^{-1} (m-Br); of the two ring deformations ν_{12} (1) occurs at 690 cm^{-1} (m-Cl) and 680 cm^{-1} (m-Br) as medium-weak peaks, while ν_{13} (6a) at 510 (m-Cl) and 535 cm^{-1}

TABLE 5.4

FUNDAMENTAL VIBRATIONAL MODES OBSERVED IN THE PHOSPHORESCENCE SPECTRA OF META-CHLORO-, META-BROMO- & ORTHO-CHLOROPHENYLACETYLENE

Symmetry	Designation[a]		Description	Frequency (cm^{-1}) b		
				m-Cl	m-Br	o-Cl
a'	4	7a	ν C - h			375
	5		ν C ≡ C	2105	2145	
	6	8a	ν C - C	1610	1605	1600
	7	19a	ν C - C	1415	1385	1385
	8	13	ν C - CC..	1245	1200	1240
	9	9a	β C - h	295	255	
	11	12		1000	1000	1045
	12	1	α C - C - C	990	980	980
	13	6a	α C - C - C	510	505	
	26	7b	ν C - h	365	355	
	31	15	β C - h		995	
	32	18b	β C - H	1095	1105	
	33		β C - CC..	655	625	
a"	17	5	γ C - H			990
	18	17b	γ C - H	915	900	890
	19	11	γ C - H	800	795	730
	21		γ C - H	590	560	550
	22	16b	ϕ C - C	460	450	465
	23	10b	γ C - h	215	190	210
	24		γ C - C ≡ C			155

a. First column gives i's of ν_i, second gives Wilson notation for substituted benzenes (Ref.30).

TABLE 3.5

VIBRATIONAL ANALYSES OF THE PHOSPHORESCENCE SPECTRA OF 10^{-3}M META-CHLORO-, META-BROMO- & ORTHO-CHLOROPHENYLACETYLENE IN METHYLCYCLOHEXANE AT 77°K

Frequency (cm^{-1})[a]			Assignment[b]
m-Cl	m-Br	o-Cl	
		155	0,24 (II)
215	190	210	0,23 (II)
295*	255*		0,9 (I)
	295*		0,11
365	355		0,[illegible]
		375	0,4 (I)
460	450	465	0,22 (II)
510*	535*		0,13 (I)
590	560*	550	0,21 (II)
655*	625	[illegible]	0,33
		730	0,19 (II)
690	680	840	0,[illegible] (I)
800	795		0,19 (II)
	830		0,9 + 21 (II)
915	900	890	0,18 (II)
		945	0,4 + 21 (II)
		990*	0,17 (II)
1000	1000	1045	0,11 (I)
1065			0,9 + 19 (I)
1095	1105		0,[illegible]
		1140	0,21 + 33
		1175	0,9 (I)

TABLE 5.5 (CONTINUED)

Frequency (cm^{-1})[a]			Assignment[b]
m-Cl	m-Br	o-Cl	
1130	1145		0,12 + 22 (II)
1215	1145		0,9 + 18 (II)
1215	1185*		0,11 + 23 (II)
1245	1200	1240	0,8 (I)
1300	1240		0,12 + 21 (II)
1300	1255		0,9 + 11 (I)
1300	1315		0,13 + 19 (II)
		1295	0,12 + 22 (II)
		1355	0,10 + 21 (II)
		1410	0,8 + 24 (II)
1370	1365		0,2 x 12 (I)
1415	1385	1485	0,7 (I)
1460	1440		0,11 + 22 (II)
1610	1605	1600	0,6 (I)
1665	1645		0,8 + 22 (II)
1690	1685		0,11 + 12 (I)
		1685	0,7 + 23 (II)
		1760	0,6 + 25 (II)
1800	1780	1805	0,6 + 23 (II)
1890	1850		0,6 + 9 (I)
	1900		0,11 + 18 (II)
		1935	0,7 + 22 (II)
		1975	0,4 + 6 (I)
1965	1970		0,2 x 11 (I)

TABLE 5.5 (CONTINUED)

Frequency (cm^{-1})[a]			Assignment[b]
m-Cl	m-Br	o-Cl	
2005	2000		0,8 + 19 (II)
2050	2040	2055	0,6 + 22 (II)
2095*	2105*		0,6 + 13 (I)
2105*	2140		0,5 (I)
2200	2171	2155	0,6 + 21 (II)
		2200	0,6 + 33
2225	2210		0,6 + 11 (I)
2290	2265		0,6 + 12 (I)
		2285	0,8 + 11 (I)
		2330	0,6 + 19 (II)
2350*	2320		0,6 + 9 + 22 (II)
2390	2390		0,6 + 19 (II)
2490	2490*		0,6 + 12 + 23 (II)
2505	2510	2465	0,6 + 18 (II)
		2535	0,4 + 6 + 20 (II)
		2590	0,6 + 17 (II)
2595	2605	2685	0,6 + 11 (I)
2650	2690*		0,2 x 11 + 12 (I)
2810	2785		0,6 + 11 + 23 (II)
		2780	0,6 + 9 (I)
2830	2805	2860	0,6 + 8 (I)
	2840		0,6 + 12 + 13 (I)
	2930		0,5 + 19 (II)
	2955		0,6 + 2 x 12 (I)
		2890	0,6 + 11 + 22 (II)

TABLE 5.5 (CONTINUED)

Frequency (cm^{-1})[a]			Assignment[b]
m-Cl	m-Br	o-Cl	
2985	2955		0,6 + 2 x 12 (I)
		2940	0,6 + 10 + 21 (II)
		3000	0,6 + 8 + 24 (II)
3010	2990	3075	0,6 + 7 (I)
3045	3040		0,6 + 11 + 22 (II)
3170*	3205	3180	0,2 x 6 (I)
3215		3275	0,6 + 7 + 23 (II)
		3350	0,2 x 6 + 23 (II)
3265	3240		0,6 + 8 + 22 (II)
3345*	3350*		0,5 + 8 (I)
3400	3385	3395	0,2 x 6 + 23 (II)
3420	3385		0,6 + 11 + 10 (II)
3490	3465	3490	0,6 + 7 + 22 (II)
3555	3565		0,6 + 2 x 11 (I)
		3565	0,4 + 2 x 6 (I)
3595	3590		0,6 + 2 x 11 (I)
3660	3670	3635	0,2 x 6 + 22 (II)
3745	3705		0,6 + 8 + 18 (II)
3790	3770*	3725	0,2 x 6 + 21 (II)
3865	3865		0,2 x 8 + 12 (I)
3935	3920		0,5 + 6 + 23 (II)
3990	3980		0,2 x 8 + 10 (II)
4045	4030*		0,6 + 2 x 11 + 22 (II)
4090	4100	4060	0,2 x 6 + 18 (II)
		4130	0,2 x 6 + 17 (II)

TABLE 5.5 (CONTINUED)

Frequency (cm^{-1})[a]			Assignment[b]
p-Cl	m-Br	o-Cl	
4205	4185	4255	0,2 x 6 + 11 (I)
4250	4235		0,6 + 2 x 11 + 12 (I)
4390*	4390		0,2 x 6 + 11 + 33 (II)
4470	4440	4445	0,2 x 6 + 3 (I)
4535	4520		0,5 + 6 + 19 (II)
4600	4575	4630	0,2 x 6 + 7 (I)
4645	4630		0,2 x 6 + 11 + 22 (II)
4715	4735		0,5 + 6 + 11 (I)
4795	4790	4765	0,3 x 6 (I)
4840	4835	4860	0,2 x 6 + 7 + 33 (II)
4940	4905		0,5 + 6 + 3 (I)
4990	4970	4940	0,3 x 6 + 33 (II)
5045	5050		0, x 6 + 11 + 1 (I)
5145	5175		0, x 11 (I)
5240	5230	5240	0,3 x 6 + 22 (II)
5580	5565	5505	0,3 x 6 + 19 (II)

* Denotes shoulder

a. Error about $\pm$ 10cm^{-1}.

b. The i of ν_i is listed (see Table 5.4); I denotes subspectrum I; II denotes Subspectrum II.

(m-Br) is a weak shoulder; thus ν_{12} decreases in frequency while ν_{13} increases in frequency compared with pheylacetylene. The acetylenic stretch ν_5, is assigned at 2105 (m-Cl) and 2140 cm^{-1} (m-Br). Nearly all the in-plane modes present in the phosphorescence spectrum of phenylacetylene are seen in the phosphorescence spectra of m-Cl and m-Br in the same ratio to the 0, 0 as in phenylacetylene. Two exceptions are ν_7, which increases in intensity, and ν_9 (now a C-h stretch), which decreases very much in intensity.

Five out-of-plane modes are observed in the phosphorescence of m-Cl and m-Br. As in phenylacetylene the out-of-plane deformation of the acetylenic group is weak in intensity, at 590 cm^{-1} (m-Cl) and 560 cm^{-1} (m-Br). The two substituent-sensitive modes ν_{22} (16b) and ν_{23} (10b) occur with strong intensities, unlike the case of the parent. The very strong out-of-plane C-h deformation, ν_{23}, decreases greatly in frequency to 215 cm^{-1} in m-Cl and 190 cm^{-1} in m-Br. Of less intensity is the out-of-plane ring deformation, ν_{22}, which also decreases in frequency to 460 cm^{-1} in m-Cl and 450 cm^{-1} in m-Br. Two new modes, ν_{18} (17b) and ν_{19} (11), both out-of-plane C-H deformations, appear at 915 and 800 cm^{-1} in m-Cl (intense and moderately intense peaks, respectively) and at 900 and 795 cm^{-1} in m-Br (intense and moderately intense peak, respectively). Here ν_{20}, a ring deformation, and ν_{24}, the deformation between the ring and acetylenic group are absent. The important point is the presence of four a'' modes, ν_{18}, ν_{19}, ν_{22} and ν_{23}, which give rise to

great vibronic activity in the phosphorescence spectra of m-Cl and m-Br and which are more positively (out-of-plane) polarized than the 0, 0 band (see Figure 5.5(B) and 5.6(B)).

The frequencies assigned are consistent with those of meta-chlorostyrene and meta-bromostyrene[71], and are with the ranges given by Varsanyi[70].

As in phenylacetylene and the para-halophenylacetylenes, the most active totally symmetric vibration is ν_6. Moderately active also are ν_8 (unlike the case of phenylacetylene) and ν_{11}. These a' modes make up Subspectrum I. Combinations and progressions in the a' modes combine with one quantum of ν_{18}, ν_{19}, ν_{22} or ν_{23}. These a'' modes act as false origins.

(d) Ortho-chlorophenylacetylene

The phosphorescence spectrum of 10^{-3}M ortho-chlorophenylacetylene (o-Cl) in polycrystalline methylcyclohexane at 77°K is shown in Figure 5.7(A). The polarizations of the major peaks in a glassy mixture of methylcyclohexane and 3-methylpentane (4 : 1 by volume) are shown in Figure 5.7(B). The assigned ground state fundamentals and vibrational analysis of the phosphorescence spectrum are shown in Tables 5.4 and 5.5 respectively.

The 0, 0 of the $S_0 \leftarrow T_1$ transition occurs at 24950 cm^{-1} showing a red shift slightly greater than the corresponding meta-derivatives of 370 cm^{-1}. A side band occurs to the blue of the 0, 0 band at 165 cm^{-1}.

As in the other derivatives, the same listing of the vibrational modes is followed. The symmetry of the ortho-derivative is C_s.

Because of the greater intensity of Subspectrum II compared to Subspectrum I many of the a' modes which appear in phenylacetylene and the para- and meta-derivatives are not observed in the phosphorescence spectra of o-Cl. Of those modes derived from a_1 in C_{2v}, ν_9 (a C-h stretch), ν_5 (the acetylenic

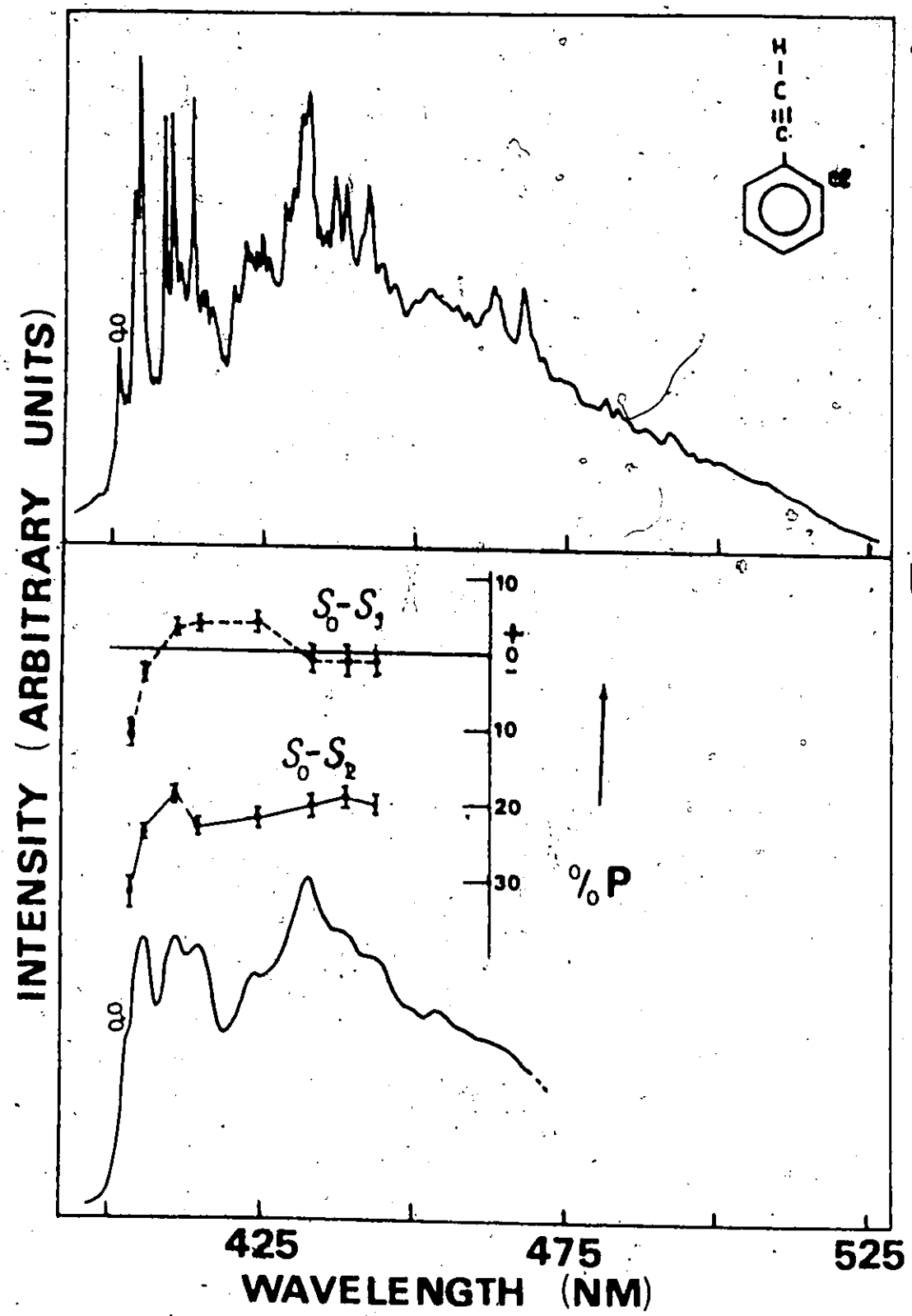

FIG. 5.1 THE PHOSPHORESCENCE SPECTRUM OF 10^{-3} M o-ClØCCH AT 77 °K (A) IN METHYLCYCLOHEXANE (B) IN A RIGID GLASS

stretch), and ν_{13} (a substituent-sensitive ring deformation) are absent.

One of the modes derived from b_2 in C_{2v} is present - $\nu_{\ldots}$. The two in-plane aromatic C-C stretches ν_6 (8a) and ν_7 (19a) occur with very little changes in frequencies compared with phenylacetylene; ν_6, the more intense of the two is a moderately intense peak at 1600 cm^{-1}; the weak peak at 1435 cm^{-1}; is attributed to ν_7. The ring breathing mode, ν_{11} (12), increases in frequency to 1045 cm^{-1}. Two substituent-sensitive modes increase in frequency. The in-plane stretch between the ring and acetylenic group, ν_8 (13), is found at 1240 cm^{-1} as a weak peak. The ring in-plane deformation ν_{12} (1) is weakly active at 840 cm^{-1}. Alternative values for the frequencies of ν_{12} are ruled out because of the intensities of the peaks and from the fit in the vibrational analyses. The weak peak at 775 cm^{-1} is assigned to ν_4 (7a), a C-h stretch (as in the para-derivatives). Thus the a' modes are in the same intensity ratio to the 0, 0 band as they are in phenylacetylene.

All eight b_1 modes (C_{2v}) appear as a'' modes (C_s) in the phosphorescence spectrum of o-Cl. Three out-of-plane aromatic C-H deformations; ν_{17} (5) is found at 990 cm^{-1} (a very weak shoulder); ν_{18} (17b) occurs as the weak peak at 890 cm^{-1}; the very strong peak at 730 cm^{-1} is assigned to the substituent-sensitive mode ν_{19} (11). The acetylenic out-of-plane C-H deformation occurs weakly at 630 cm^{-1}.

The intense peak at 465 cm^{-1} is assigned to ν_{22}(16b) an oop ring deformation. The out-of-plane C-h mode ν_{23} is assigned to the strong peak at 210 cm^{-1}. Because of the proximity of the two substituents in the ortho-position, it is expected that ν_{23} and ν_{24}, the out-of-plane deformation between the ring and the acetylenic group couple strongly. Thus ν_{24} appears as the strong peak at 155 cm^{-1}.

The vibrational analysis is similar to that of phenylacetylene for Subspectrum I, with ν_6 being the most active mode. However, most of the spectra is dominated by Subspectrum II which consists of one quantum of a'' vibration acting as a false origin.

5.6 Interpretation of the Phosphorescence Polarizations

(a) General

The polarizations of the major peaks in the phosphorescence spectra of phenylacetylene and the monohalophenylacetylenes in MC/3MP(4:1) glass at 77°K are used to identify the major mechanistic pathways by which the $T_1 \rightarrow S_o$ transition gains radiative intensity as a function of both the mass of the heavy-atom and its position in the ring.

In glassy solvents, neighboring bands overlap greatly and the observed polarization is the net contribution of all the overlapping bands. Even if monochromatic excitation could be achieved, and depolarization effects minimised, the limiting values of +50% and -33% are not expected, since more than one sublevel of the lowest triplet state can be emissive. However trends in the polarizations across partially resolved bands are important. Consideration must be given not only to the degree of polarization but also whether the polarization represents a maximum or a minimum.

(b) Phenylacetylene (C_{2v})

The percentage polarizations of the 0,0 band and the major peaks of the phosphorescence of phenylacetylene (Figure 4.10) remain relatively constant with respect to both ^1L_a (P equals - 25%) and ^1L_b (P is about -15%). The 0,0 band is predominantly oop (x-axis) polarized with some short-axis (y)

contribution. There is no long-axis *(z) contribution (See Section 4.7(c)). Similarly polarized are all the bands assigned to totally symmetric modes. Band 2, containing a hidden b_1 vibrational mode, shows no preferential y- or x-axial polarization as the maxima are about the same (relative to the other bands) for both ^1L_a and ^1L_b excitation.

The main radiative mechanism for $T_1 \rightarrow S_o$ 0,0 band intensity is direct SO coupling (the first term in the RHS of equation 2.13). The matrix elements involved are

$$< {}^3\psi_o | \hat{e}_x \hat{r} | {}^1\psi_j > < {}^1\psi_j | \hat{H}_{so} | {}^3\psi_i >$$

where the intermediate singlet states $^1\psi_j$ (Table 2.1) are of $\sigma\pi^*$ -type. The in-plane triplet spin sublevels of planar aromatics T^y and T^z are mixed with $^1(\sigma\pi^*)$ or $^1(\pi\sigma^*)$ states via one-center terms because of symmetry (one is x-polarized and the other is forbidden). The radiative decay rate from sublevel T^x is quite small since T^x couples with the main $^1(\pi\pi^*)$ states only through three-center terms which are small. Therefore, the 0,0 band of phenylacetylene is typical of all planar aromatics with a dominant (about 90%) oop polarized component. The in-plane polarized component, via $\pi\pi^*$ intermediate states is about 10 times smaller. This holds for all the band attributed to totally symmetric modes, which together with the 0,0 make up Subspectrum I.

Subspectrum II arises via spin-orbit-vibronic (sov) coupling through the second term in the RHS of equation 2.13. This first order HT-coupling term cannot contribute to Sub-

spectrum I. First order HT-coupling for transitions to vibronic states with one quantum of an oop mode (b_1) has terms

$$\langle S_o | er_{y,z} | S_k \rangle \left[\frac{\partial}{\partial Q_p} \langle S_k | H_{so} | T_1 \rangle \right]$$

from where S_k is a $\pi\pi^*$ type state. These in-plane polarized bands become polarized according to the symmetry of the oop modes as is seen for band 2.

(c) Para-halophenylacetylenes (C_{2v})

For the para-halophenylacetylenes the in-plane polarization component of the phosphorescence become increasingly stronger as the mass of the halogen increases (see Figure 5.1(B)-5.4(B)). There is a rapid increase in the contribution of Subspectrum II to the overall radiative $T_1 \rightarrow S_o$ transition. The amount of Subspectrum II ranges from 0.1 (C_6H_5CCH), 0.25 (p-F), 0.65 (p-Cl), 0.85 (p-Br) to 0.95 (p-I). The in-plane contribution to the polarization of the 0,0 band increases C_6H_5CCH (25%, -15%), p-F (-9%, -5%), p-Cl (-18%, -4%), p-Br (-6%, -2%) to p-I (+5%, +7%) for both ^1L_a and ^1L_b excitations, respectively.

There are large increases in %P subsequent to the 0,0 region. After the first band due to the b_1 mode oscillations on this large increase is seen, but the minima never get to be as negative as the 0,0 band. The minima are found for peaks assigned to totally symmetric modes (a_1), from the vibrational analysis, which are polarized similarly as the 0,0 band.

The oscillations increase in going from p-F to p-Cl, then decrease from p-Br. In p-I this oscillation is not seen. These oscillations follow the increase of Subspectrum II (small in p-F, dominant in p-I).

The observed increase of the in-plane polarized component of the 0,0 transition in the phosphorescence spectra is not due merely to finite slit width of observation since the resolution of the achieved for the slits used in the detecting monochromator was 20 cm^{-1}, or due to the proximity of the low by C-h mode since no dramatic an effect is not observed in the corresponding ortho- and meta-halophenylacetylenes.

In the para-halophenylacetylenes three mechanisms are responsible for the radiative rate of the 0,0 band. The first two are due to direct spin-orbit coupling via $\sigma\pi^*$ or $\pi\sigma^*$ intermediate states (to give an oop polarized component) and via a very small amount of $\pi\pi^*$ states involving three-centre integrals i.e. over the halogen and two adjacent carbon atoms, as in the parent phenylacetylene. The third mechanism is via second order H-F coupling discussed next.

The only way a positive polarization contribution to the 0,0 transition can come about is by mixing in some in-plane transitions such as $\pi\pi^*$ transitions. To mix in $\pi\pi^*$ transitions directly requires integrals over three-centers, i.e., over the halogen and two adjacent carbons. Evaluation of equation 2.13 in terms of the one electron operators r_i (dipole) and

H_{so} (spin-orbit) in the space of the single excited configuration of $\pi\pi^*$- and $\pi\sigma^*$- types over MO's ϕ_i, ϕ_j led to integrals

$$\langle \phi_i | r_x | \phi_j \rangle \quad \text{and} \quad \langle \phi_i | L_u | \phi_j \rangle$$

(where L_u is the orbital angular momentum operator on atom u) in the theory discussed in Section 2.10. The three-center integrals are in the spin-orbit part. These integrals are much smaller than the corresponding one- and two-center integrals. Therefore, for direct mixing of intermediate $\pi\pi^*$ states to be important in the electronic transition there must be a striking increase in the oscillator strength of the $S_o \rightarrow S_i$ transitions from which the radiative $T_1^* \rightarrow S_o$ transition gains intensity in the parent hydrocarbon when a heavy atom is introduced. Examination of Table 5.1 shows no such striking increase in either the ^1L_b or ^1L_a transition strengths as the mass of the heavy atom is increased. This observation is similar to the case of the halonaphthalenes discussed by El-Sayed[18] and by Friedrich et al[20, 69]. The experiment values of $\int \epsilon d\bar{\nu}$ for the halophenylacetylenes show that there is hardly any change of the $\pi\pi^*$-transition probabilities compared with the parent phenylacetylene. Furthermore, since the heavy nucleus is shielded by the surrounding electrons, Friedrich et al were able to show theoretically that the three-centre terms are very insensitive to heavy-atom substitution. Thus this mechanism is ruled out both by theory and experimental spectroscopic observations. Thus the third mechanism (second order H T coupling) leads to the enhancement of the $T_1 \rightarrow S_o$ transition for the

para-halophenylacetylene 0,0 transition though coupling of the type

$$\langle \frac{\partial}{\partial Q_p} T_1^x | H_{so} | \frac{\partial}{\partial Q_p} S_i \rangle$$

The most efficient states are assumed to be of charge-transfer $\pi\pi^*$-configurations, where the electron is transferred from a non-bonding π-orbital from the halogen to π^*-orbitals of the aromatic ring.

Subspectrum II is positively polarized i.e. parallel to the ^1L_a and ^1L_b excitations while subspectrum I is perpendicular to these excitations. Subspectrum II is due to one quantum of non-totally symmetric vibrations (b_1) which are identified as out-of-plane modes (see Table 5.9). These modes include C-H, ring and C-X deformations, some of which are already seen in phenylacetylene, while others are seen only in the phosphorescence spectra of the halophenylacetylenes. Thus, as in the case of the naphthalenes, heavy-atom substitution enhances the SO coupling mechanism already present in the parent hydrocarbon, and introduces a new strong coupling scheme of its own.

The almost constant separation gap for the polarizations after $S_o \rightarrow S_1$ and $S_o \rightarrow S_2$ excitation, with the values after $S_o \rightarrow S_2$ excitation more positive, shows that the original polarization of the parent is being modulated by the polarization of Subspectrum II via b_1 modes.

As the heavy atom increases (in p-Br, and p-I) the second order HT-mechanism dominates the zero order HT-mechanism in the 0,0 transition. Support of this comes from the study

of the halobenzenes[103] where it was shown that the radiative rate of the T^x spin-state increases rapidly as a function of the mass of the heavy-atom relative to the T^y and T^z spin-states. The greater long-axis in-plane polarization may indicate that A_1 singlet states are more important than B_1 singlet states in enhancing the radiative $T_1 \rightarrow S_o$ 0,0 rate of the para-halophenylacetylenes.

Another mechanism which can be proposed involves contribution from the d-orbitals at the halogen atom, by causing the in-plane rate via zero order coupling terms to increase. The percentage of Subspectrum II is already significant in the parent phenylacetylene. This percentage progressively increases as the mass of the heavy atom is increased in the para-halophenylacetylenes. In phenylacetylene d-orbitals are not occupied. Similarly d-orbitals are not occupied in p-F and p-Cl. Hence a delocalization of the π-electrons into empty d-orbitals of the halogen can be assumed to be very small. For p-Br and p-I, the spin-orbit coupling via $d_\pi \; p_\pi$ -interaction is small compared to $p_\pi \; p_\pi$ -coupling because of small overlap. Therefore zero order coupling involving the halogen d-orbitals is much smaller than the usual zero order term.

It was argued by Mothandaraman and Tinti[103] that the relative increase in the relative in-plane polarized rate observed in halogenated benzenes may arise because of distortion of the molecular plane by crystal cage constraints. However, for molecules in glassy solutions it is hardly likely that any such geometry change of the solute molecules exists.

(c) The meta and ortho-phenylacetylenes

The 0,0 polarizations of m-Cl (Figure 5.5(B)), m-Br (Figure 5.6(B)) and o-Cl (Figure 5.7(B)) are negative for both ^1L_a and ^1L_b excitations with a more negative value for the ^1L_a excitation. For molecules of C_s symmetry the emitting $\pi\pi^*$ triplet must be $^3A'$. Also all three sublevels of T_1 can be dipole emissive in the 0,0 region. The π-electron clouds probably retain pseudo C_{2v} symmetry.

For the ortho- and meta-halophenylacetylenes there is no group-theoretic distinction between the y and z (in-plane) axes of C_{2v}. The ^1L_a and ^1L_b states do not necessarily maintain z and y axes polarizations. However, from absorption measurements, the intensities of the $^1L_a - {}^1A'$ transition in the ortho- and meta-halophenylacetylenes do not drastically change. Therefore the assumption that these states retain their C_{2v} polarizations seems reasonable, but open to question.

Because of the formal reduction in symmetry the detailed group-theoretical arguments used in the case of the para-halophenylacetylenes are not possible. In the ortho- and meta-phenylacetylenes excitation to the ^1L_a band produces a polarization of the 0,0 band of phosphorescence which is more negative than the polarization obtained after ^1L_b excitation. This is in-line with the observations in phenylacetylene and its para-halo-derivatives. However, the polarizations of the major bands are almost constant, unlike the case in the para-halophenylacetylenes.

For the meta-derivatives, the polarizations of the major bands are almost the same values for both ^1L_a and ^1L_b excitations, with that after ^1L_a being slightly more negative. All the major bands have about the same polarizations as the 0,0 band after ^1L_b excitation while the 0,0 is more negatively polarized after ^1L_a excitation. (See Figure 5.5(B) and 5.6(B)). Since the bands are negatively (out-of-plane) polarized as in phenylacetylene itself, there is only a slight positive (in-plane) contribution. This in-plane contribution is greater after ^1L_a excitation than after ^1L_b excitation.

In o-Cl (see Figure 5.7(B)) the major bands are less negatively polarized than the 0,0 band after both ^1L_a and ^1L_b excitations, with polarizations after ^1L_a excitations more negative. For ^1L_b excitation the major band are almost depolarized. For the ortho-derivatives, therefore, the main contribution is out-of-plane (negative) with a small in-plane (positive) contribution after both ^1L_a and ^1L_b excitations.

From the vibrational analysis of the phosphorescence spectrum of o-Cl (Table 5.5) most of the spectral intensity arises from oop (a") modes. The large negative values of the polarizations of the 0,0 band for both ^1L_b and ^1L_a excitations show that Subspectrum I of o-Cl is just like phenylacetylene itself. Very little second-order HT-coupling is present. However, first order HT-coupling is responsible for the vibronic bands having more positive polarizations than the 0,0 band. It

seems that first order HT-coupling does not lead to as large positive polarizations here as for the para-derivatives.

The m-Cl and m-Br polarization data indicate that the second-order HT-coupling mechanism is operative (since the 0,0 region is more positively polarized than in phenylacetylene) but it is not the dominant mechanism for the in-plane rate.

Assuming that the vibrational analyses are correct, negative polarizations observed for the vibronic bands are difficult to interpret since Subspectrum II is over 80% in m-Cl, m-Br and o-Cl. This negative polarization is also seen in the β-halonapthalenes[18, 20, 69]. One possible explanation is that the directions of ^1L_a and ^1L_b transitions may be parallel and that of the intermediate $\pi\pi^*$ states are orthogonal to this direction. Another possibility, if the ^1L_a and ^1L_b directions are orthogonal (as in phenylacetylene and the para-derivatives), then "pure" ^1L_a and ^1L_b excitations were not achieved experimentally for the meta- and ortho-derivatives. Until the relative directions of the ^1L_a and ^1L_b transitions are determined, the interpretation of the negative polarizations of the $T_1 \rightarrow S_o$ bands in these compounds remains unsolved.

CHAPTER

ENVIRONMENTAL EFFECT

ON THE LUMINESCENCE SPECTRA

(a) Guest-host fit

The luminescence spectra of many aromatic molecules undergo a dramatic increase in structure when studied in certain polycrystalline aliphatic hydrocarbons and other compounds at low temperature. For phenylacetylene and its halogenated analogues detailed structure of the fluorescence and phosphorescence spectra were obtained in the polycrystalline matrices formed by the branched saturated aliphatic hydrocarbon isopentane (IP) and by the ring saturated hydrocarbon methylcyclohexane (MC). For the ortho- and meta- halo substituted phenylacetylenes polycrystalline MC also proved to be the solvent in which the sharpest phosphorescence spectra were obtained. For the para-halo phenylacetylenes (1, 4 - disubstituted benzenes) trans-1, 4 - dimethylcyclohexane (DMC) was the most suitable solvent. All these Shpol'skii-like spectra were very sharp with half-bandwidths ~ 25 cm^{-1}. From these observations it can be concluded that the sharpest spectra are obtained in hosts in which the guest molecules can fit into the lattice space. Similarly, for the isoelectronic molecules, benzonitrile[59, 60] and phenyl isocyanide[57, [illegible]], MC was the most suitable solvent since the -C ≡ CH, -C ≡ N and -N ≡ C groups are approximately the size as the cyclohexane ring. For the para- halophenylacetylenes

the coherent spectrum in the DBC host was for the para-bromophenylacetylene. The iodo group is a bit too large while the fluoro group is so small that the fit is poorest.

(b) Problem of 0, 0 band Assignment

As in gases, the problem of the pure electronic transition, or 0, 0 band assignment can be complicated by the presence of "hot bands". Furthermore, multiple sites can be obtained in rigid solutions at 77°K. In the phenylacetylenes (and the halo-derivatives) there appear to be no multiple sites due to solvent splitting of the bands. In contrast, the other members of the isoelectronic series show evidence of splitting in polycrystalline DBC. For phenylisocynide[57, 58] there are two sites in the fluorescence and one in the phosphorescence, while in benzonitrile[59, 60] the reverse is observed - one site for the fluorescence and two sites for the phosphorescence. However in the phosphorescence spectra of the halophenylacetylenes side bands occur to the blue of the assigned 0, 0 band. (Section 5.5) These bands are of low frequencies and assigned as "hot" bands. To the red of the 0, 0 bands in phenylacetylene and its halo-derivatives some low frequency bands of low intensity are assigned to lattice vibrations coupling to the electronic transitions (Sections 4.3, 4.5 and 5.5).

An alternative interpretation was recently presented for the assignment of the 0, 0 band of the phosphorescence spectrum of phenylacetylene. Friedrich et al[35] suggested that the observed first transition band cannot be assigned as the 0, 0

band. These authors developed a theoretical "quasi π-model" in which they used both theoretical and spectroscopic values to qualitatively and quantitatively explain the radiative properties of the lowest triplet state of phenylacetylene. By using their phosphorescence yield $\phi_p = 0.3 \pm 0.2$, the observed τ_p of Laposa and Singh[68], and by assuming the ISC yield as close to unity they concluded that the phosphorescence is nearly completely vibrationally induced. Also, unlike the case in most aromatic hydrocarbons, these authors found, in agreement with the results here (Section 4.7) that the polarization of the major bands in the phosphorescence spectrum of phenylacetylene exhibit nearly no vibronic structure. From this they conclude that the very strong band at 25300 cm^{-1} is not the 0, 0 but is due to the first excitation of the degenerate promoting modes γ (C-CCH) and β C-CCH at $\Delta\bar{\nu} \simeq 350$ cm^{-1}. Since the lowest triple state is calculated to be of A_1 orbital symmetry this means that second order - spin orbit coupling dominates the orbitally allowed first-order spin-orbit coupling.

In benzene the emitting triplet state is a B_{1u} (in D_{6h}) state[79] and thus the $S_o - T_1$ transition is both spin and orbitally forbidden. Although the phosphorescence spectrum is vibrationally induced the 0, 0 band appears in rigid solutions, because of solvent perturbation. Even in weakly perturbing solvents such as argon matrix[78] at 20°K and cyclohexane[80] (CH) at 77°K the intensity of the 0, 0 band is about 10 to 15% of most intense band (the 0, 1600 transition).

For strongly perturbing solvents such as carbontetrachloride[35] at 90°K the 0, 0 band reaches up to 60% of the intensity of the 0, 1600 band. Weak chemical perturbation by the methyl group enhances the intensity of the 0, 0 band. In toluene the 0, 0 band of the phosphorescence ranges from 25% (in MC[86] at 77°K) to 60% (in CH[87] at 90°K and in benzene[88] at 4°K) of the intensity of the most intense band. For the xylenes[87], in CH at 90°K, this intensity is 20% for ortho-, 30% for para- and 40% for meta-xylene. It seems reasonable that for stronger chemical perturbation, as in the isolectronic phenylacetylene, phenylisocyanide and benzonitrile, the 0, 0 transition, which is orbitally allowed should be strong, and, in the absence of heavy-atom substituents, first-order spin-orbit coupling should dominate the vibronically induced second order process. In these three molecules the phosphorescence spectra are similar, with the first band being of strong spectral intensity. No small or hidden bands has yet been detected for phenylisocyanide or benzonitrile. A careful examination of the spectrum of phenylacetylene in both IP and MC reveals no such band, which could have been easily detected for a band as small as 0.2% the intensity of the strongest band. Further chemical perturbation by halogens, and especially further reduction in symmetry, support the assignment in this work. In the halo-derivatives Y-C-CCH should not change much in frequency. However no bands $\sim$ 350 cm^{-1} are detected to the blue of the assigned 0, 0 band. The bands detected to the blue are of much

lower frequencies (less than $\sim 200\ cm^{-1}$) and are presumably "hot bands". A temperature dependence study could determine this.

The polarization data (Figure 4.10) is also consistent with the interpretation presented for the vibrational analysis of the phosphorescence spectrum of phenylacetylene. Band 2 is more positive than the other bands partly because of contribution of a b_1 mode (Section 4.7).

Paramagnetic molecules such as oxygen perturb the spin-forbidden S - T transition. By saturating solutions of aromatic hydrocarbons in chloroform with oxygen at high pressure Evans[13] introduced a technique for observing singlet-triplet absorption spectra. The 0, 0 absorption band is found to coincide with the corresponding transition E_T in the $T_1 \rightarrow S_o$ phosphorescence spectrum. Table 6-1 displays comparisons of $T_1 \leftarrow S_o$ (in chloroform) and $T_1 \rightarrow S_o$ (in rigid solutions) data for benzene and some substituted benzenes. The data supports the present assignment of the 0, 0 band of the phosphorescence spectrum of phenylacetylenes.

TABLE 6.1

COMPARISON OF THE 0,0 BAND FOR THE $S_o - T_1$ TRANSITION IN SOME BENZENES

Molecule	Absorption[a] (cm^{-1})	Emission (cm^{-1})	Solvent*
Benzene	29440	29350	CCl_4[b]
		29515	A[c]
		29445	CH[d]
Toluene	29000	28890	EPA[e]
		28920	CH[f]
		29010	MC[g]
Benzonitrile	26880	26985	A[h]
		26760	CH[h]
		27010	MC[h]
Phenylacetylene	25190	25285	EPA
		25230	3MP
		25240	IP
		25215	IP[i]
		25320	MC

* A = alcohol, CH = cyclohexane, MC = methylcyclohexane, 3MP = 3-methylpentane, IP = isopentane, EPA = a 5 : 5 : 2 mixture of ethyl ether, IP and A..

a. In $CHCl_3$ from Ref. 13
b. Ref. 85
c. Ref. 89
d. Ref. 80
e. Ref. 90
f. Ref. 87
g. Ref. 86
h. Ref. 59
i. Ref. 3

CHAPTER 7

CONCLUSIONS

The $\pi\pi^*$ luminescence of phenylacetylene-h_0, $-d_1$, $-d_5$ and $-d_6$ were investigated for the fluorescence ($S_1 \rightarrow S_0$) and phosphorescence ($T_1 \rightarrow S_0$) emissions in dilute solutions at 77°K.

In polycrystalline methylcyclohexane these spectra were quasi-linear (with half-bandwidths ~ 25 cm^{-1}). Shifts in frequencies of the normal modes on deuteration attest the confidence in the vibrational analyses (all spectra from a given emissive state were similar for $-h_0$, $-d_1$, $-d_5$ and $-d_6$).

The fluorescence spectrum of phenylacetylene was analysed in terms of an allowed component and a forbidden component. The allowed component (in C_{2v} notation) involves the 0,0 of the $^1B_2(S_1) \rightarrow {}^1A_1(S_0)$, short-axis ($y$) in-plane transition, and the totally symmetric (a_1) modes. This allowed component is very small. The forbidden component, which is based on one quantum of a b_2 mode, is about 95% of the fluorescence radiation. This large forbidden component is seen in the isoelectronic phenylisocyanide but not in benzonitrile.

The phosphorescence spectrum of phenylacetylene is different from the fluorescence spectrum. In phenylacetylene the 0,0 band of the phosphorescence is the most intense spectral band of the transition, like the isoelectronic

phenylisocyanide and benzonitrile. Polarization of the 0,0 region was used to assign a_1 symmetry to T_1. Most of the vibronic structure is due to a_1 modes. A weak component based on one quantum of a b_1 vibration is also seen.

In terms of the Franck-Condon principle, the vibrational analyses of the fluorescence spectra are consistent with a planar, slightly expanded, regular hexagonal structure for phenylacetylene in the first excited state (S_1). This is found for benzene and most substituted benzenes.

The phosphorescence spectra indicate that the first triplet (T_1) state of phenylacetylene of planar, non-regular hexagon geometry, either quinoidal or antiquinoidal. A calculation, assuming overall expansion of the ring in the T_1 state, indicates that the T_1 state of phenylacetylene is antiquinoidal in polycrystalline isopentane and methylcyclohexane matrices. For phenylacetylene, and other substituted benzenes, the T_1 state is different from that of benzene itself where it is a regular hexagon in some matrices.

Deuteration reduced the $T_1 \rightsquigarrow S_0$ non-radiative rate rather than lengthening the observed phosphorescence lifetime. The importance of the exocyclic triple bond as an energy sink was demonstrated by the fact that replacement of the acetylenic hydrogen by deuterium causes an increase in phosphorescence lifetime equal to that caused by replacement of all the ring hydrogens.

Seven halogen monosubstituted phenylacetylenes were used to investigate changes in the radiative and non-radiative processes on heavy-atom substitution, as a function of both the position on the ring and the mass of the halogen.

Phosphorescence lifetimes decreased markedly with increasing mass of halogen, and the effect was greatest for the para position in accordance with the Platt vector diagrams. Similar effects were seen in the fluorotoluenes and the halobiphenyls. The values of $\int \epsilon d\bar{\nu}$ for the $S_1 \leftarrow S_0$ and $S_2 \leftarrow S_0$ absorptions were not very sensitive to heavy atom perturbation. Intersystem crossing yields increased with halogen mass, again the effect was greatest for the para position.

Vibrational analyses of the phosphorescence spectra showed that the main spectral component (based on the 0,0 transition) of the parent molecule (Subspectrum I) was still present in the halophenylacetylenes though the component based on one quantum of an out-of-plane mode increased. This component (Subspectrum II) increased regularly with increasing mass of the heavy-atom in the para-derivatives. In meta-chloro-meta-bromo- and ortho-chlorophenylacetylene the Subspectrum II was over 80%.

Polarizations of the 0,0 band and the major bands of the phosphorescence spectra (in rigid glasses) of phenylacetylene and monohalo derivatives were used to interpret the main spin-orbit coupling mechanisms by which the $T_1 \rightarrow S_0$ rate was enhanced on halogen substitution. For the "pure" aromatic hydrocarbon

(phenylacetylene) the out-of-plane polarized rate was dominant over the in-plane polarized component in the 0,0 region. This component was direct spin-orbit (zero order Herzberg-Teller) coupling. The in-plane polarized component of the 0,0 band gained intensity via second order Herzberg-Teller coupling. The in-plane polarized radiative component increased with the increasing mass of the halogen in the para-derivatives. A similar effect was seen in the α-halonaphthalenes. The polarizations of bands subsequent to the 0,0 also demonstrated the increasing importance of Subspectrum II (of first order Herzberg-Teller coupling mechanism) with increasing mass of the halo-substituent in the para position. For the ortho- and meta-halophenylacetylenes the mechanisms for $T_1 \rightarrow S_o$ rate enhancement remained unsolved.

Finally, guest-host fit showed that trans-1, 4-dimethylcyclohexane was a suitable host for quasi-linear spectra of the para-halophenylacetylenes while methylcyclohexane was suitable for phenylacetylene and its ortho- and meta-halo-derivatives. Also, the effects of solvent perturbation on the intensity of the phosphorescence 0,0 band of benzene and substituted benzenes indicated that the band assigned to the 0,0 transition is the "true" 0,0 band.

BIBLIOGRAPHY

1. J. M. Robertson, J. F. Music and F. A. Matsen, J. Am. Chem. Soc. 72 5260 (1950).

2. M. R. Padhye and B. S. Rao, J. Sci. Ind. Research (India) 19B 1 (1960); 18B 499 (1959).

3. T. S. Zhuraleva, Optics and Spec. 22 489 (1967); [Optika i Spectroskopiya 22 898 (1967)].

4. A. D. Walsh, Proc. Roy. Soc. (London) A191 32 (1947).

5. H. W. Thompson and P. Torkington, J. Chem. Soc. 595 (1944)

6. W. Veil, M. Ninnewisser, H. K. Bodenseh and H. Buchert, Z. Naturforsch. A15 1011 (1960)

7. M. Borgael and P. Daure, Bull. Soc. Chim. 47 1349 (1930)

8. M. J. Murray and F. F. Cleveland, J. Am. Soc. 61 3546 (1939)

9. J. C. Evans and R. A. Nyquist, Spectrochim. Acta 16 918 (1960)

10. S. P. So, Ph.D. Thesis, McMaster University, (1969).

11. G. W. King and S. P. So, J. Mol. Spec. 33 376 (1970).

12. G. W. King and S. P. So, J. Mol. Spec. 36 468 (1970).

13. D. F. Evans, J. Chem. Soc. 1351 (1957); 2753 (1959).

14. E. F. Harrigan, T. C. Wong, and N. Hirota, Chem. Phys. Lett. 14 549 (1972).

15. G. Wade and J. E. Nebbor, J. Chem. Phys. 56 1619 (1972)

16. T. S. Zhuravleva and D. N. Shigorin, Zh. Fiz. Khim. 39 3118 (1965).

17. G. C. Nieman, J. Chem. Phys. 50 1674 (1969).

18. T. Pavopoulos and M. A. El-Sayed, J. Chem. Phys. 41 1082 (1964).

19. S. P. McGlynn, T. Azumi, and M. Kinoshita, Molecular Spectroscopy of the Triplet State, Prentice-Hall, Englewood Cliffs, New Jersey (1969).

20. J. Friedrich, F. Metz and F. Dorr, Ber. Bunsenges. physik. Chem. 11 1214 (1974).

21. W. Siebrand and D. Williams, J. Chem. Phys. 46 403 (1967).

22. W. Siebrand, J. Chem. Phys. 46 440 (1967); 44 4055 (1966).

23. L. Pauling, and E. B. Wilson, Jr., Introduction to Quantum Mechanics, McGraw-Hill, New York (1935).

24. F. A. Cotton, Chemical Applications of Group Theory, Interscience, New York (1963).

25. G. Herzberg, Electronic Spectra and Electronic Structure of Polyatomic Molecules, Van Nostrand, Princeton (1966).

26. G. W. King, Spectroscopy and Molecular Structure, Holt, Rinehart and Wilson, New York, (1964).

27. R. S. Mulliken, J. Chem. Phys. 23 1997 (1955).

28. D. R. Lide, J. Chem. Phys. 22 1577 (1954).

29. B. Bak, D. Christensen, W. B. Dixon, L. Hansen-Nygaard, and J. Rastrup-Andersen; J. Chem. Phys. 37 2027 (1962)

30. E. B. Wilson, Phys. Rev. 45 706 (1934).

31. H. Sponer and E. Teller, Rev. Mod. Phys. 13 75 (1941).

32. M. Born and R. Oppenheimer, R. Ann. Physik, 84 457 (1927).

33. J. B. Birks, Photophysics of Aromatic Molecules, Wiley-Interscience, London (1969).

34. B. Meyer, Low Temperature Spectroscopy, Elsevier Publishing Co., New York (1971).

35. S. Friedrich, R. Griebel, G. Hohlneicher, F. Metz and S. Schneider, Chem. Phys. 1 319 (1973).

36. S. Friedrich, R. Griebel, G. Hohlneicher, F. Metz and S. Schneider, Chem. Phys. 1 330 (1973).

37. S. K. Lower and M. F. A. El-Sayed, Chem. Revs. 66 199 (1966).

38. H. F. Hameka, The Triplet State; Proceedings of an International Symposium held at the University of Beirut, Feb., 1967, (A. B. Zahlan, ed.), Cambridge University Press,

39. R. M. Hochstrasser, Molecular Aspects of Symmetry, Benjamin, New York (1966).

40. A. C. Albrecht, J. Mol. Spectrosc., 6 84 (1961).

41. T. Azumi and S. P. McGlynn, J. Chem. Phys. 37 2413 (1962).

42. D. S. McClure, J. Chem. Phys. 17 665 (1949).

43. A. H. Kalantar, Chem. Phys. 1 207 (1973).

44. G. W. Robinson, Excited States, Vol.1, (E.C. Lim, ed.) Academic Press, New York (1974).

45. E. B. Wilson, J. C. Decius and P. C. Cross, Molecular Vibrations, McGraw-Hill, New York (1955).

46. J. Laposa, E. Lim and R. Kellog, J. Chem. Phys. 42 3025 (1965).

47. B. R. Henry and W. Siebrand, Chem. Phys. Lett. 3 327 (1969).

48. T. E. Martin and A. H. Kalantar, J. Phys. Chem. 72 2265, (1968).

49. N. C. Yang, E. L. Murov and T. Shieh, Chem. Phys. Lett. 3 6 (1969).

50. K. Higashiuru, K. Tanimoto, N. Hamaji, and M. Oiwa, Kogyu Kazaku Zasshi (Japan) 66 (3) 374 (1963).

51. T. L. Jacobs, Organic Reactions, Vol. 5, John Wiley, New York (1949).

52. A. D. Allen and C. D. Cook, Can. J. Chem. 41 1084 (1963).

53. L. Brandsma, Preparative Acetylenic Chemistry, Elsevier Publishing Co., New York (1971).

54. G. Herzberg, Infrared and Raman Spectra, Van Nostrand, Princeton, New Jersey (1945).

55. D. H. Whiffin, J. Chem. Soc. 1350 (1956).

56. S. Leach, R. Lopez-Delgado and L. Grajar, J. Chim. Phys. 63 194 (1966).

57. R. A. Nalepa, M.Sc. Thesis, McMaster University, (1973).

58. R. A. Nalepa and J. D. Laposa, J. Luminescence, 8 429 (1974).

59. G. L. LeBel, M.Sc. Thesis, McMaster University, (1971).

60. G. L. LeBel and J. D. Laposa, J. Mol. Spectrosc., 41 249 (1972).

61. J. R. Platt, J. Chem. Phys. 17 484 (1949).

62. Alan R. Muirhead, Allen Hartford, Jr., Kwo-Tsair Huang, and John R. Lombardi, J. Chem. Phys. 56 4385 (1972).

63. A. C. Albrecht, J. Chem. Phys. 33 156 (1960).

64. J. C. D. Brand and P. D. Knight, J. Mol. Spectry. 36 328 (1970).

65. G. W. King and A. A. G. van Putten, J. Mol. Spectry. 42 514 (1972).

66. K. Takei and Y. Kanda, Spectrochim. Acta 18 1201 (1962).

67. H. Singh and J. D. Laposa, J. Luminescence 3 287 (1971).

68. J. D. Laposa and H. Singh, Chem. Phys. Lett. 4 918 (1969).

69. J. Friedrich, F. Metz and F. Dorr, submitted to Mol. Phys.

70. G. Varsanyi, Vibrational Spectra of Benzene Derivatives, Academic Press, New York (1969).

71. J. C. Fateley, G. L. Carlson and F. E. Dickson, Appl. Spect. 22 650 (1968).

72. T. E. Martin and A. K. Kalantar, J. Chem. Phys. 48 4996 (1968).

73. T. E. Martin and A. K. Kalantar, Chem. Phys. Lett. 1 623 (1968).

74. T. M. Rabalais, H. J. Maria and S. P. McGlynn, Chem. Phys. Lett. 3 59 (1969).

75. L. J. de Groot and J. H. van der Waals, Mol. Phys. 4 189 (1961).

76. E. C. Lim and J. D. Laposa, J. Chem. Phys. 41 3257 (1964)

77. E. W. Schlag, S. Schneider and S. F. Fischer, Ann. Rev. Phys. Chem. 22 465 (1971).

78. P. M Johnson and L. Ziegler, J. Chem. Phys. 56 2169 (1972)

79. A. C. Albrecht, J. Chem. Phys. 38 354 (1963).

80. J. D. Sprangler and N. G. Kihner, J. Chem. Phys. 48 698 (1968).

81. F. Metz, S. Friedrich and G. Hohlneicher, Chem. Phys. Lett. 16 353 (1972).

82. S. Fischer and E. W. Schlag, Chem. Phys. Lett. 4 393 (1969).

83. E. C. Baum and J. N. Pitts, Jr., J. Phys. Chem. 70 3063 (1966).

84. E. M. R. Stacie, Atomic and Free Radical Reactions, 2nd ed. ACS Monograph No. 215, Vol. 1, Reinhold Publishing Corp. New York, N.Y., (1954).

85. Y. Kanda and R. Shimada, Spectrochim. Acta 17 7 (1961).

86. V. J. Morrison, M.Sc. Thesis, McMaster University (1975).

87. Y. Kanda and R. Shimada, Spectrochim. Acta 17 279 (1961).

88. D. M. Haaland and G. C. Nieman, J. Chem. Phys. 59 4435 (1973).

89. F. P. Dikun and V. Ya. Sveshnikov, Dolk. Akad. Nauk SSSR 65 637 (1949).

90. Y. Kanda and H. Sponer, J. Chem. Phys. 28 798 (1958).

91. C. M. O'Donnell, K. F. Harbaugh and J. D. Winefordner, Spectrochim. Acta 29A 753 (1973).

92. J. K. Roy, Indian J. Phys. 35 143 (1961).

93. D. S. McClure, J. Chem. Phys. 17 905 (1949).

94. V. Ermolaev and K. Switaskev, Optics and Spec. 1 399 (1959).

95. G. Porter and B. Ward, Proc. Roy. Soc. (London) A 287 457 (1965).

96. A. J. Jackson, Ph.D. Thesis, McMaster University (1971).

97. A. Stojiljkovic and D. H. Whiffen, Spectrochim Acta, 12 47 (1958).

98. P. R. Griffiths and H. W. Thompson, Proc. Roy. Soc. (London) A298 51 (1967).

99. A. A. G. van Putten, Ph.D. Thesis, McMaster University (1974).

100. M. A. El-Sayed, J. Chem. Phys. 43 2864 (1965).

101. L. Goodman and V. J. Krishna, Rev. Mod. Phys. 35 541 (1963).

102. Y. H. Lui and S. P. McGlynn, J. Luminescence 9 449 (1975).

103. G. Kothandaraman and D. S. Tinti, Chem. Phys. Lett. 19 225 (1973).

105. [illegible] and J. [illegible], J. Luminescence 9 449 (1975)

106. [illegible] and [illegible], Jr., J. Phys. Chem. 70 2066 (1966).

106. [illegible] and E. E. Millard, J. Phys. Chem. 72 1918, 3344 (1968).